

NASA CR-132758

MULTISPECTRAL SCANNER SYSTEM FOR ERTS

FOUR BAND SCANNER SYSTEM

NASA Contract NAS 5-1125j

SPACE AND COMMUNICATIONS GROUP
HUGHES AIRCRAFT COMPANY
EL SEGUNDO, CALIFORNIA

(NASA-CR-132758) MULTISPECTRAL SCANNER SYSTEM FOR ERTS: FOUR-BAND SCANNER SYSTEM. VOLUME 1: SYSTEM DESCRIPTION AND PERFORMANCE (Hughes Aircraft Co.) 133 p HC \$8.75 N73-25474 CSCI 14B GR/14 Unclas 06202

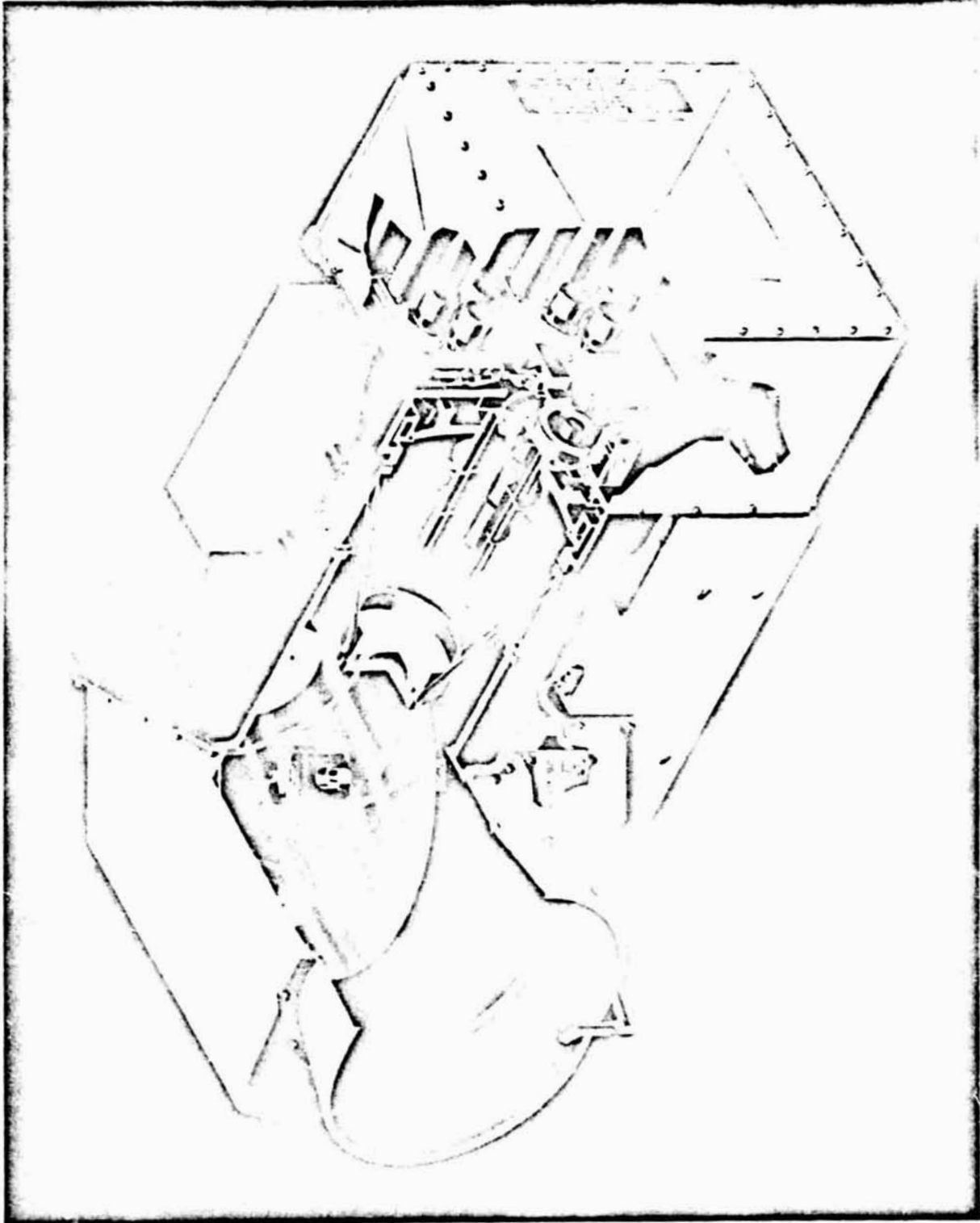
August 1972

FINAL REPORT
VOLUME I
SYSTEM DESCRIPTION
AND PERFORMANCE



Prepared for:
GODDARD SPACE FLIGHT CENTER
GREENBELT, MARYLAND 20771

REPRODUCIBILITY OF THE ORIGINAL PAGE IS POOR.



PRECEDING PAGE BLANK NOT FILMED

INTRODUCTION

The Final Report for the Multispectral Scanner System program is provided in two portions. The first portion is written at the conclusion of the 4-band program, and the second portion will be written subsequent to completion of the 5-band program.

The 4-band final report is in three volumes. The first volume describes the system and compares its performance with the original objectives. The second volume describes some field experiments performed at the end of the program using the Engineering Model scanner and multiplexer. Volume III will be an analysis of in-orbit performance and will be written later.

This document is Volume I. It contains an overall functional description of the system with a summary of the initial design guidelines and the final design parameters (Chapter 1); a description of the design of the major components of the scanner and multiplexer (Chapter 2); an explanation of the processing of the calibration system output (Chapter 3); a summary of calibration data (Chapter 4); and a performance summary (Chapter 5). Detailed descriptions can be found in Operation and Maintenance Manuals and the Qualification and Acceptance test reports shown in the list of applicable documents.

PRECEDING PAGE BLANK NOT FILMED

CONTENTS

VOLUME I. SYSTEM DESCRIPTION AND PERFORMANCE

	Page
1. MULTISPECTRAL SCANNER SYSTEM	1-1
1.1 System Objectives	1-1
1.2 System Description	1-1
1.3 General Description	1-5
1.4 Summary of System Parameters	1-15
2. MSS SPACECRAFT EQUIPMENT	2-1
2.1 Scanner	2-1
2.2 Multiplexer	2-35
3. CALIBRATION PROCESSING THEORY	3-1
3.1 Purpose of Calibration System	3-1
3.2 Processing Requirements	3-3
3.3 Calibration System Processing in General	3-3
3.4 Processing Techniques	3-5
3.5 Ingredients Needed for Lookup Table Computation	3-13
3.6 Generation of Lookup Table	3-15
3.7 Sun Calibration Pulse	3-18
3.8 Limitations	3-18
4. CALIBRATION DATA	4-1
4.1 Scanner Spectral Response	4-1
4.2 Radiometric Response	4-1
4.3 Registration and IFOV	4-14
4.4 Multiplexer Calibration	4-18
4.5 Scan Characteristics	4-18
4.6 Sun Calibration System	4-21
4.7 Internal Calibration System	4-23
4.8 Telemetry Calibration	4-26
4.9 Special Engineering Model Sun Calibrate Measurements	4-26
5. PERFORMANCE EVALUATION	5-1
5.1 Prototype Subsystem (S/N 001) Test Program Summary	5-1
5.2 Prototype Subsystem (S/N 001) Performance Results	5-3

- 5.3 Backup Subsystem (S/N 002) Test Program Summary
- 5.4 Backup Subsystem (S/N 002) Performance Results
- 5.5 Typical Signal-to-Noise and MTF Performance

APPLICABLE DOCUMENTS

1. MULTISPECTRAL SCANNER SYSTEM

1.1 SYSTEM OBJECTIVES

The 4-band Multispectral Scanner System (MSS) is designed to provide the capability for collecting earth imagery from the Earth Resources Technology Satellite (ERTS). The scanner portion of the system employs all reflective optics to accommodate the four spectral bands which occupy a broad spectral range from visible to near infrared. Using a single optical system for all spectral bands assures the excellent registration needed for signature analysis of agricultural scenes. Systematic coverage of the earth with nearly uniform lighting is obtained by the ERTS near-polar sun synchronous orbit. The sun synchronous orbit assures that lighting angles are little changed for contiguous areas imaged and for subsequent images of the same areas. The 496 n. mi. altitude permits the scanner to image with usable resolution in 225 feet wide areas. Subsequent data sampling and processing have been carefully designed to preserve the registration inherent in the point scan technique.

Table 1-1 shows the initial design goals which were used as guidelines for the MSS system design. Measurements made on the prototype subsystem (S/N 1) and the backup subsystem (S/N 2) verify that all initial design goals have been met or exceeded. A complete performance summary, including all parameter measurements made during environmental Qualification and Acceptance Testing, is included in Section 5.

1.2 SYSTEM DESCRIPTION

The Multispectral Scanner System consists of a scanner and multiplexer mounted on ERTS as shown in Figure 1-1, and a configuration of ground equipment to process the video data channels to a condition suitable for photographic reproduction and computer processing of signatures. Several specialized units of test equipment are also provided to permit testing to the required precision. These units are transportable so that they can accompany the scanner/multiplexer subsystem through the test cycle.

Earth imagery data collected by the scanner are multiplexed into a single 15 Mbps data stream on board the spacecraft and transmitted to

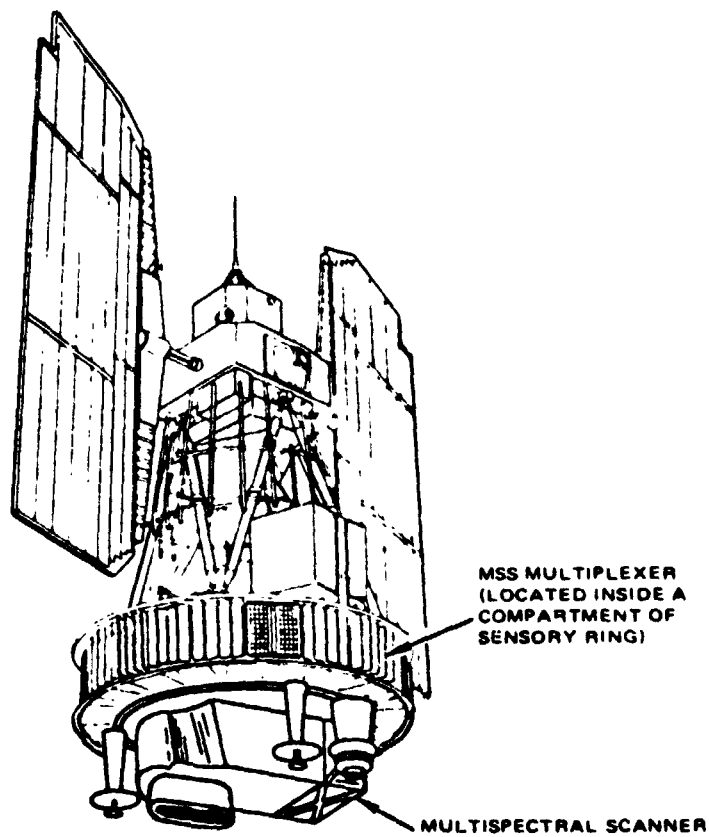


Figure 1-1. MSS Shown on ERTS

TABLE 1-1. IMAGING DESIGN GOALS

Quality of imaging	Radiance levels from observables represented by agricultural crops in areas as small as 225 feet across should be measured with good relative fidelity among the reflective bands.
Spectral bands	
Band 1	0.5 to 0.6 microns
Band 2	0.6 to 0.7 microns
Band 3	0.7 to 0.8 microns
Band 4	0.8 to 1.1 microns
Interval between repeated mapping of areas	Approximately 3 weeks (swaths of 100 n. mi.)
Registration	Approximately 40 feet
Viewing angles	No greater than 10 degrees from normal
Minimum lighting condition	Sun zenith angle \leq 55 degrees
Orbit	9:30 a. m., sun-synchronous at 496 n. mi. altitude (99 degrees retrograde)
Velocity	3.49 n. mi. /sec
Weight	Approximately 120 pounds

receiving sites via a 20 MHz bandwidth downlink. The received data are recovered and demultiplexed into the original channels and formatted for binary recording on multitrack tapes. The tapes are then forwarded to the NASA Data Processing Facility (NDPF) where output data in the form of both images and digital data are procured. This process is shown schematically in Figure 1-2.

Binary data recorded on the magnetic tapes includes timing and radiometric calibration information that can be converted by computer programs into spectral signatures. While signature analysis is not provided by the MSS system, the signature analysis function has greatly influenced MSS requirements.

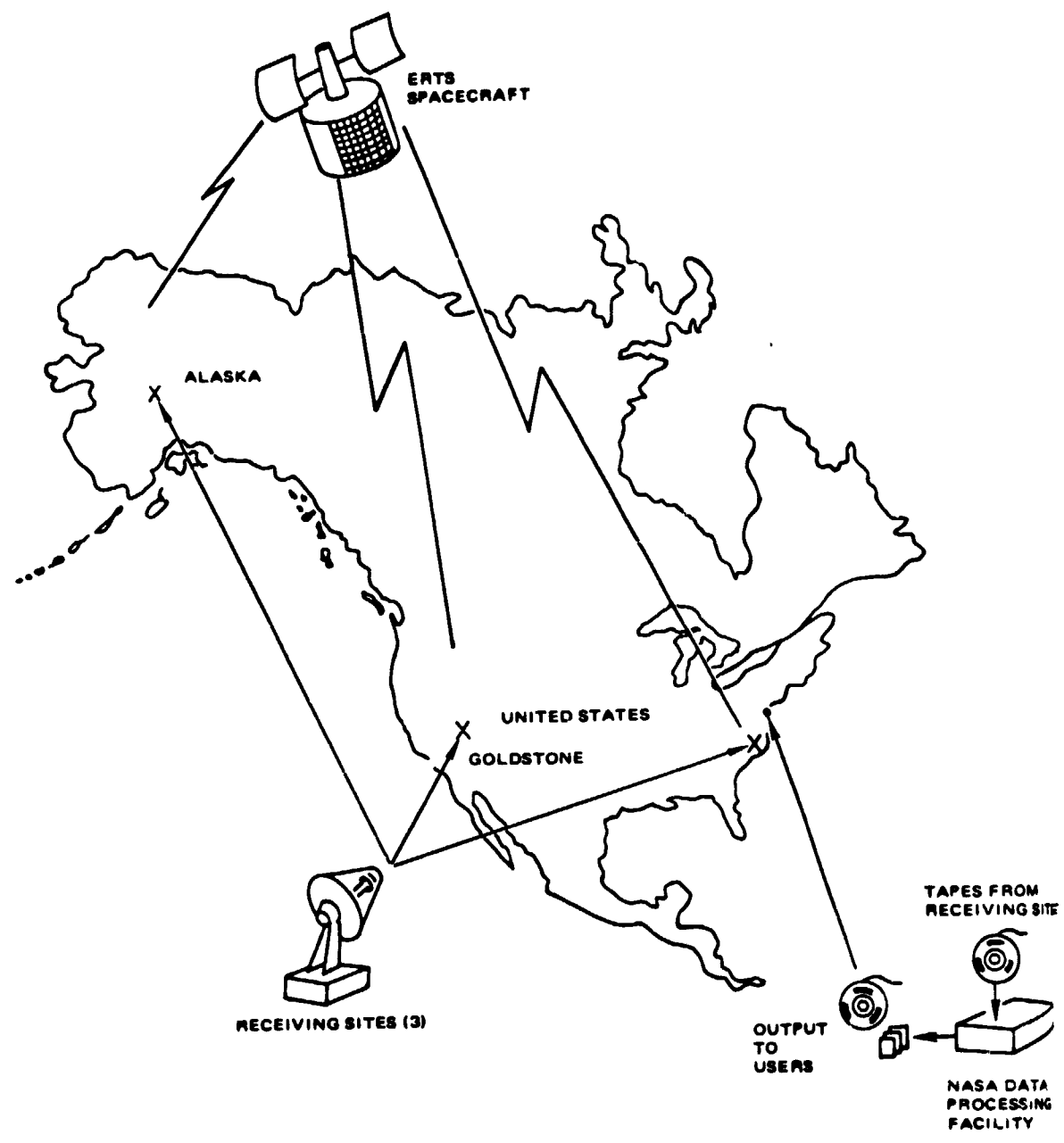


Figure 1-2. Earth Resources Technology Satellite System

A later mission is planned that incorporates a fifth (IR) band. This can be added to the existing four-band design because the optical components are common to all five bands except for the final detector stage of the fifth band.

1.3 GENERAL DESCRIPTION

The flight subsystem, shown schematically in Figure 1-3, consists of a scanner and multiplexer. The spacecraft provides the scanner and multiplexer with command signals, regulated thermal surfaces, regulated power, power for telemetry, and time code signals. The MSS equipment sends a binary data stream suitable for transmission or storage to appropriate spacecraft subsystems. Pertinent parameters for spacecraft interface are summarized in Table 1-2.

The following subsections treat the units of the MSS system in a general manner. The flight subsystem is then repeated in Section 2 in more detail.

1.3.1 Scanner

The scanner is designed to scan a 100 n. mi. swath on the earth, imaging six lines across in each of four spectral bands simultaneously. An oscillating mirror provides the crosstrack scan, and the orbital progress of the spacecraft provides the scan along the track, as shown in Figure 1-4. The flat mirror is at 45 degrees with respect to the scene and the double-reflector, telescope type optics. The scan motion of the mirror subtends a field of view of 11.5 degrees. This is achieved by ± 2.9 degrees of motion.

TABLE 1-2. INTERFACE PARAMETERS

Item	Value
Scanner weight	105 pounds
Multiplexer weight	6 pounds
Scanner size	Approximately 14 by 15 by 35 inches
Multiplexer size	4 by 6 by 6.5 inches
Regulated power, -24.5 volts	20 watts (system A)
Unregulated power, -39 volts	22 watts
Command capability	72 (55 assigned)
Telemetry channels	97

about a nominal 45 degree position. The scanner configuration is illustrated schematically in Figure 1-5, and an isometric cutaway view of the scanner is shown in Figure 1-6.

The six lines in each of the four spectral bands are imaged by a 4 by 6 fiber optics array located at the focused area of the telescope. The square end of each glass optical fiber forms the field stops which determine the instantaneous field of view (IFOV) of the system. Each IFOV of 0.086 mr subtends a square of 259 feet on the earth from the ERTS orbit. The telescope configuration (Ritchey Chrétien) provides a relatively wide area of focus which reduces the system sensitivity to thermal and mechanical misalignments.

An image of the earth in the 100 n. mi. swath is swept across the fiber array each mirror scan. Light impinging on each glass fiber is conducted to an individual detector via an optical filter, each chosen for the four spectral bands. The band 1, 2, and 3 detectors are photomultiplier tubes, while band 4 uses silicon photodiode detectors. The amplified detector outputs (bands 1 and 2 have a commandable times 3 high gain mode) comprise the video signal output for each of the scanner's 24 channels. By operating the mirror at a rate of 13.62 Hz, the orbital velocity is precisely such that the subspacecraft ground track has advanced six IFOVs, and the next line imaged by the first detector in each band is contiguous to the sixth line of the previous scan. Figure 1-7 illustrates the field stop pattern projected on the earth's surface. The channels (A through F) in each of the four bands (1 through 4) are also identified on this figure.

The 24 video outputs are sampled (at a 100,000 sample/sec rate) by the multiplexer during the forward trace (west to east) sweep of the mirror in the southbound part of orbit. The sampling is initiated at the start of each scan by the mirror scan monitor located at the edge of the aperture in the scanner. This device projects a light beam onto the scan mirror and has detectors that cause a pulse to be emitted at angle crossings that correspond to the west edge, center, and east edge of the 100 n. mi. swath.

During the retrace interval, when the scan mirror makes the transit from east to west, a shutter wheel closes off the optical fiber view to the earth, and an internal light source is projected on the fibers via a prism. A continuously variable neutral density filter (NDF) is swept across the light path so that each video channel contains a nearly right triangular pulse of about 10 ms duration, which begins with an abrupt transition from black to white and descends at a lower rate monotonically to black. This internal calibration signal provides a check on the relative radiometric levels and a means for equalizing gain changes that may have occurred in the six channels of one spectral band. Experience has shown that the eye discerns very slight variations among adjacent lines. Corrections are performed in the ground processing equipment to equalize these levels to within 2 percent so that line-to-line density variations, called striping, will be reduced to an acceptable minimum.

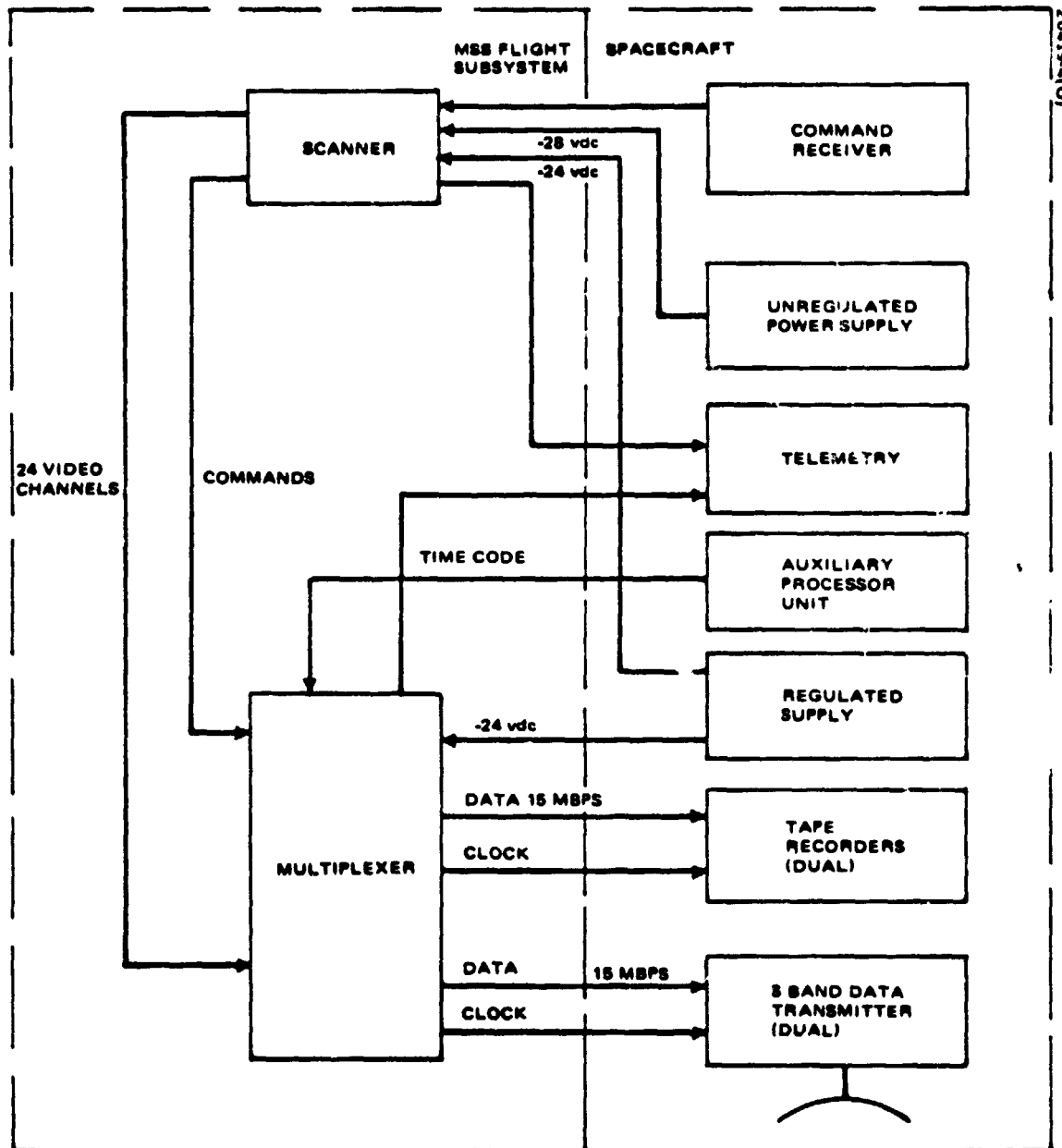


Figure 1-3. MSS Flight Subsystem and Spacecraft Interface

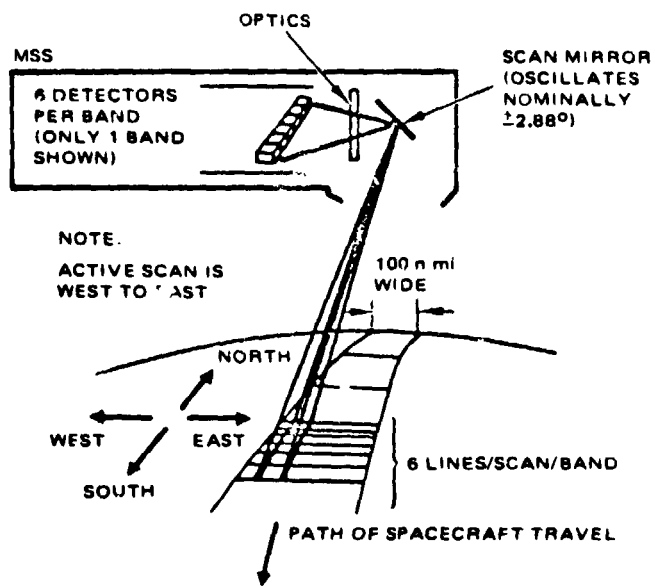


Figure 1-4. MSS Ground Scan Pattern

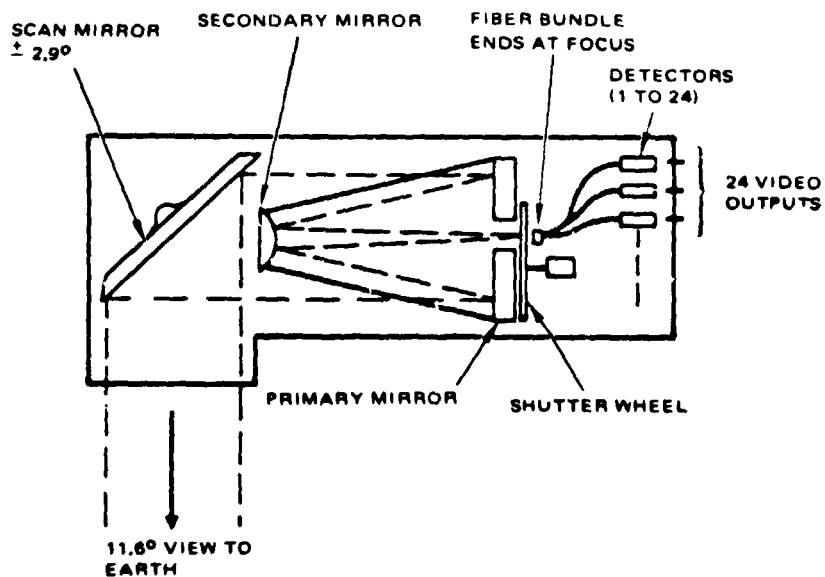


Figure 1-5. Scanner Schematic

20419-7(U)

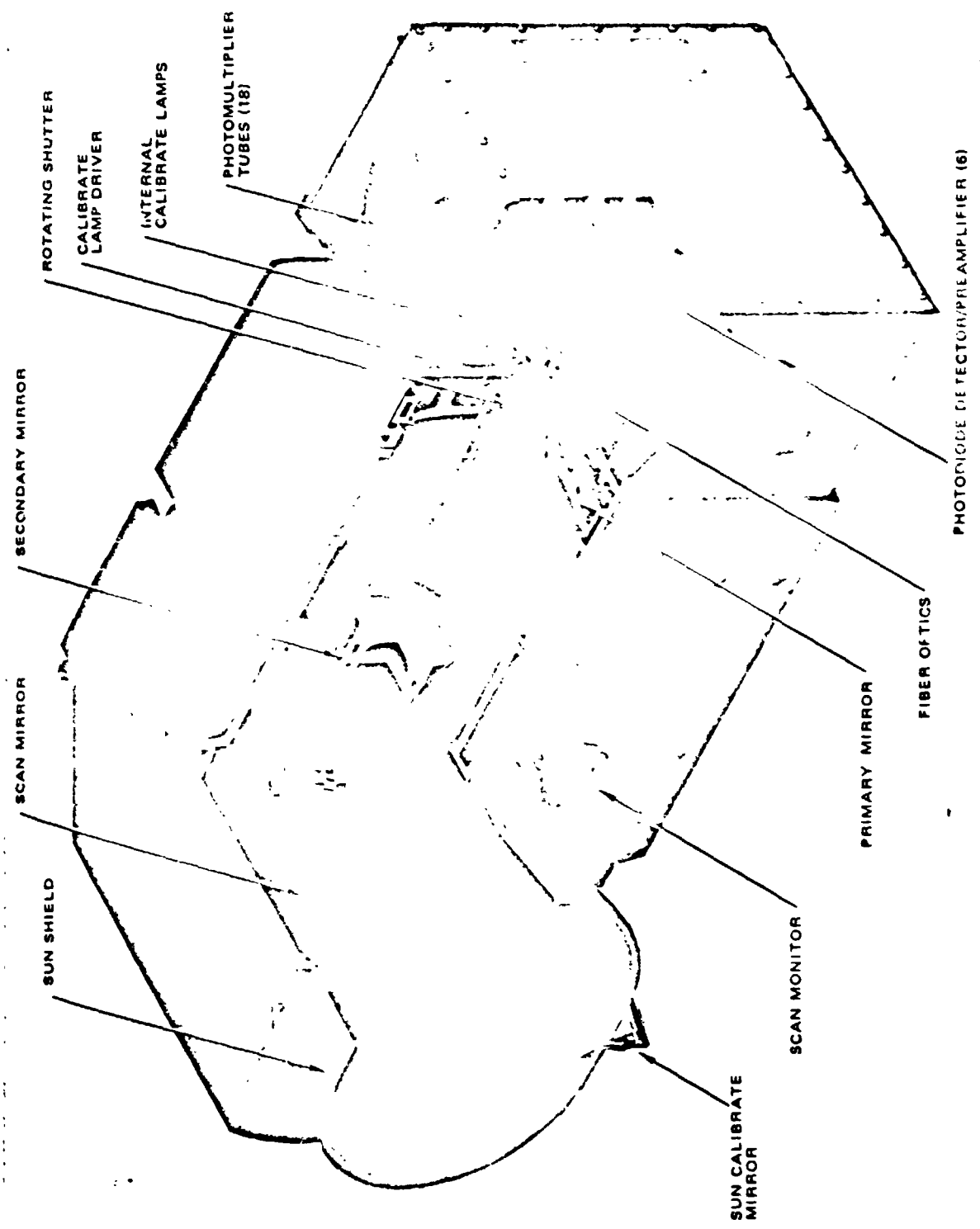
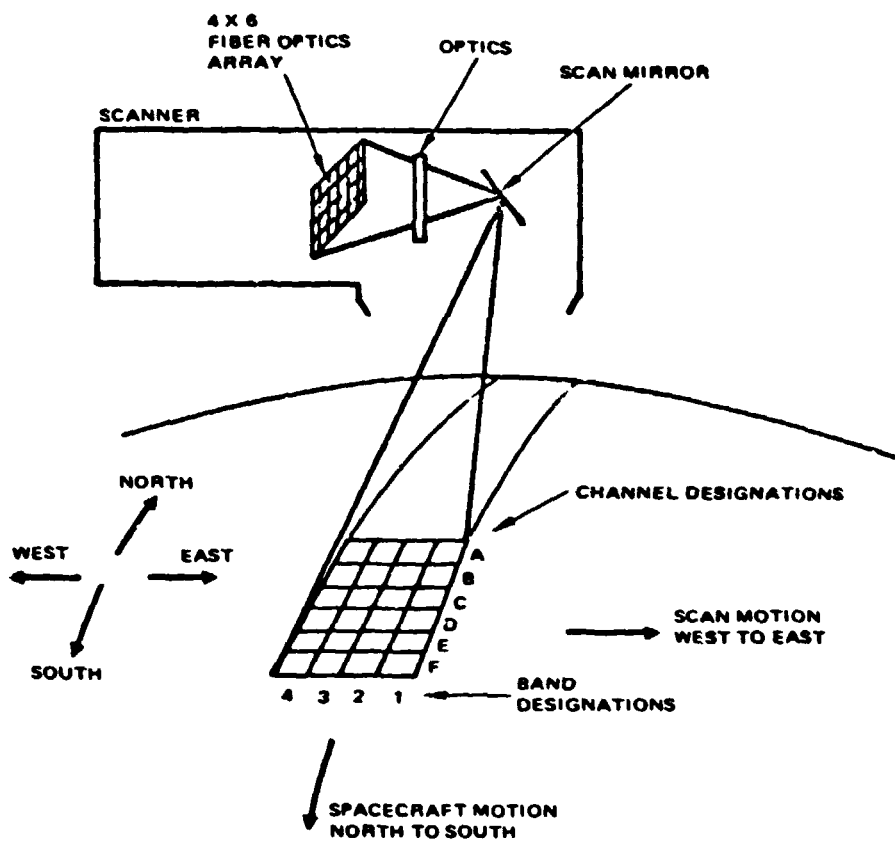


Figure 1-6. Scanner Isometric View



20419-8(U)

Figure 1-7. Field Stop Pattern Projected on Earth's Surface

The continuously variable filter is so located on the shutter wheel to provide calibration signals during alternate retrace intervals. During the intervening periods, a dark area of the shutter wheel produces a black signal level.

Once in each orbit, a small, four-faceted mirror located below the scan mirror deflects a sample of direct sunlight across the optical fibers. The output appears as a 1 to 2 ms pulse on each scan line for about 9 seconds of data. This provides the primary in-orbit calibration source by which the output level of the calibration lamps may be monitored.

Each video channel from the scanner is sampled and commutated once every 10 microseconds and multiplexed into a pulse amplitude modulation (PAM) stream. The commutated samples of video are then transferred to the analog-to-digital converter either for direct (linear) encoding or through a signal compression amplifier prior to conversion to digital form. The compression amplifier compresses the higher light levels and expands the lower levels to more nearly match the quantization noise to the photomultiplier detector noise. Photomultipliers have noise levels which limit system signal-to-noise performance at high light levels, but for low light levels, quantization noise becomes the limiting factor. Thus, the compression amplifier provides better signal-to-noise performance at low light levels.

Noise for the channels of band 4 is established by the equivalent load resistor noise and is best matched by the linear quantization. For these six channels, the signal compression path is bypassed. The different modes available by band are shown in Table 1-3.

The scan monitor pulse marking start of forward scan occurs during a time when the multiplexer is transmitting a 6 bit word pattern which is termed the data preamble. The arrival of this scan monitor pulse is marked by the inversion of the next word from the pattern of a preamble code. A minor frame sync code then follows, and the multiplexer commutator is reset so that channel A of band 1 is always sampled first and the other channels follow in a standard commutation pattern. This standard commutation pattern is actually preempted during the first sampling cycle so that spacecraft time signals may be inserted in lieu of image data. Resetting the sampling frame with the scan monitor makes the start of sampling completely angle dependent and, therefore, immune to small timing variations that could arise from the scan mechanism.

TABLE 1-3. MSS MODES BY BAND

Scanner Gain, Modes	Multiplexer Modes	
	Linear, Bands	Compression, Bands
High gain	1, 2	1, 2
Low gain	1, 2, 3, 4	1, 2, 3

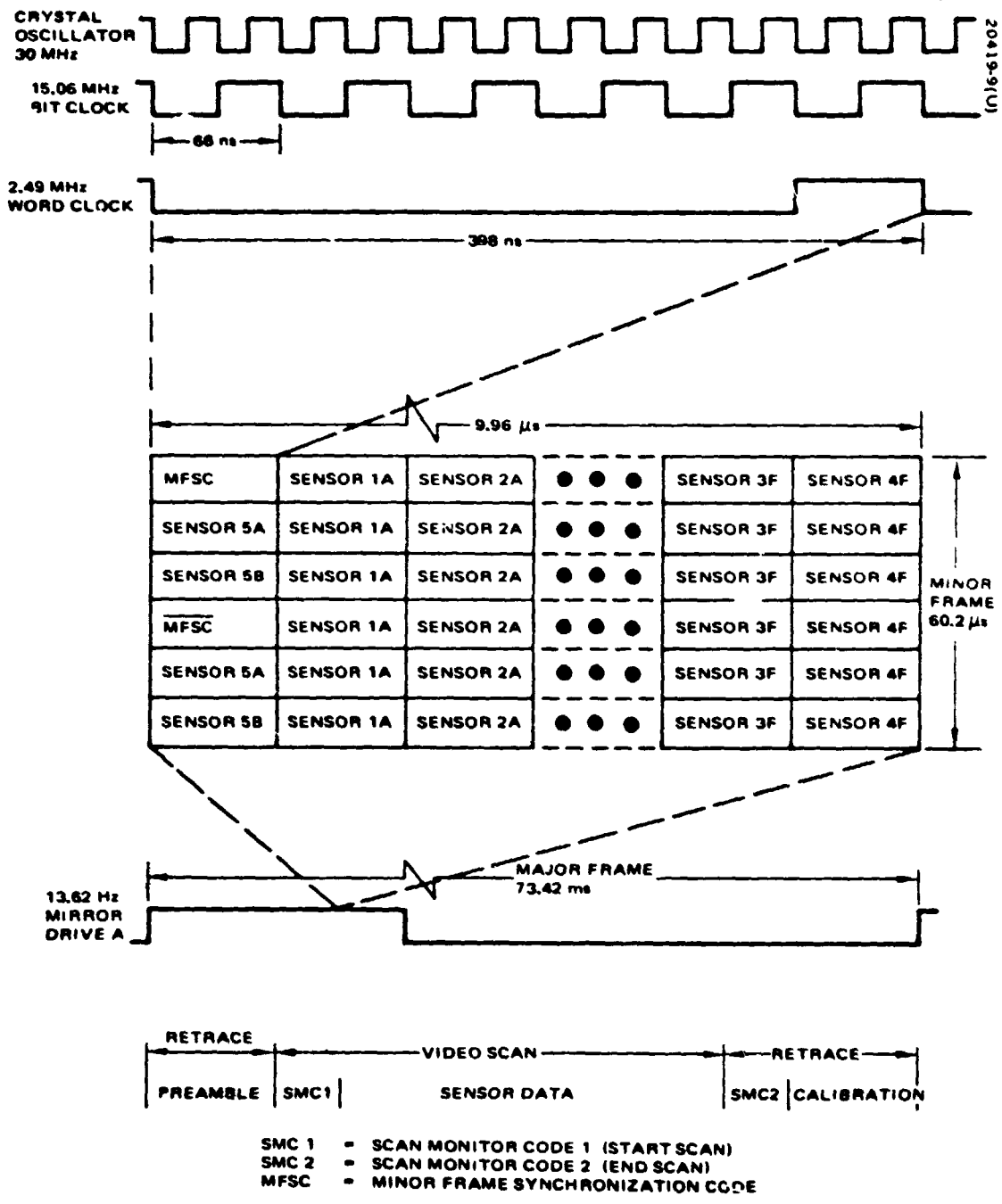


Figure 1-8. Multiplexer Digital Format

The 13.62 Hz mirror drive signal is derived by the multiplexer from its master oscillator of approximately 30 MHz. Word and bit rate are derived from internal division of the 13.62 Hz scan cycle and are maintained uniformly from scan to scan. Bit and word synchronization are maintained continuously by the demultiplexer. Only the line start and minor frame synchronization need be acquired in each scan and this is facilitated by having the word synchronization information. The channels are multiplexed into a 15 Mbps stream which is sent along with a bit clock to the spacecraft recorders and transmitters. An illustration of the multiplexer digital format is shown in Figure 1-8.

1.3.2 Receiving Site Equipment

A pictorial diagram of the receiving site equipment is shown in Figure 1-9. The ground receiver accepts signals from the spacecraft transmitter and supplies demodulated baseband and timing data to the other subsystems at the receiving site.

The demultiplexer receives the demodulated bit stream along with a bit clock. At the beginning of an orbital pass, the demultiplexers progress through an acquisition sequence to obtain word synchronization and then to a routine in which the minor frame code is acquired for every scan line. The 24 channels are decommutated and presented in binary form for tape recording on an in-line, 28 track tape recorder/reader. Each of the 24 lines scanned in the four spectral bands of Mission A is assigned a separate track.

A status monitor gives an oscilloscope analog representation of the video sweeps corresponding to the original analog scanner outputs in the spacecraft and permits the operator to verify that each channel is functioning from the scanner through the demultiplexer.

1.3.3 Test Equipment

1.3.3.1 Ground Processing Test Equipment

A pictorial diagram of the ground processing test equipment used to evaluate the MSS system is shown in Figure 1-10. The ground processing equipment input is reels of tape delivered from the test site (spacecraft integrator or Hughes). The tapes are read on a tape recorder that is identical with the one at the test site. The outputs are connected directly to the digital processor for film reproduction. Each channel is clocked out of the tape recorder with line start and finish information sufficient to permit independent reconstruction. This makes it possible to select only the six tracks pertaining to one spectral band and to operate on these independently. However, spacecraft time code reconstruction requires access to all channels

The processing circuits are designed to serialize data for six lines imaged in each band during a scan and present four composite spectral bands

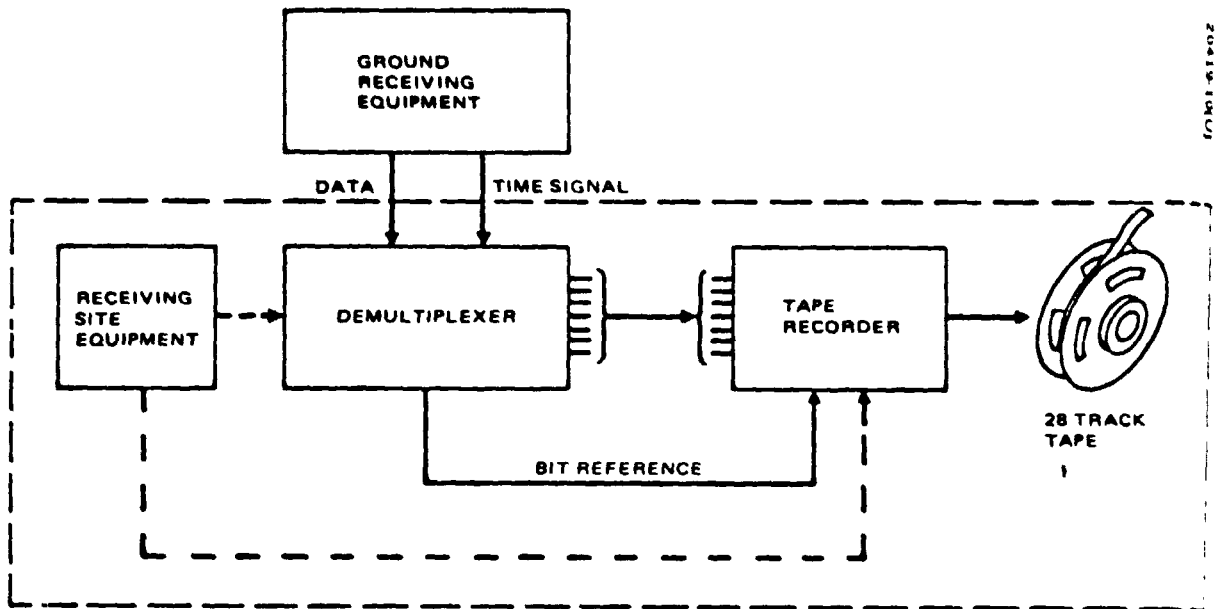


Figure 1-9. Receiving Site

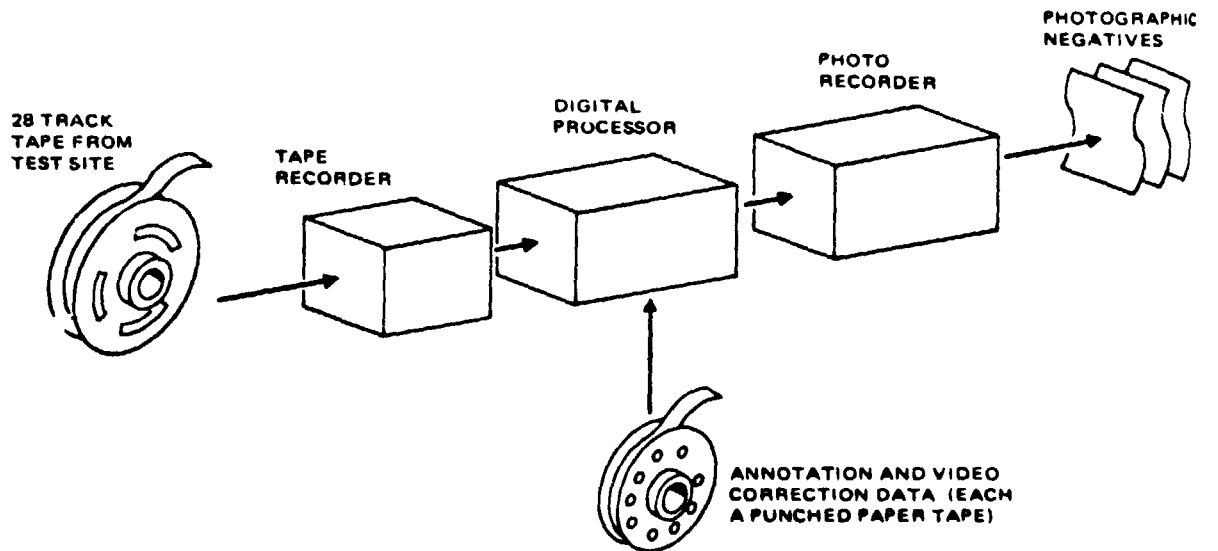


Figure 1-10. Ground Processing Test Equipment

to the photorecorder. The processing circuit also restores the time base which could become distorted by the tape recorders.

Images of scenes in all four spectral bands are reproduced in one operation of a precision drum photorecorder on one film transparency 16.5 by 24 inches. Each spectral image is 7.3 inches square and represents a square of ground 100 n.mi. on a side. Annotation data, geographic ticks, and a photographic gray scale are reproduced with each spectral frame making an overall 8 by 9 inch rectangle.

1.3.3.2 Test Equipment for Flight Subsystem Units

There are two different types of test equipment which were used for checking the scanner and multiplexer together or singly. Equipment for testing the scanner and multiplexer is assembled in a group called bench test equipment (BTE). This equipment is used for all formal testing of the assembled scanner and for the scanner/multiplexer combined test (e.g., subsystem environmental qualification and acceptance tests).

A slightly different set of testing functions is required after delivery to the spacecraft integrator. An assembly of test components called the spacecraft test equipment (STE) is used for these tests.

1.3.3.3 Test Equipment for Receiving Site Equipment

Equipment is mounted permanently with the demultiplexer and tape recorder at the receiving site. This equipment consists of a test set which allows diagnostic testing and checkout of the operational equipment at any time during the mission.

1.4 SUMMARY OF SYSTEM PARAMETERS

Table 1-4 summarizes the MSS system design parameters.

TABLE 1-4. SUMMARY OF SYSTEM PARAMETERS

SPACECRAFT EQUIPMENT	
<u>Scanner</u>	
Telescope optics	9 inch Ritchey-Chrétien type with 3.5 inch secondary mirror, f/3.6
Scanning method	Flat mirror oscillating ± 2.9 degrees at 13.62 Hz
Scan duty cycle (forward trace)	31.5 ms of 73.42 ms cycle minimum
Instantaneous field of view	0.086 mr (includes fiber cladding)
Optical fiber core	2.8 milli-inches
Spectral band and detectors	0.5 to 0.6 microns, PMT 0.6 to 0.7 microns, PMT 0.7 to 0.8 microns, PMT 0.8 to 1.1 microns, SiPd
Focal length	32.5 inches
Number of lines scanned per scan per band	6
Limiting resolution from 496 n. mi.	100 feet
Operational resolution	225 feet
Sampling distance	184 feet
Video bandwidth (-3 dB)	42.3 kHz per channel
<u>Multiplexer</u>	
Number of channels	24
Quantization	6 bits
Quantization accuracy	With ± 30 mv at any quantum level
Processing modes	Linear and signal compression
Clock stability	$\pm 1 \times 10^{-4}$ /year

Table 1-4 (continued)

<u>Multiplexer (continued)</u>	
Output bit rate	15.06 x 10 ⁶ bps
Sampling rate (each channel)	100,418 samples/second
Crosstalk	> 40 dB rejection
RECEIVING SITE EQUIPMENT	
<u>Demultiplexer</u>	
Input bit rate	15.06 x 10 ⁶ bps
Output bit rate capability (25 channels)	602 x 10 ³ bps/channel
Output channels	25
Probability of not acquiring	1 in 10 ¹² for a bit error rate of 1 x 10 ⁵
Scan monitor beginning of line pulse misrate	1 per 1.7 x 10 ⁵ pictures
Scan monitor beginning of line pulse false alarm rate	1 per 3.06 x 10 ¹⁷ pictures
<u>Tape Recorder/Reader</u>	
Number of tracks	28 (sized for 32)
Number of speeds	7
Normal record/playback speed ratio	4:1
Record mode	Digital
Record/playback bit error rate	1 x 10 ⁶
Start time	< 8 seconds
Stop time	< 4 seconds

Table 1-4 (continued)

GROUND PROCESSING TEST EQUIPMENT	
<u>Digital Processor</u>	
Inputs	25 video tape channels, STADAN time code from tape channel, annotation and indexing paper tape, and video correction paper tape
Output	Video signals polarized for either negative or positive transparency
<u>Photo Recorder</u>	
Type	Mechanical facsimile
Format	Four spectral bands at 10^6 to 1 scale
Rate of reproduction	One-fourth record rate
Gray scale fidelity	$16 \sqrt{2}$ gray shades
Optical system	Two optic heads on a common carriage
Light source	Zirconium arc crater lamp
Drum speed	1225.8 rpm

2. MSS SPACECRAFT EQUIPMENT

2.1 SCANNER

A functional block diagram illustrating the major subassemblies comprising the scanner is shown in Figure 2-1.

2.1.1 Scan Mirror Assembly

2.1.1.1 Functional Description

An isometric view of the scan mirror assembly is shown in Figure 2-2. The scan mirror which causes the sweep across the 100 n. mi. swath need only scan half the angle of the full field of view because of the angle doubling effect that occurs at reflection. The mechanism has a nearly symmetrical scan pattern; i. e., the west to east forward scan and east to west retrace occur in practically equal time intervals, as shown in Figure 2-3.

The mirror is lightly suspended on flexure pivots, and its motion is reversed from scan to retrace and from retrace to scan by impacting bumper/dampers which are in contact with the mirror for the 4 ms (nominal) period shown as turnaround. The rest of the scan phase may be used for imaging and amount to approximately 43 percent of the total cycle. Between impacts, during the scan phase, the mirror drifts at a constant angular rate except for very mild rate changes caused by the restoring forces of the flexure pivots.

The system is comprised of a mirror, mounting structure, mirror pivot springs, two bumper/damper units, and a torque coil. Once in motion, the mirror scans back and forth between impact springs indefinitely if the system were lossless. In practice, the system loses energy from damping during impacts and from spacecraft motion. A magnetic torquer is included to restore these energy losses by applying a moment during the retrace interval. The torquing interval is controlled by appropriate feedback to compensate for variations in the energy dissipators.

The basic characteristics of mirror motion are described in Figure 2-4 by means of a one-dimensional analog and a phase-plane plot of the limit cycle motion. During the scan interval, the mirror moves at nearly constant velocity to the right until impact occurs. The bumper/damper causes a rate reversal to the left. During impact, the bumper dashpot generates damping forces

which prevent the mirror from recovering all of its initial rate amplitude. As the mirror retrace motion proceeds to the left, the torquer coil continues to accelerate the mirror in anticipation of the velocity loss during the coming impact at the start of scan. The arrival velocity at the latter impact is precisely that necessary to result in proper scan velocity after impact which is identical to the scan of the previous cycle.

Periodic torquing is physically accomplished by exciting the magnetic coil with a 13.62 Hz square wave pulse and terminating coil excitation when the mirror crosses a particular point (sensed with an optical switch) near the mid-scan point of the retrace interval.

Figure 2-5 illustrates mirror velocity, system mechanical energy, and applied torque for typical steady state limit cycle motion at 13.62 Hz.

2.1.1.2 Mechanical Design

The components that comprise the scan mirror assembly are shown in Figure 2-2, and described in the following paragraphs.

2.1.1.2.1 Mirror. The mirror is an ellipse with a major axis of 13.98 inches and is 1 inch thick. The front and back plates, along with integral connecting ribs, are formed by electric discharge machining from a solid beryllium billet. The front surface is electroless nickel plated to give a good optical finish and the rear receives the same plating for stress balancing. An enhanced silver coating (OCLI 6065001) is vacuum deposited on the front surface for uniform spectral response across the MSS spectral range. A protective coating is then applied to prevent tarnishing.

2.1.1.2.2 Flex Pivots. Two flexure pivots support the scan mirror with the smallest restoring torque that is compatible with stress requirements. Bendix cross-spring flexures with a diameter of 5/8 inch are used.

2.1.1.2.3 Support Structure. An aluminum structure supports the mirror assembly. This structure is bolted to an extended edge of the scanner telescope casting with dowel pins at the casting interface for precise alignment. Mirror to mounting surface alignment is held to 1.5 arcmin accuracy.

2.1.1.2.4 Bumper/Damper Units. Two bumpers with damping mechanisms act at each end of the mirror traversal to change the direction of rotation of the mirror. Figure 2-6 is a cutaway view of one unit. A bumper cup which is integral with the torquer armature is set into the mirror. Turn-around occurs as the front and back ends of the nylon clad cup strike the impact bars. The front surface impact of one cup occurs simultaneously with the rear surface impact of the cup at the other end and vice versa. In this way the turn-around force is a couple so that translation forces on the pivots are minimal. The impact bar is mounted to the support structure through a helical spring, and controlled damping is introduced to the system through a pair of silicon rubber mounts affixed to each impact bar (one of pair shown). These two dampers are placed in shear when the impact bar is displaced back and forth by impacts with the mirror.

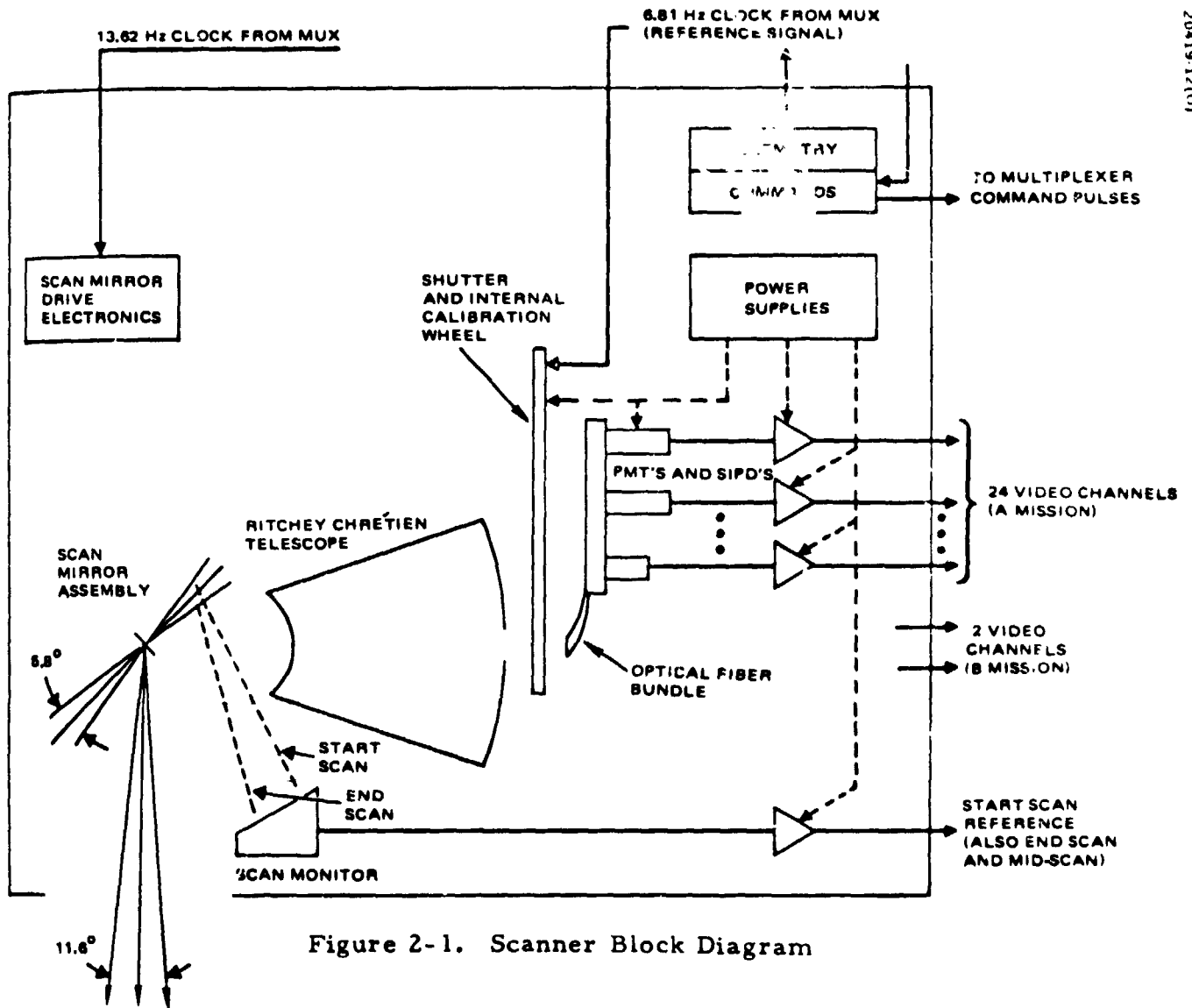


Figure 2-1. Scanner Block Diagram

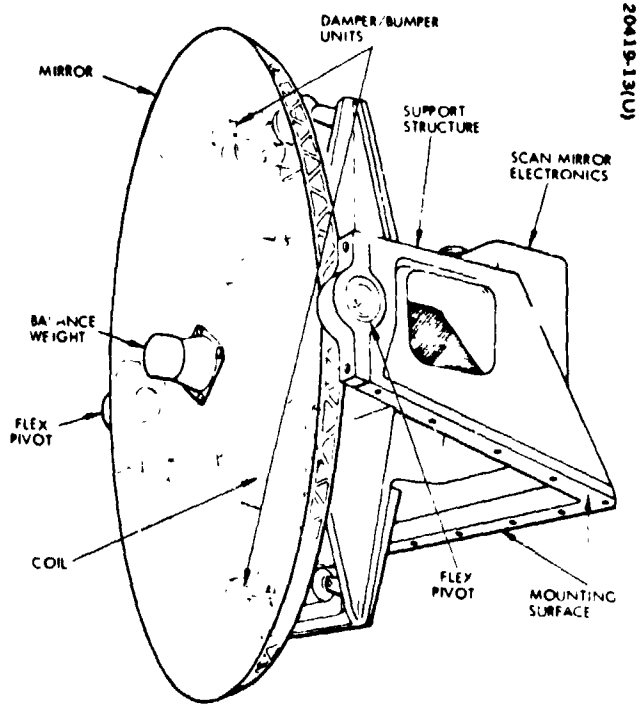


Figure 2-2. Scan Mirror Assembly

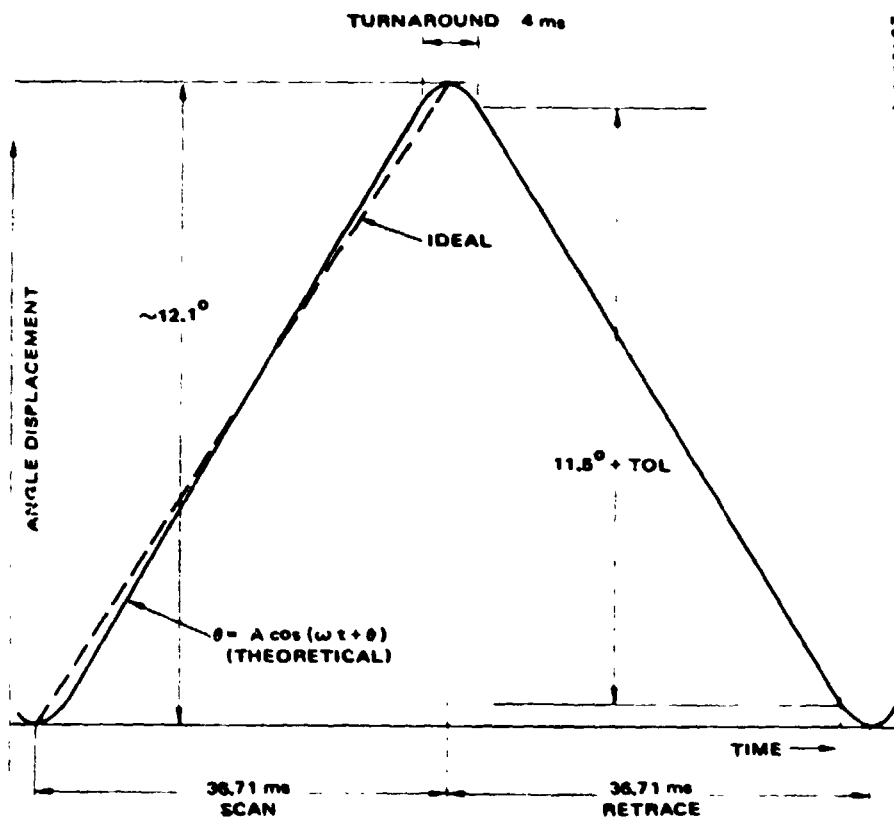


Figure 2-3. Angle Displacement Versus Time for Scan Mirror Assembly

BASIC CHARACTERISTICS OF MIRROR MOTION

- MIRROR UNDERGOES LIMIT CYCLE MOTION WITH IMPACTS PROVIDING MOMENTUM REVERSALS THAT GENERATE SCAN-RETRACE MOTION
- BUMPER SPRINGS ARE MOMENTUM SWITCHES DURING IMPACT
- BUMPER DASHPOTS ARE ENERGY SINKS DURING IMPACT
- MAGNETIC TORQUER IS ENERGY SOURCE DURING RETRACE

20419-15(U)

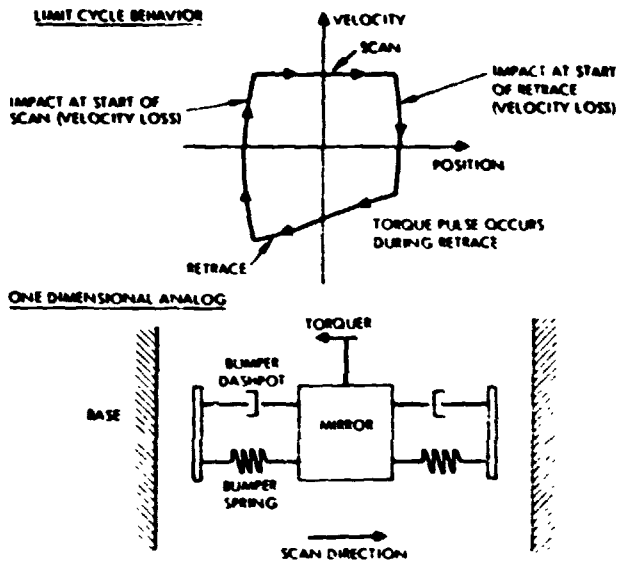


Figure 2-4. Basic Characteristics of Mirror Motion

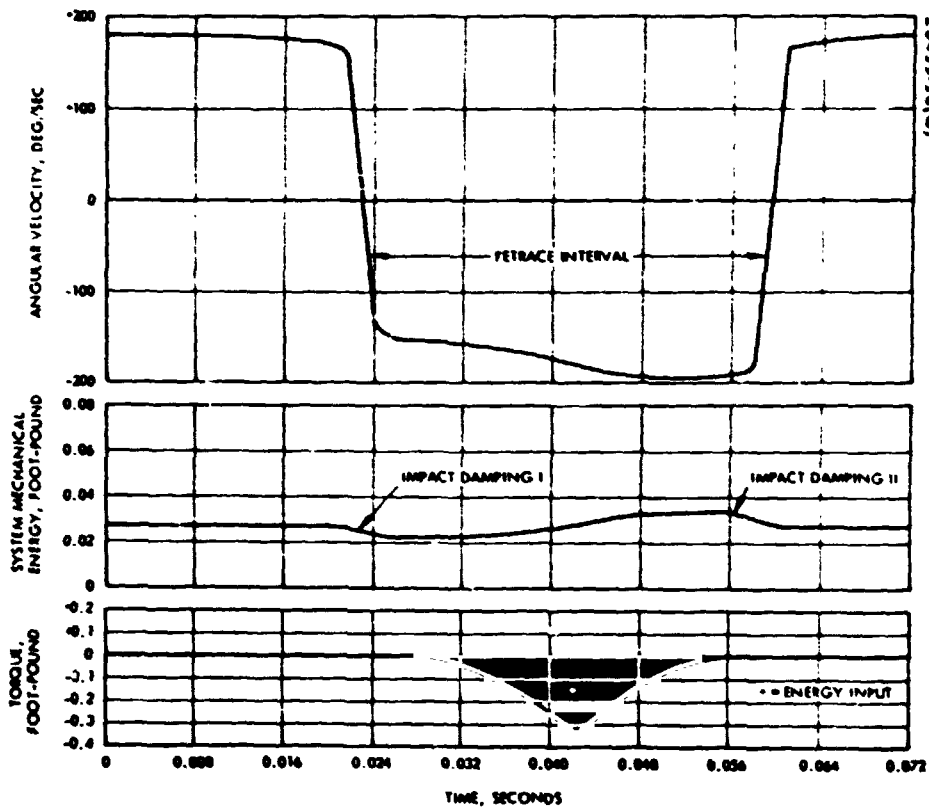
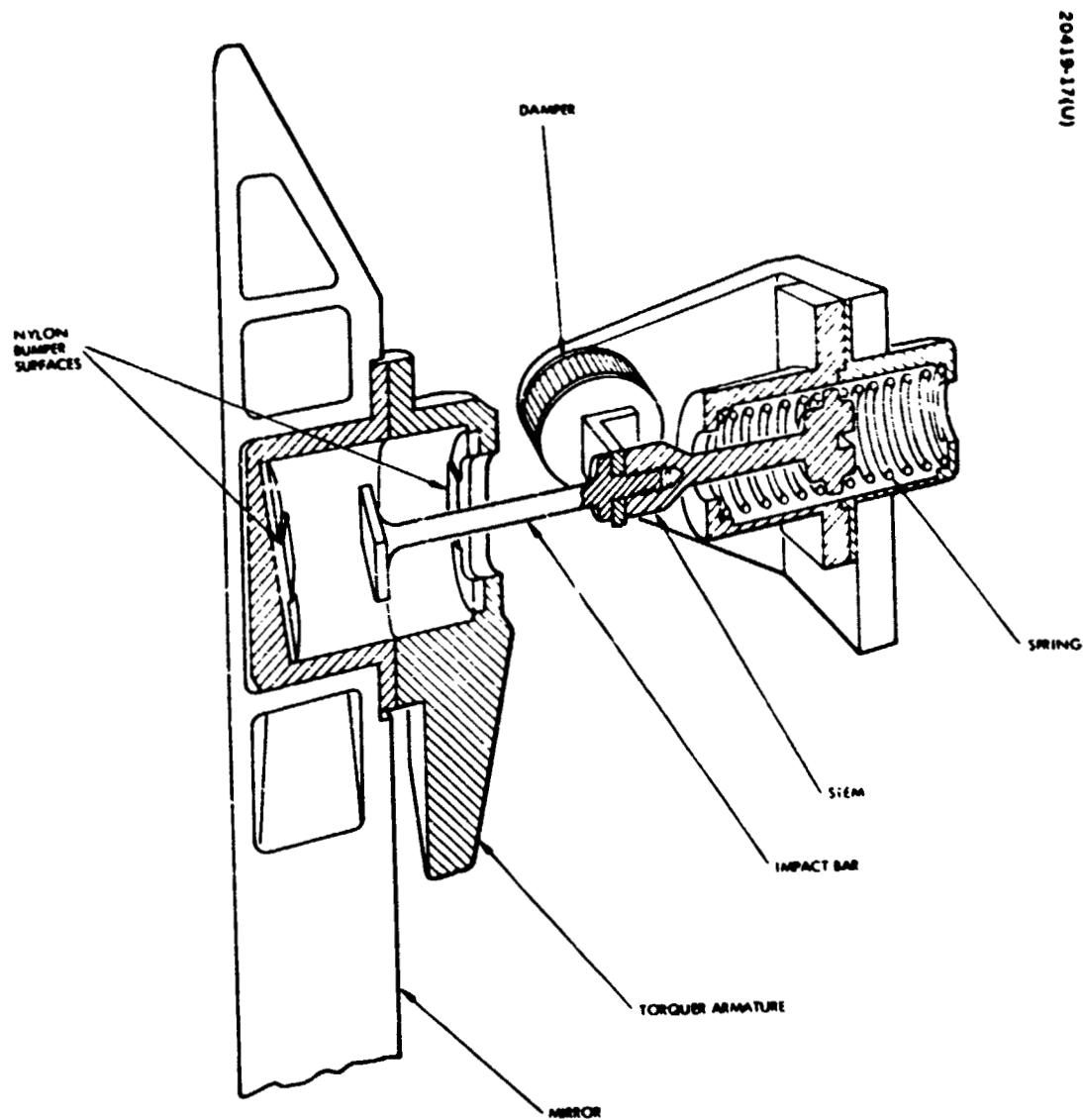


Figure 2-5. Scan Mirror Angular Velocity, Energy and Torque History (Drive Frequency 13.62 Hz)



20419-17(U)

Figure 2-6. Cutaway View Bumper/Damper Unit

2. 1. 1. 2. 5 Electromagnetic Drive Assembly. The electromagnetic drive assembly consists of a drive coil/core assembly mounted on the support structure and an armature mounted on the mirror. The core is manufactured from Allegheny-Ludlum No. 4750 magnetic iron around which a cc (1300 turns No. 24 AWG) is wound on a nylon bobbin. The armature is also manufactured from Allegheny-Ludlum No. 4750 magnetic iron and forms part of the bumper cup as shown in Figure 2-6.

2. 1. 1. 2. 6 Optical Switch. An optical switch consisting of tungsten filament lamps, silicon phototransistor detectors, and collimating optics is used for turning off the torquer at the mid-scan point. Light from the two bulbs passes through a defining slit, a beamsplitter, the two lenses, and an aperture, and is focused to a line approximately 0.3 inch long and 0.002 inch wide. The switching mirror, one-half of which is highly reflective and the other half absorbent, is placed at the focal point of this assembly. When the switching mirror is in position to reflect the focused beam, the beam is then reflected back through the lenses to the beamsplitter where it is reflected at 90 degrees and refocused on the detectors. Redundant lamps and detectors are used for reliability reasons.

2. 1. 1. 3 Scan Mirror Electronics

The scan mirror electronics provides power to the scan mirror drive coil of the scan mirror mechanism with a synchronized voltage pulse of fixed amplitude and variable duration to maintain stable scan mirror performance. These electronics form the interface between the scanner and the scan mirror assembly.

Through the scanner, the scan mirror electronics receives:

- 1) unregulated spacecraft power, with redundant wire paths,
- 2) system on/off command,
- 3) scan mirror normal/inhibit command,
- 4) power line 1 or 2 select command, and
- 5) scan mirror drive signal (clock).

In addition, regulated telemetry power is received from the scanner for thermistor bias in the temperature sensing networks. Scan mirror position information is provided from the optical switch on the scan mirror mechanism.

Telemetry outputs are:

- 1) power line 1 confirm,
- 2) power line 2 confirm,
- 3) line select confirm,
- 4) system on confirm,
- 5) scan mirror normal confirm,
- 6) regulator output voltage,
- 7) regulator temperature,
- 8) drive electronics temperature,
- 9) coil temperature,
- 10) mounting frame temperature at flexural pivot, and
- 11) detected scan mirror drive signal.

Outputs 1 through 5 are digital; outputs 6 through 11 are analog.

The scan mirror drive electronics and their functions are shown schematically in Figures 2-7 and 2-8, respectively. Electronic components and subassemblies external to the scan mirror electronics are also shown in Figure 2-7.

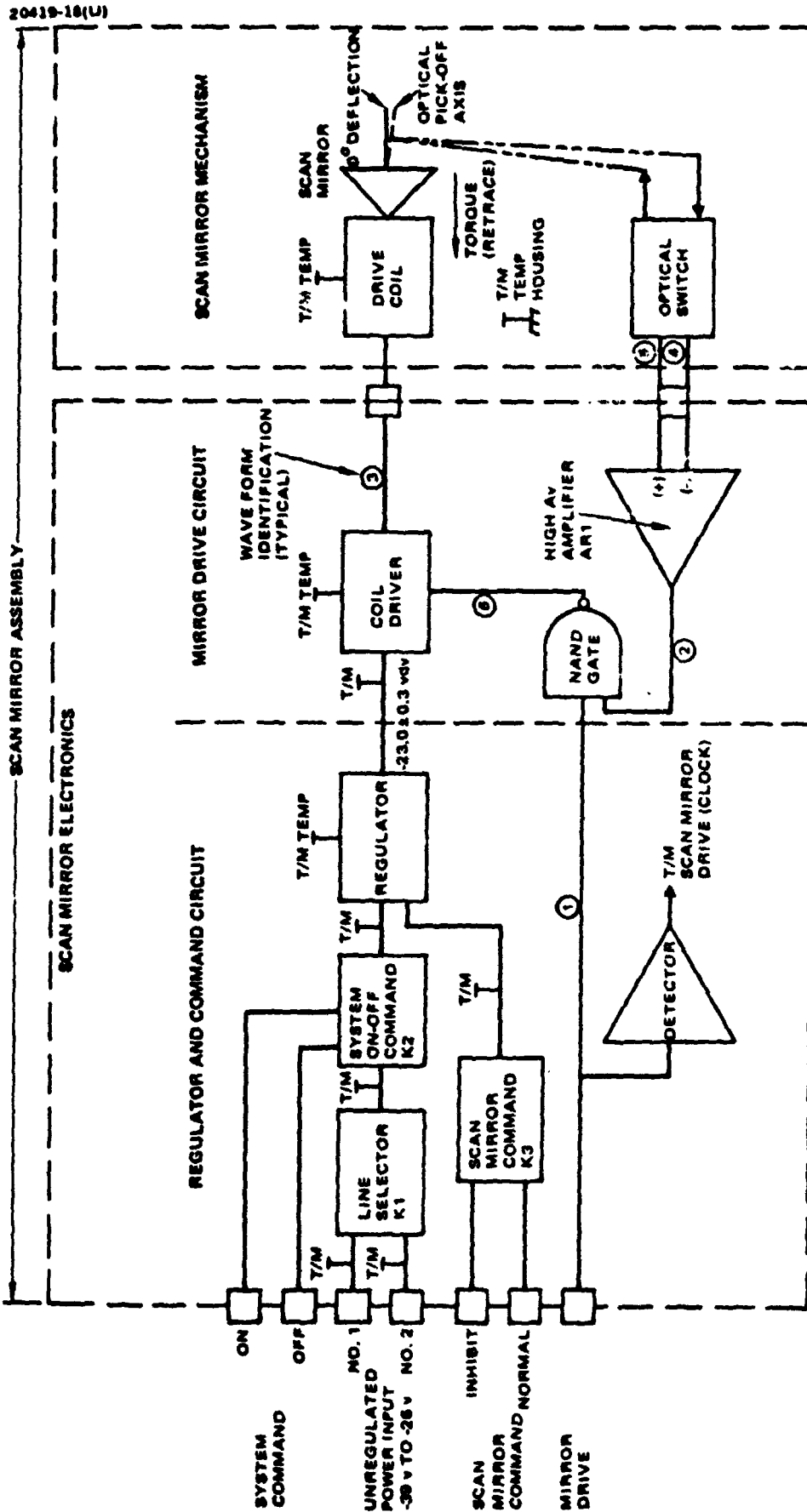


Figure 2-7. Scan Mirror Assembly Functional Block Diagram

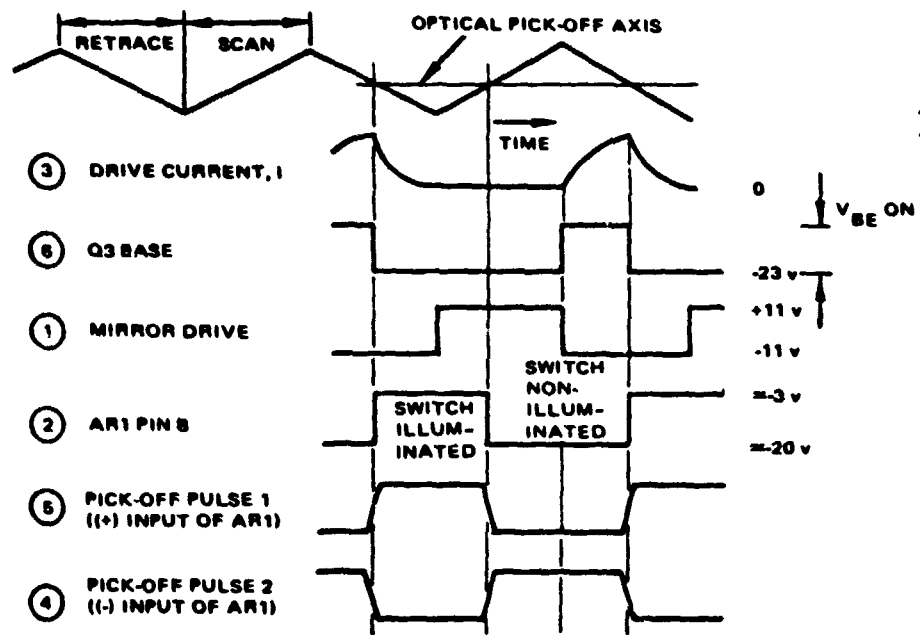


Figure 2-8. Scan Mirror Assembly Waveforms

The linear series regulator has a matched differential transistor pair, operated with one input referenced to a temperature-compensated zener diode, and the other input sampling the regulated output voltage remotely at the mirror coil. The error is sensed, amplified, and fed to a Darlington pair, which in turn drives the series pass stage.

2.1.2 Optics

The basic optical elements of the scanner described here are the telescope and the transfer optics used to transmit the image spot intensities to the appropriate detectors. These form the primary image path through the scanner. Optical elements are used in other parts of the scanner such as optical pickoff devices; however, these are described as part of the particular devices. The primary optical path is shown in Figure 2-9.

2.1.2.1 Telescope

Although the actual focused area occupied by field stops intercepts less than 1 mr, a larger focused area is needed to assure good performance over combinations of temperature, misalignments, and materials changes. The Ritchey Chrétien design was selected for the superior off-axis quality. As shown in Figure 2-10, the 90 percent blur circle diameter does not reach 50 percent of the instantaneous field of view until the off-axis angle exceeds 0.25 degree (4.4 mr). The reflecting pair, shown in Figure 2-9, has a focal length of 32.50 inches and an $f/\#$ of 3.6. The reflectors are made of fused silica and the supporting rods are Invar (see Figure 2-11).

2.1.2.2 Fiber Optics Assembly

Twenty-four fibers are arranged in the focal plane in the configuration shown in Figure 2-12. As the scan mirror sweeps across this matrix as indicated, six lines are simultaneously imaged in each of the first four spectral bands. These fibers carry the energy from the focal plane through a supporting tube to the aluminum base plate where the 24 fibers branch out in channels and are directed to 24 individual detectors. The fibers are epoxy bonded at each end and throughout their length. The square fibers are 0.0028 inch on a side, including the inner glass core of 0.0024 inch and exterior cladding.

Transfer lenses collimate the energy at the output of the fibers of bands 1 to 3 to within ± 5 degrees. The energy is then efficiently transferred to the photomultiplier tubes by means of enhancement prisms. For band 4, the transfer lenses image the optical fibers onto the detectors with magnification of approximately four. Between each lens and detector assembly is an appropriate spectral filter.

The transfer lens is a plano-convex lens of high index glass with an antireflective coating to minimize transmission loss. Optical coupling between each lens and fiber is accomplished with Dow Corning 93-500.

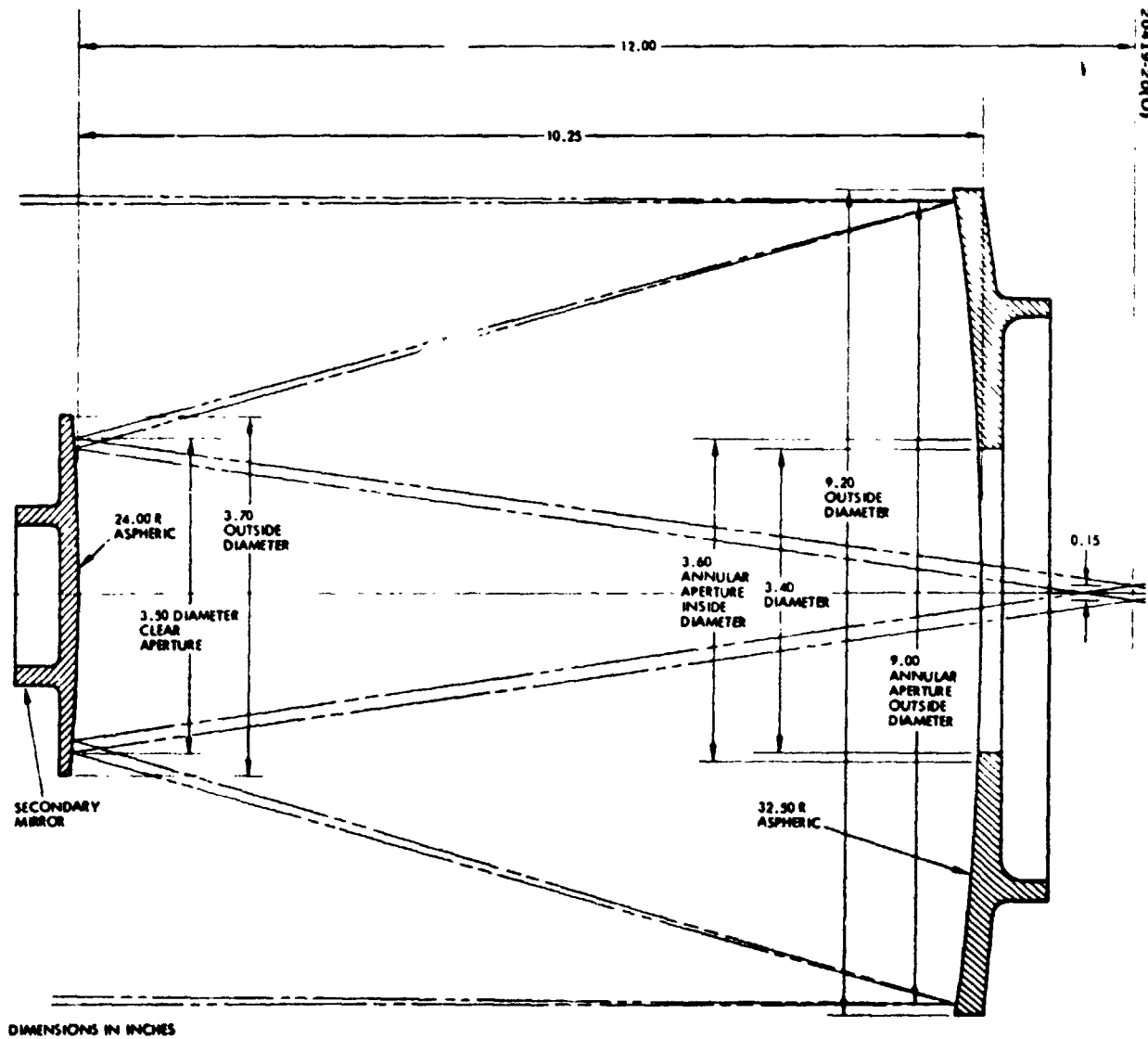


Figure 2-9. Telescope Optics Design

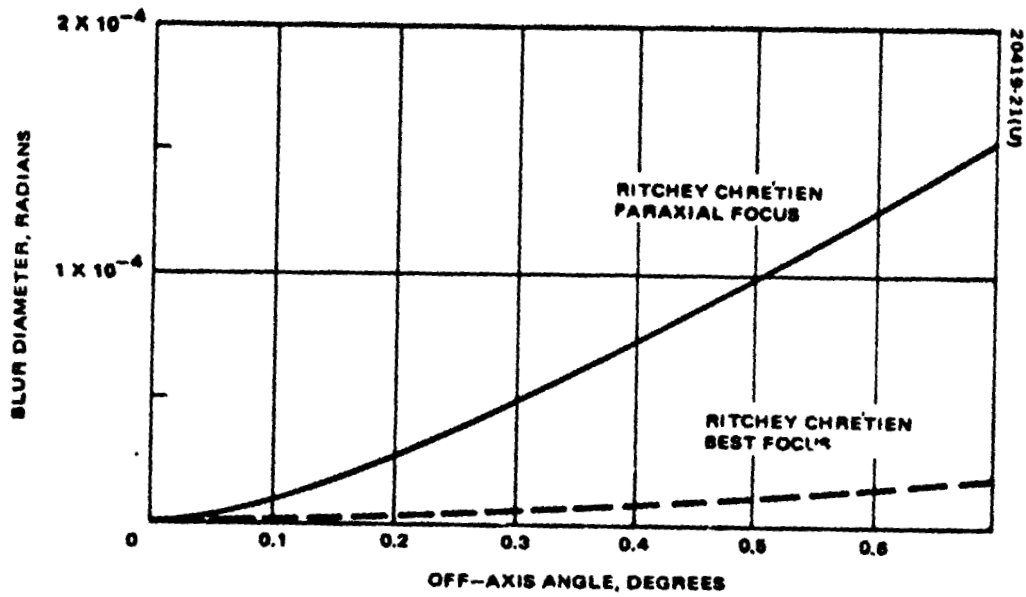


Figure 2-10. Off-Axis Image Blur for Ritchey Chrétien Optical System

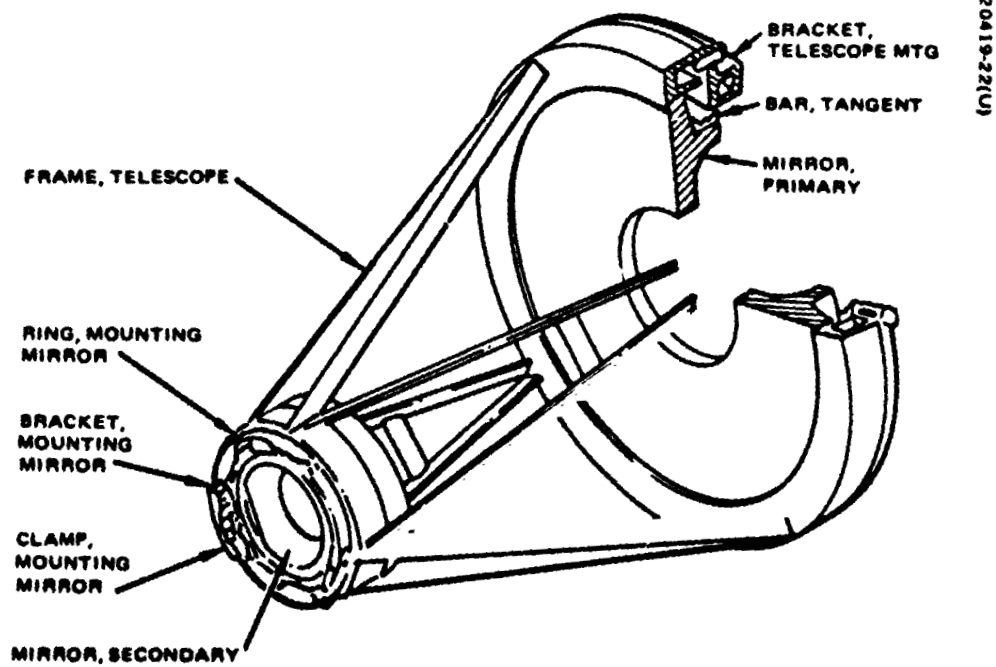


Figure 2-11. Telescope Assembly

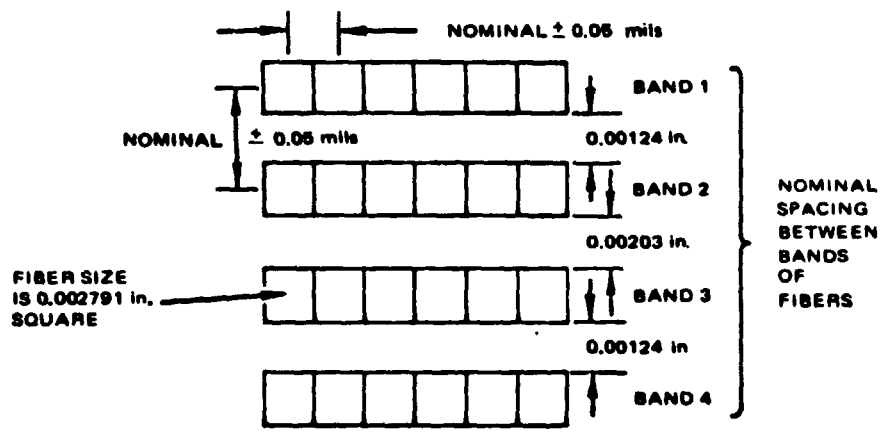


Figure 2-12. Channels at Field Stop Viewed From Object Side

m
in
2.

in
sp
4

in
el
in
so
go
pe
m

a
to
F
o
r

l
n
v
le

i:
a
p
i:
2

r
d
n

The lens and filter are cemented into a mounting block which is then moved about to position the optical center line relative to a set of index holes in the fiber optics plate. These holes also locate the detector assembly.

2. 1. 3 Photomultiplier Tube (PMT) Detectors

PMT detectors are used for bands 1 through 3. The PMT subassembly includes the enhancement prism, the tube itself, divider resistor chain, and space for the preamplifier. Relative spectral response for bands 1 through 4 is shown in Figure 2-13.

2. 1. 3. 1 Preamplifiers and Buffers

The PMT preamplifier is a current mode amplifier with a differential input stage, followed by an integrated operational amplifier. An input field effect transistor (FET) matched pair provides low input bias current and low input offset voltage which appears with unity gain at the output due to the high source impedance and current mode configuration. High loop gain provides good gain stability and output impedance. Inclusion of a Butterworth three-pole filter within the preamplifier decouples the loop from the output line, making the preamplifier insensitive to load capacitance.

The PMT buffers and 15 volt regulators for each band are packaged on a separate printed circuit card assembly. The integrated circuit (IC) regulators use discrete component transistors to handle the 60 ma load current. Foldback current limiting is provided. The individual channel buffers consist of two cascaded IC operational amplifiers, both inverting, to provide the required overall noninverting gain of nominally 8.

Gain may be set within a range of ± 3 dB before launch, and in bands 1 and 2 is commandable to the high gain mode which provides an additional nominal gain increase of a factor of three. Output offset is adjustable ± 0.3 volt in 10 mv steps by resistor selection. This provides a resolution slightly less than the least significant bit.

2. 1. 3. 2 Packaging

The PMT packaging arrangement is shown in Figure 2-14. The tube is potted into an aluminum cylinder which provides shielding, light baffling, and mechanical support. An aluminum bulkhead separates the tube from the preamplifier area. The enhancement prism is cemented to the tube face and is so located that incoming radiation makes two passes at the photocathode.

2. 1. 4 Silicon Photodiode Detectors

Silicon photodiode detectors are used in band 4. A curve showing relative response for band 4 is given in Figure 2-13. With this silicon photodiode, the equivalent load resistance of the current source establishes the noise level.

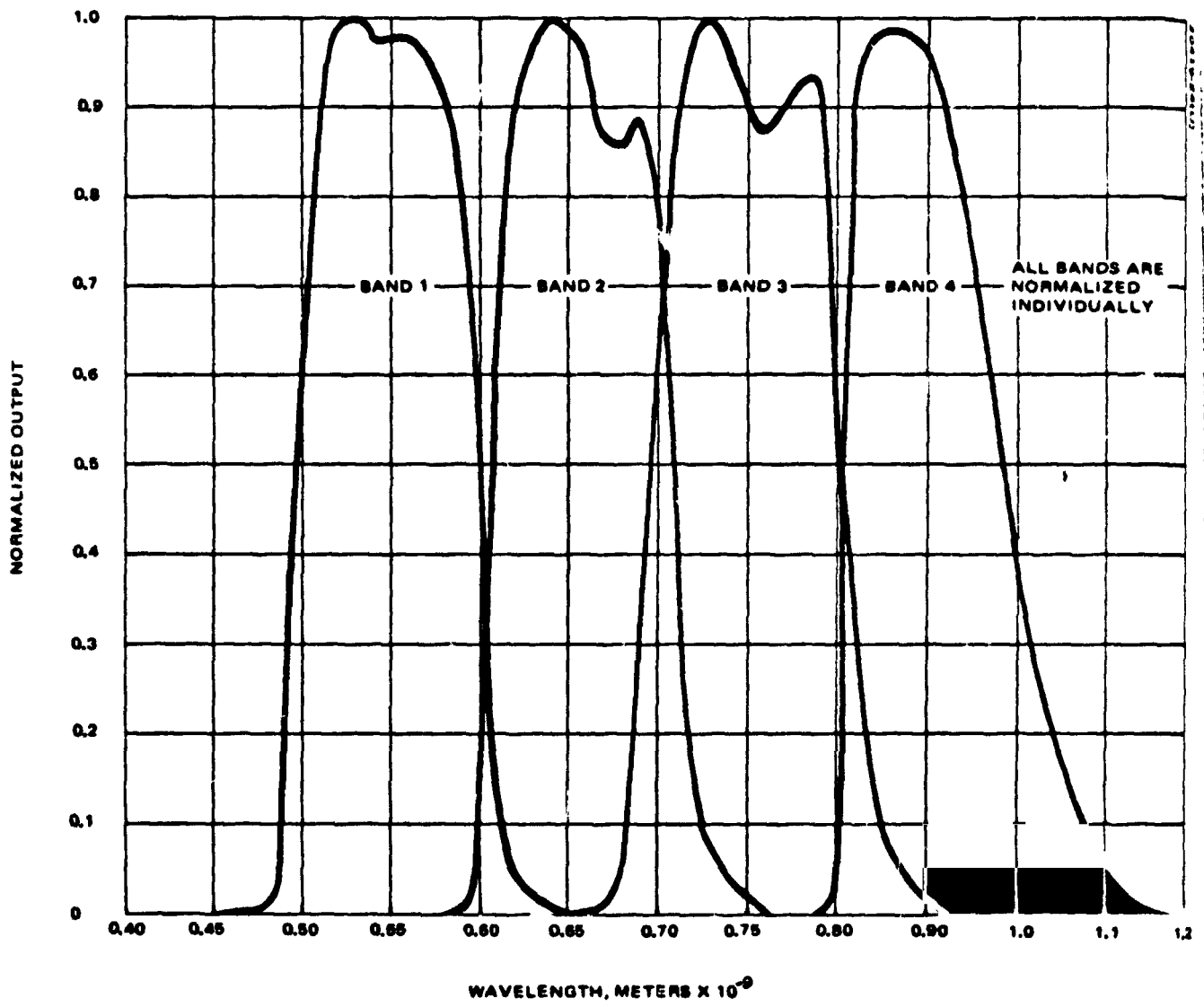


Figure 2-13. Relative Spectral Response

20419-25(1)

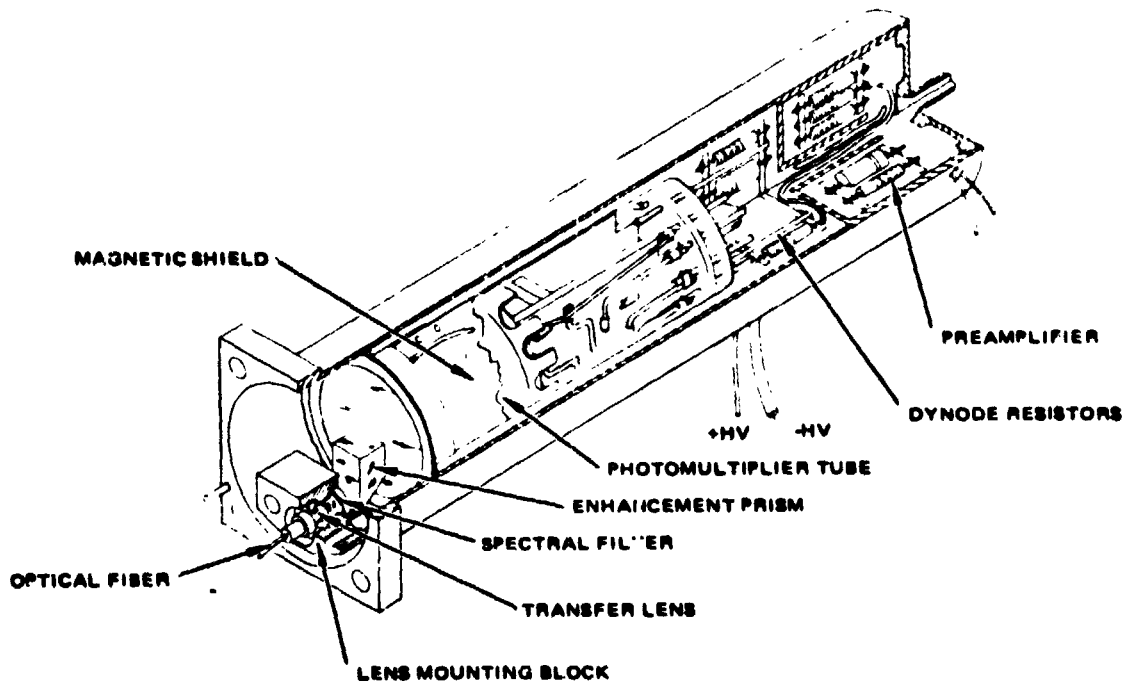


Figure 2-14. MSS Photomultiplier Tube Detector Assembly

2. 1. 4. 1 Preamplifier

The preamplifier is a current mode amplifier with a single ended FET input stage. The biased operation of the diode makes it necessary to use a blocking capacitor to restore the dc reference level by means of a no-light clamping signal. It is important that input capacitance be kept low to minimize the output noise due to the input FET. For this reason, a source follower input stage has been designed with careful attention to layout. The first stage has unity voltage gain, and a low noise bipolar stage run at 100 microamperes is used for the second stage.

2. 1. 4. 2 Packaging

The packaging arrangement of the photodiode subassembly is shown in Figure 2-15. Mounting and alignment of the detector employs an eccentric nylon sleeve into which the can containing the diode is lightly pressed. The orientation and amount of the eccentricity are selected to center the sensitive area, to place it at the focus of the transfer optics. Potting over the lead end of the can and surroundings retain the position.

2. 1. 5 Rotating Shutter and Calibration Components

A large rotating shutter performs several reference and calibration functions during the scan retrace intervals. Some of the components used for internal calibration are mounted on the shutter wheel at angular positions chosen to provide proper timing for calibration signals. Descriptions of these components have been collected in this section because of their proximity and interdependence.

2. 1. 5. 1 Shutter Wheel

The shutter rotates (6.81 Hz) once for every two scan mirror cycles and has annular slits which disclose the focused region of the optics system during the two corresponding scan intervals. Alternative targets are substituted during the time the focused region is closed to the optics. These targets include a variable density wedge with a mirror to direct a continuously diminishing light level into fibers for calibration purposes. Figure 2-16 shows the shutter wheel with all of the cutouts and special targets indicated.

2. 1. 5. 2 Shutter Wheel Control Circuits

The shutter wheel is maintained in synchronism with the scan cycle by means of a phase locked loop which compares the output of an optical monitor on the shutter with a signal from the scan monitor which senses the start of scan. The timing relationship for the shutter wheel in terms of sun mirror reference is shown in Figure 2-17. The time origin is shown as the scan monitor pulse which controls the shutter wheel; however, this is a convenience only, since the oscillator establishes the time frame and the scan monitor pulse follows with some line-to-line jitter. Figure 2-18 is a block diagram of the phase locked loop which drives the shutter wheel in phase with the scan mirror.

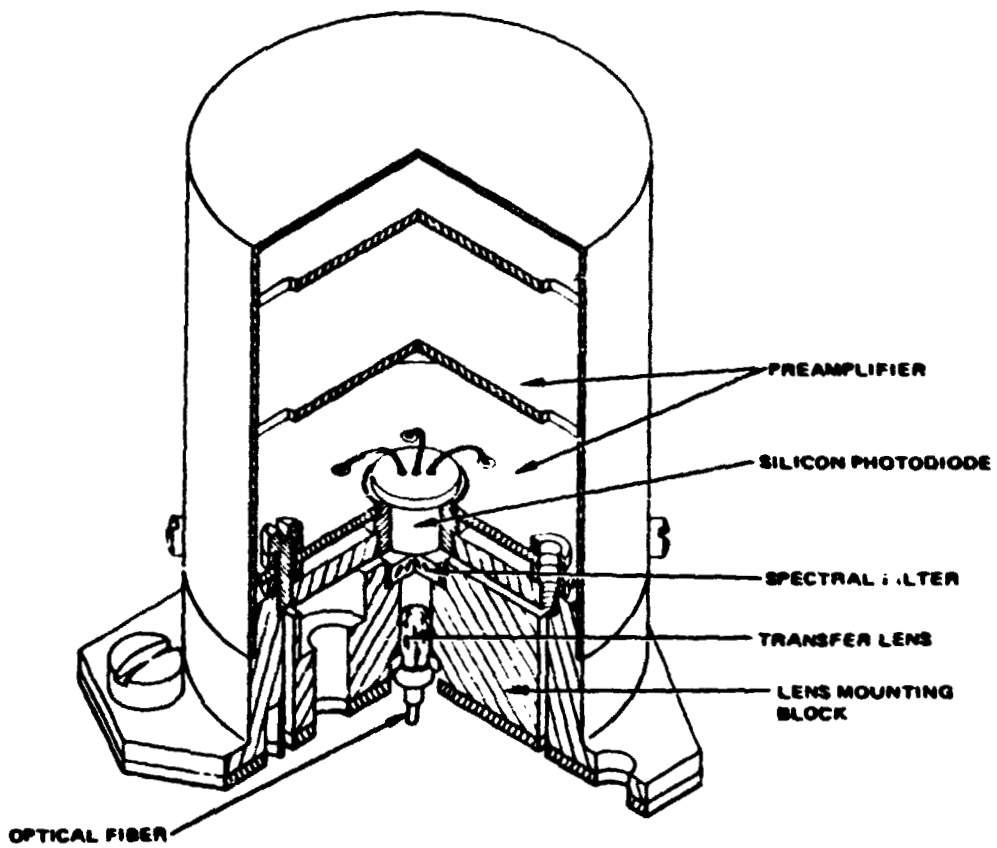


Figure 2-15. Silicon Photodiode Detector Assembly

20419-26(U)

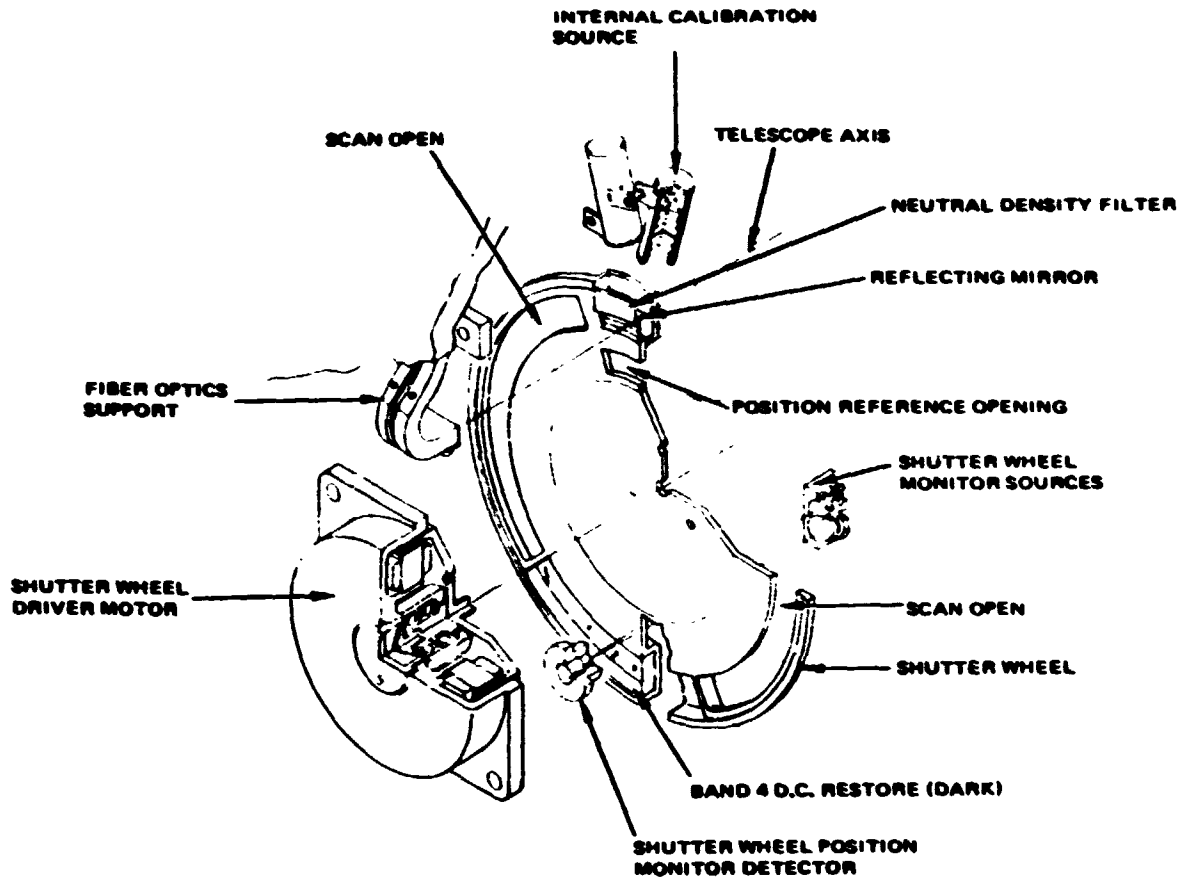


Figure 2-16. Shutter Wheel Assembly

- NOTES 1) PER SCAN MUX - 18432.0 WORDS DEMUX - 7372.8 WORDS
 2) GRAY WEDGE ALTERNATES WITH CLOSED SHUTTER ON SUCCESSIVE SCANS
 3) MIDSCAN CODE BY COMMAND ONLY

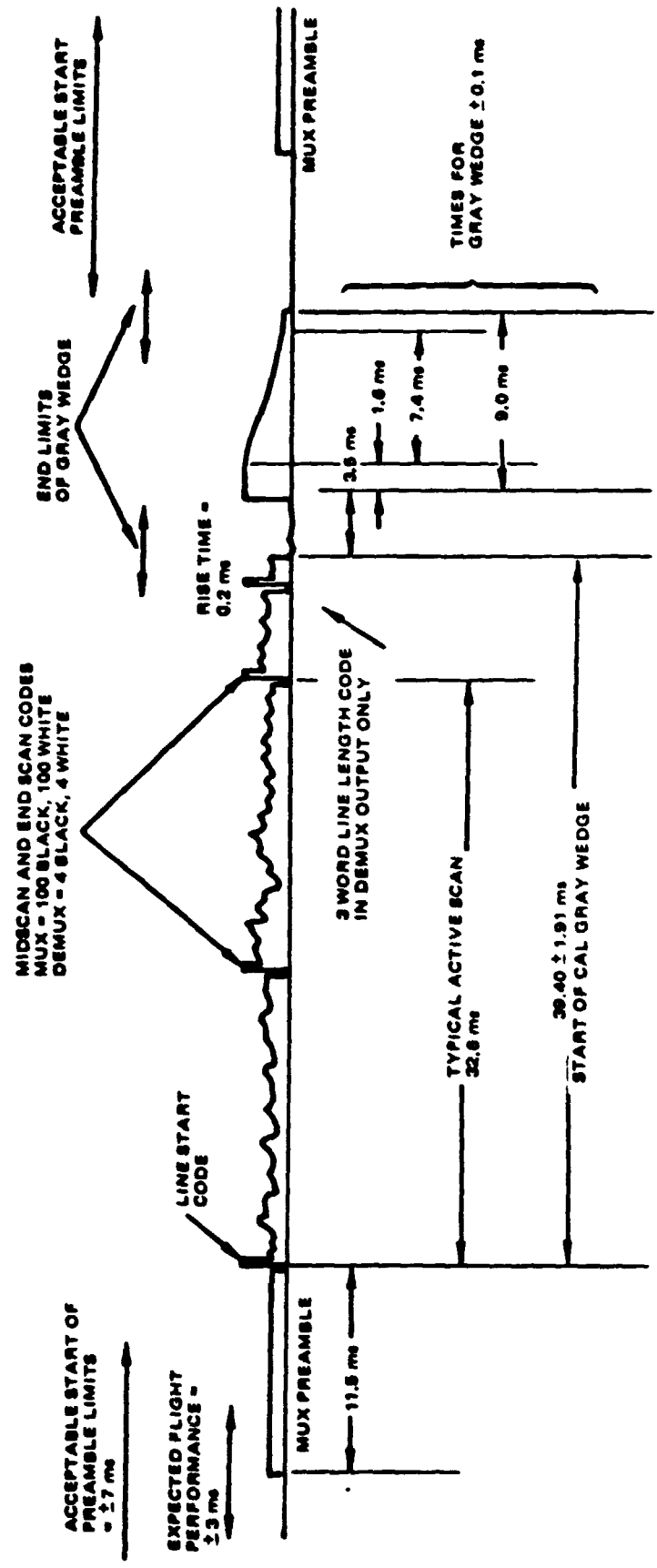


Figure 2-17. MSS Video Data Timing Format

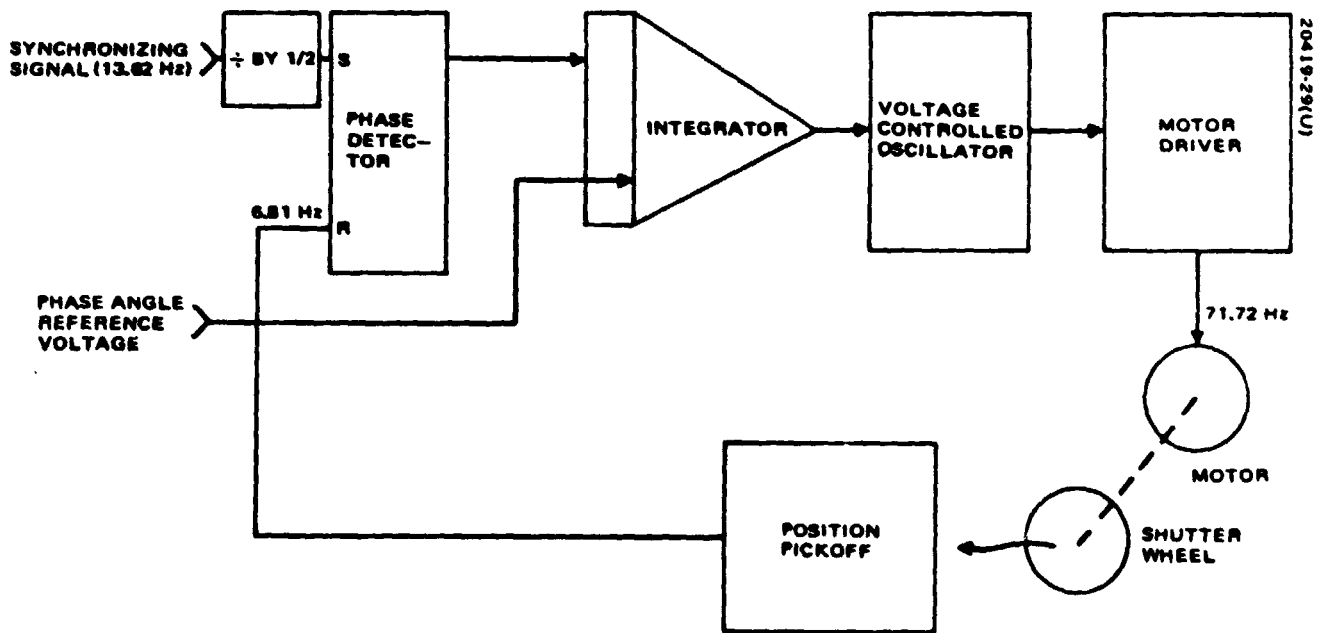


Figure 2-18. Phase Lock Loop Block Diagram

Should the scan monitor fail, an alternate signal is injected onto the reference signal line by the multiplexer. This signal has been incorporated in the multiplexer to initiate sampling and maintain shutter synchronization in the event of such a failure. Both optical pickoffs, which are compared in the phase locked loop, employ dual light sources for redundancy.

2. 1. 5. 3 Internal Calibration

The internal calibration system consists of redundant tungsten lamps with optics, a folding mirror, and a neutral density filter (NDF). The tungsten lamps are selected by ground command. Each lamp is filtered to achieve a relative spectral distribution similar to that of the sun. A typical lamp spectrum is shown in Figure 2-19. The optical components are used after each lamp to concentrate the light output onto the fiber optics array as illustrated in Figure 2-20. The NDF varies continuously from 100 percent transmission (completely transparent) on one end to approximately 1 percent transmission on the other. The NDF is used to attenuate the light that falls on the fiber optics array to provide light samples at all levels between zero and full scale. Shown in Figure 2-21 is an approximation to the profile of the NDF transmission as a function of the angle of the shutter wheel to which it is attached.

All elements of the lamp calibration system are shown in Figure 2-22, with the optical fiber array moved away from the NDF for clarity. The redundant set of tungsten lamps and optics which are identified as the source assemblies are stationary. Attached to the shutter wheel are the NDF and folding mirror. The focused light beam is transmitted through the NDF to the fiber optics array by means of the folding mirror. Correct positioning of the beam on the fiber optics array while the shutter wheel rotates is accomplished by the folding mirror. Passing the NDF through the light beam causes the light to be attenuated so its intensity profile resembles the NDF transmission profile given in Figure 2-23. As the shutter wheel rotates, the calibration system generates a voltage waveform out of the scanner which resembles that shown in Figure 2-23. The maximum scanner output can exceed 4 volts, but the multiplexer converts all signal levels above 4 volts to the digital word corresponding to 4 volts as shown. This output waveform is commonly called the calibration gray wedge.

The calibrate lamp current is regulated by a switching regulator which operates synchronously with the main supply inverter. Current regulation is maintained to ± 0.2 percent for input voltages in the range of -20 to -30 volts. Power of 0.357 watt is delivered to the lamp, with 0.29 watt dissipated in the regulator.

2. 1. 5. 4 Band 4 DC Restore Circuit

The purpose of the dc restore circuit is to set the channel output periodically to a predetermined value (0 volt) for zero input signal. The dc restore circuit is enabled by the same comparator in the phase locked loop that controls the shutter phase. The shutter covers the detectors to provide a black or zero light input for a period overlapping the 20 ms enabled time of the dc restore circuit.

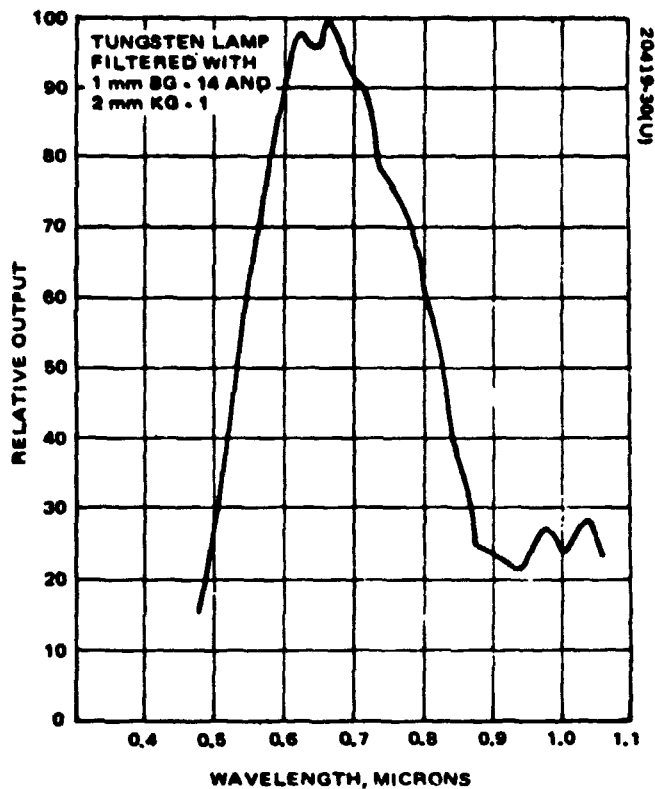


Figure 2-19. Relative Spectral Distribution of Calibration Lamps

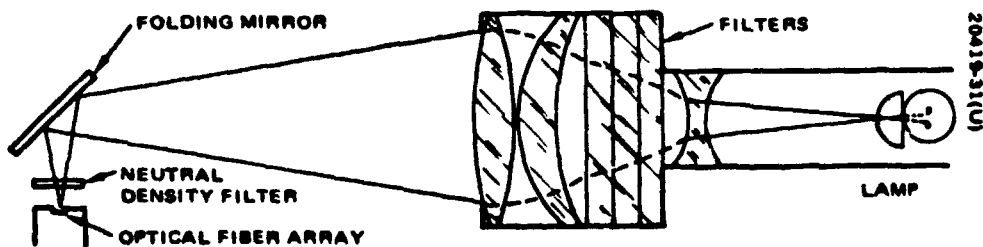


Figure 2-20. Internal Calibration Optics

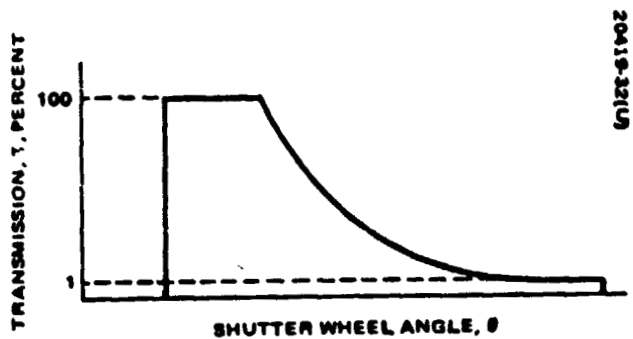


Figure 2-21. NDF Transmission Versus Shutter Wheel Angle

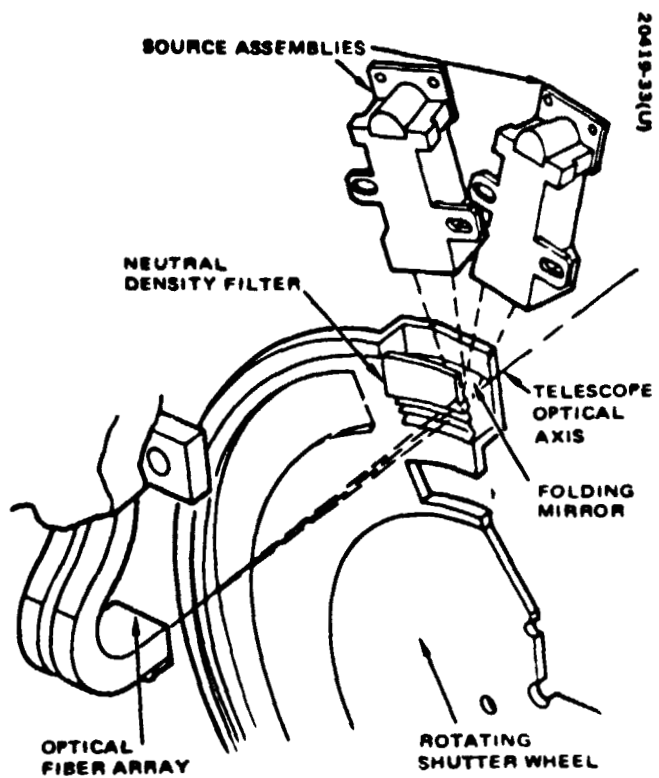


Figure 2-22. Internal Calibration System

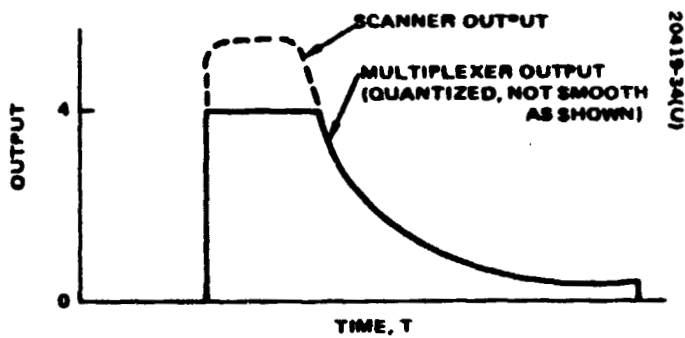


Figure 2-23. Typical Channel Output

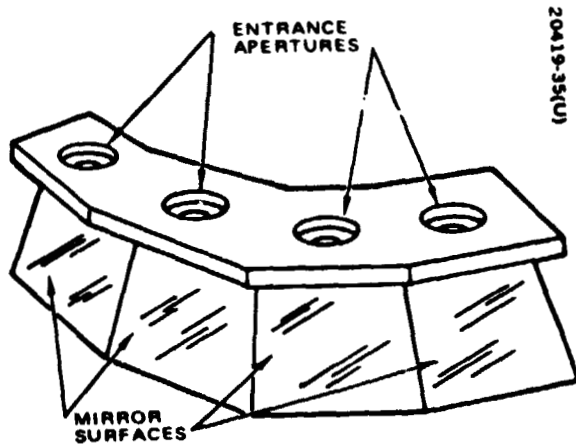


Figure 2-24. Sun Calibration System

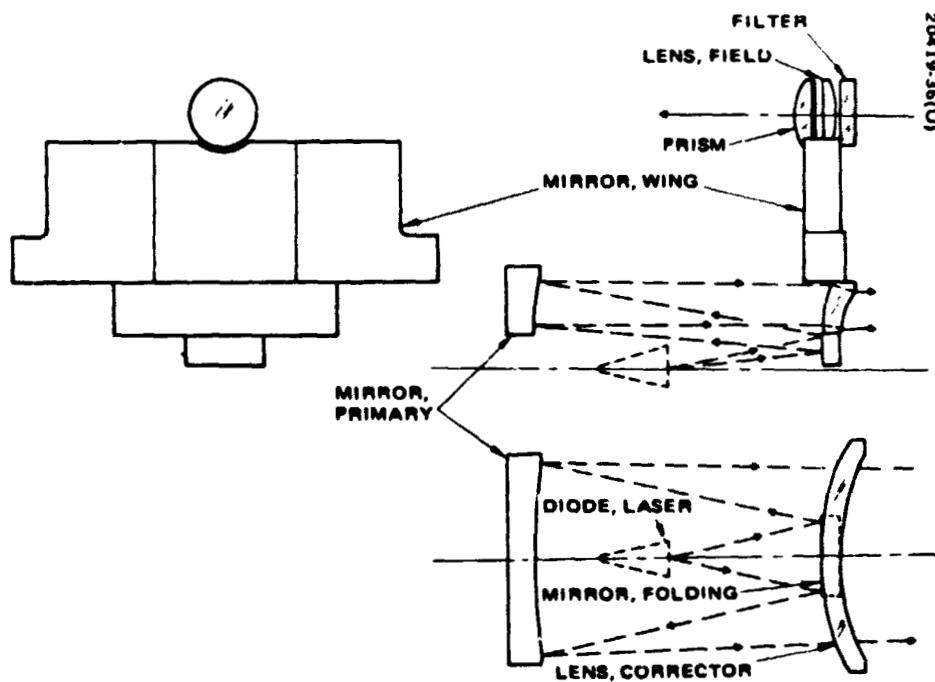


Figure 2-25. Scan Monitor Optical Schematic

The dc restore card contains a complete band of six dc restore circuits. The forward loop or unrestored signal path contains the dc restore capacitor. During the restore period an FET switch is turned on by the restore command, and the restorer output is set to zero volts. The charge required to set the output in the presence of zero light input is stored on the capacitor and maintained when the restore command is removed. The restoring time constant is 3 ms. The loop also performs the function of switching the dc restore circuit into and out of the video circuits for bands 4 and 5.

2. 1. 5. 5 Sun Calibration Mirrors

The sun calibration system consists of a four-faceted mirror and an entrance aperture for each facet. The sun calibration system is shown in Figure 2-24. The mirrors are fixed in position and oriented to reflect the sun through the apertures. The angles of the mirrors are selected so that the sampling of the sun's energy occurs just before the ERTS crosses the northern terminator. In this way competing light from the scene is made negligible. This sampling will appear in the scan interval for each channel of bands 1 through 4 and can be used as a primary standard by which changes in the internal light calibration system can be assessed and corrected.

2. 1. 6 Scan Monitor

Angle crossing of the scan mirror denoting the west edge, center, and east edge of the 100 n. mi. swath is indicated by means of an optical pickoff situated to view the scan mirror essentially orthogonally. The beginning pulse is supplied to the multiplexer where it is used to initiate video sampling. The center pulse can be transmitted upon command and is provided for checkout and troubleshooting. The end of line pulse is transmitted in the data to allow line-to-line corrections should the scanning mirror show minor variations in time to scan a line.

The scan monitor system consists of a gallium arsenide laser diode emitter (operating in sublasing mode), an optical projection system, a series of reflectors, and a pair of detectors.

The system has a built-in redundancy in the form of two light sources in one package, only one of which will operate at any given time, one is installed on-axis, while the backup must be offset by their minimum center-to-center dimension. If one source fails, the redundant unit is selectable by ground originated commands.

The optical system consists of segments of spherical and plane elements as per Figure 2-25. Spot diagrams indicate that 100 percent of the energy from a point on the emitter is concentrated within a 0.010 inch diameter circle, 92 percent within a 0.004 inch circle at the first image, which is at the 30 degree prism, and 100 percent within a 0.032 inch circle at the detectors.

The system is folded, utilizing the scan mirror four times to "walk" the spot from the emitter plane to the detector plane. Thus, a 60 inch optical path is attained in 7.5 inches and, by reason of the multiple reflections, is actually equivalent to a 240 inch optical lever.

2.1.6.1 Scan Monitor Electronics

The purpose of the scan monitor circuitry is to determine the optical zero crossing within 0.5 microsecond, as determined by the 0.5 volt point on the leading edge of its output pulse.

The two silicon photodiodes are followed by a preamplifier. The photodiodes are placed physically side by side and polarized oppositely with respect to the preamplifier input. The result when a narrow "slit" of light passes over the two diodes is an output signal, going first positive and then negative (or vice versa, depending on the direction of light travel), resembling a single cycle sine wave.

The preamplifier outputs are ac coupled into three comparators which sense a positive, zero, and negative level. These, in conjunction with two one-shots, produce an output signal only for falling zero crossings which correspond to scan as opposed to retrace. The signal is supplied to the multiplexer.

The power supply regulators for the integrated comparators are included on the board. Integrated regulators are used with series pass transistors to handle the required current, and foldback current limiting is provided.

2.1.7 Command and Control Telemetry

2.1.7.1 Commands

The flight subsystem receives the following type of command pulse from the spacecraft command subsystem:

- | | |
|----------------------------|-----------------|
| 1) Command pulse amplitude | -23.5 ±1.0 volt |
| 2) Command pulse width | 40 ±5 ms |
| 3) Maximum load current | 200 ma |
| 4) Source impedance | 60 ±10 ohms |

The MSS flight subsystem has its own internal command submatrix located in the scanner unit, but also receives some commands directly from the spacecraft command matrix. The internal submatrix consists of a 6 MA x 7 MB real time matrix and a 4 MA x 4 MB stored command matrix. The command input line is grounded. Redundant steering and suppression diodes are used on all relays.

2.1.7.2 Telemetry

The flight subsystem is designed to provide the following outputs to the spacecraft telemetry subsystem:

1) Analog

Range:	0 to -6.375 volts dc
Output impedance:	10 kilohms maximum
Effective accuracy:	8 bits
Resolution:	25 mv

2) Digital (single bit words)

Off condition:	-0.5 ±0.5 volts dc
On condition:	-7.5 ±2.5 volts dc
Output impedance - on:	1 megohm maximum
Output impedance - off:	50 kilohms maximum

The flight subsystem does not have the capability to store telemetry data, but the spacecraft telemetry subsystem has this capability. The telemetry cycling period is 16 seconds. A detailed telemetry handbook with calibration curves and output circuitry description is contained in Appendix A of the MSS Operation and Maintenance Manual, Vol. 1, Reference H5324-4365.

2.1.8 Power Supplies

Block diagrams of the scanner electronics and main power supply are shown in Figures 2-26 and 2-27, respectively. Transformer isolation is provided between the main supply and ±15 volt supply returns. The transformer is driven by the same inverter source as the PMT supply. This eliminates slow modulations or "beats" in the supply outputs caused by interfering sets of inverter transients. An external line noise filter is provided to reduce reflected transients onto the spacecraft -24.5 volt line to an acceptable level. The driven inverter produces less spiking than a standard self-oscillating inverter, since core saturation is not required for oscillation. Regulated outputs are obtained using standard feedback circuits.

The high voltage power supply configuration is illustrated in block diagram form in Figure 2-28. The output voltage is obtained by a fixed voltage multiplier which converts input levels in the range of 117 to 270 volts up to 1000 to 2300 volts with a 5 megohm load. The voltage level is controlled by means of a feedback loop which divides the output voltage and compares the resultant voltage with a -3.6 volt reference. The difference is used to correct the drive level to the multiplier chain. The output level is selectable within the range from -1000 to -2300 volts. This is accomplished by selecting precision resistors which determine the level of the feedback control voltage and hence set an appropriate bias on the input drive voltage.

20419-37(U)

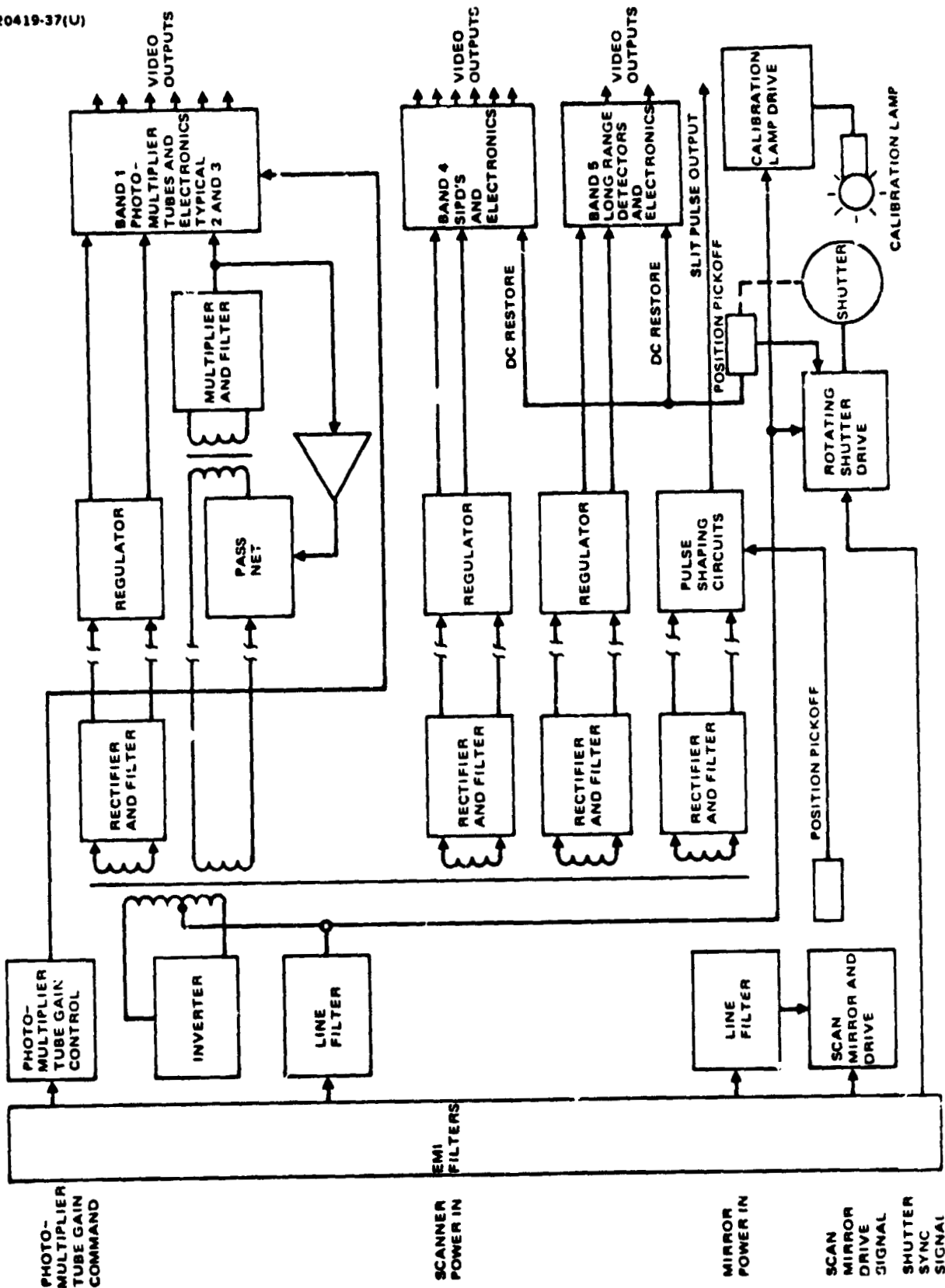
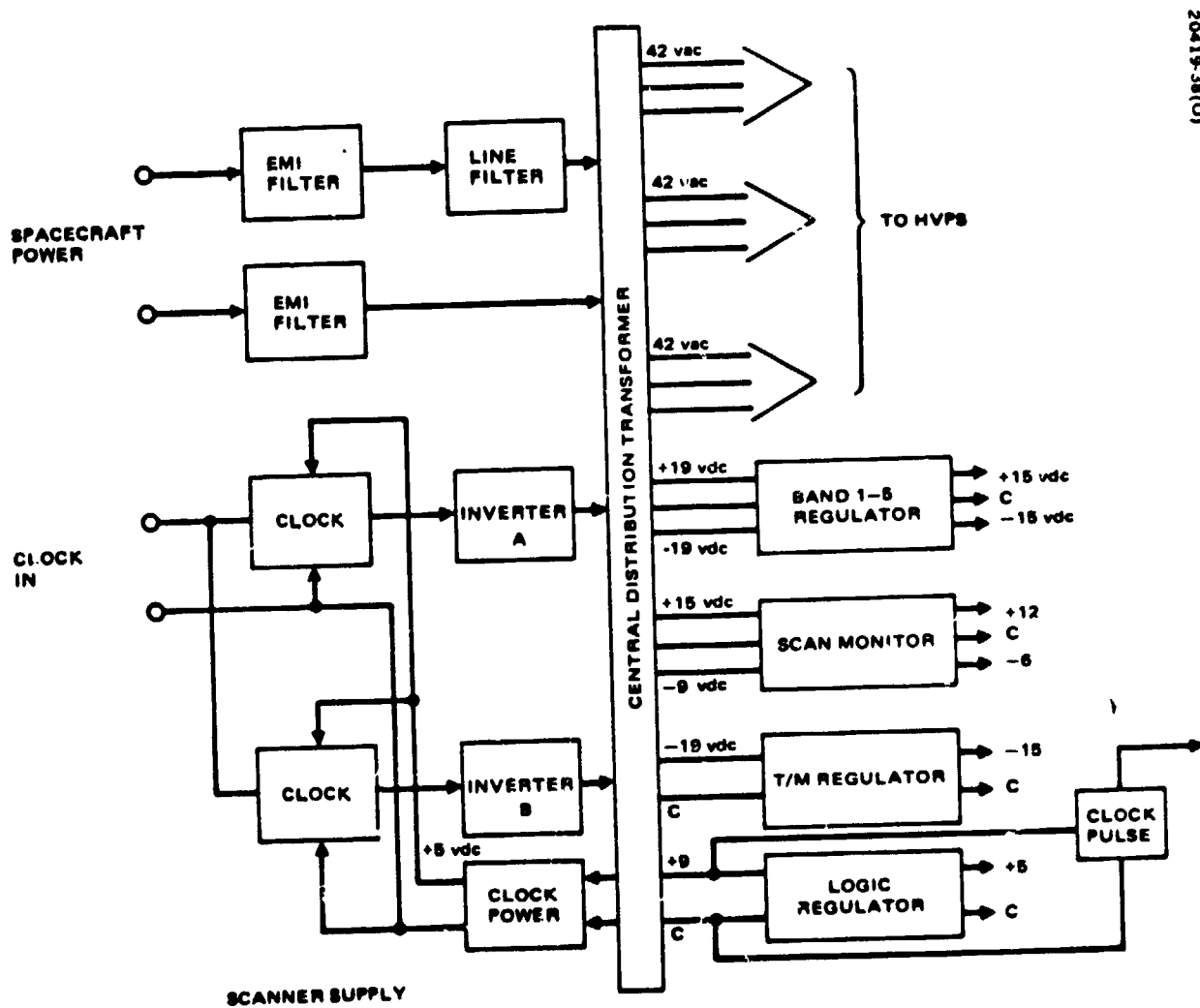
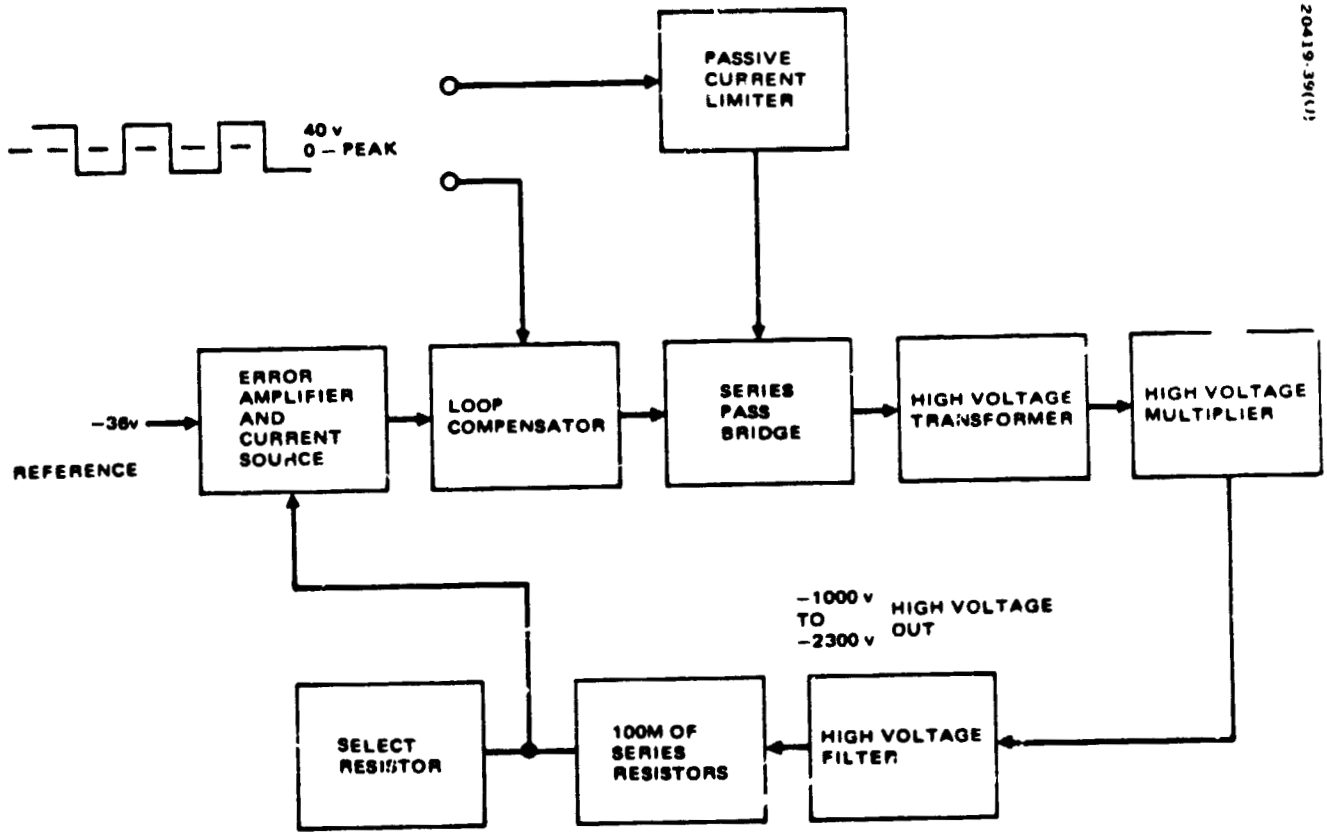


Figure 2-26. Scanner Electronics Block Diagram



20419-38(U)

Figure 2-27. Main Power Supply



20419-39(1)

Figure 2-28. High Voltage Power Supply

Figure 2-29 is a summary block diagram which illustrates the redundancies in the power system.

2.1.9 Structural and Thermal Design

The instrument's packaging configuration (see Figure 1-6) is a cylindrical magnesium casting with the scan mirror assembly housed at one end and the aft optics/sensor package mounted at the opposite end. The telescope assembly is housed inside of the cylindrical portion of the main frame, and the electronics chassis is packaged around the cylindrical portion of the main frame. At the scan mirror end of the instrument, a sun shield surrounds the scan drive and scan monitor in roughly the shape of a cylinder, whose axis coincides with the scan field of view and is normal to the telescope axis. The support post that positions the sun calibrate mirror directly below the scan mirror pivot axis extends down past the sun shield, but except for the actual mirror mounting bracket, its major portion remains outside of the scanner field of view to minimize aperture obscuration. The sun shield has been designed to mount independently from the other subassemblies at the scan mirror end of the frame in order to provide easy access for assembly and alignment operations.

The total weight of the scanner is 105 pounds. The center of gravity is measured during environmental qualification and acceptance testing. The moments of inertia (engineering units) are as follows:

<u>Parameter</u>	<u>Moment of Inertia, lb-in.²</u>
I, orbital	13,400
I, horizontal	4,230
I, vertical	13,600

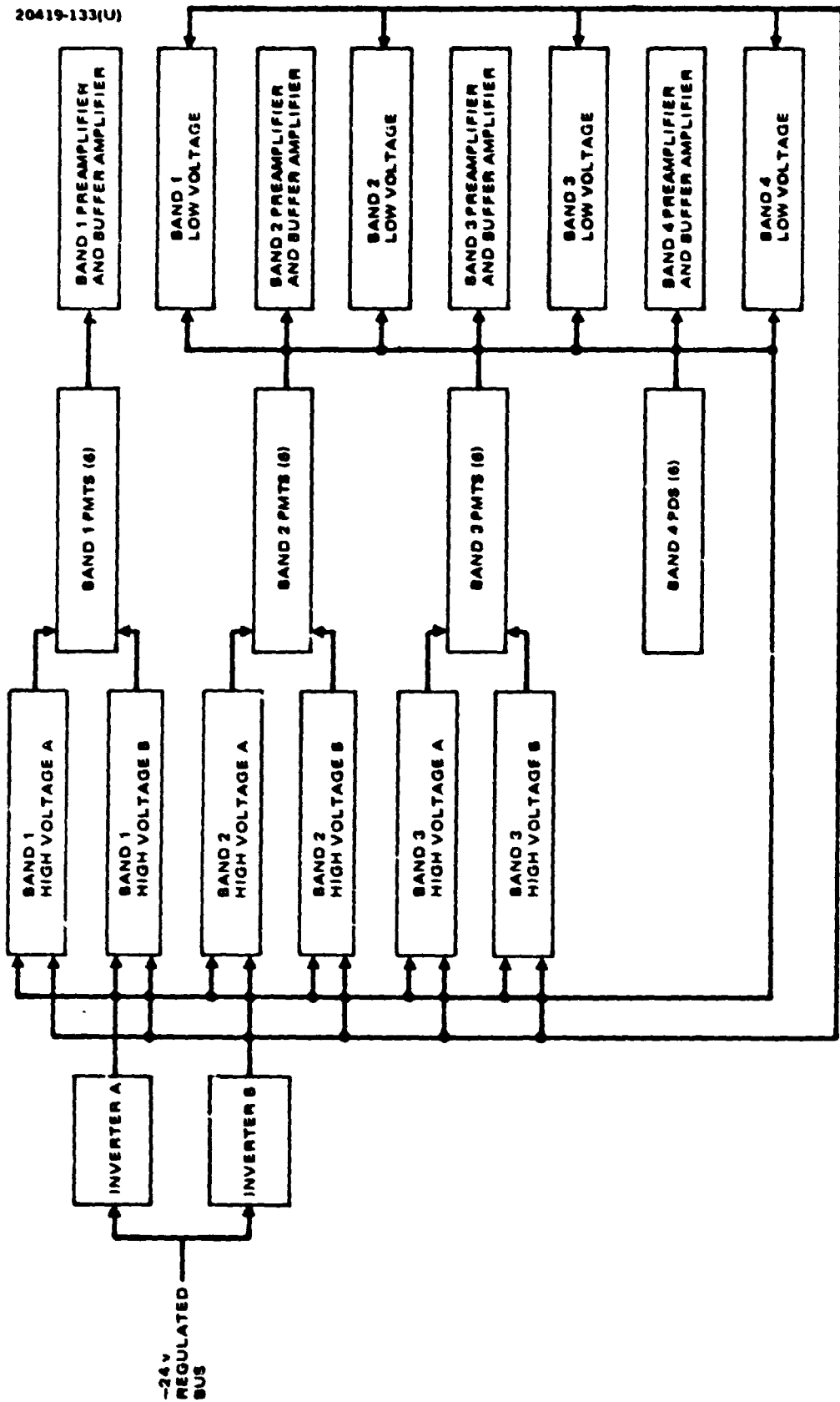
The unbalance angular momentum due to the rotating shutter wheel and motor is 0.35 in-lb-sec.

2.1.10 Mechanical Interface

The scanner will be located such that the end opposite from the scan mirror points west during the normal picture taking period. It will also be mounted so as to view the nadir within an elliptical cone of ± 15 degrees cross orbital track and ± 10 along orbital track.

The spacecraft and scanner mounting surfaces will be flat within ± 0.005 inch. The spacecraft scanner mounting surface is aligned and drilled using an alignment drill fixture. The drill fixture is aligned optically to within ± 0.05 degree about three orthogonal axes referenced to the spacecraft axes. Mounting surfaces may be shimmed as necessary and no further alignment should be necessary during scanner installation.

The telescope axis is not aligned to the scanner mounting surface, but is measured to within ± 0.03 degree with respect to two orthogonal optical



POWER SYSTEM AVAILABLE COMBINATIONS

- 1) ALL A'S (INVERTER A, HIGH VOLTAGE POWER SUPPLY A)
- 2) ALL B'S (INVERTER B, HIGH VOLTAGE POWER SUPPLY B)
- 3) AB (INVERTER A, HIGH VOLTAGE POWER SUPPLY B)
- 4) BA (INVERTER B, HIGH VOLTAGE POWER SUPPLY A)

Figure 2-29. Summary Block Diagram of Scanner Power System Redundancies

alignment surfaces (mirrors). Telescope misalignment data is related to the scanner mounting surface.

2.2 MULTIPLEXER

The functional block diagram of the multiplexer is shown in Figure 2-30; an actual photograph of the multiplexer is shown in Figure 2-31.

2.2.1 Theory of Operation

The primary function of the multiplexer is to commutate and digitize analog signals from the 24 scanner sensors. The multiplexer also generates and inserts the digital codes into the data bit stream in order that the receiving site equipment can determine each line length for the particular mirror scan rate at which that line was scanned.

Drive signals provided to the scanner shutter and to the scanner mirror are obtained by dividing down from the multiplexer word rate, thereby assuring a known integral number of words in each scan cycle. Both bit rate clocks and digitized data stream are supplied to on-board magnetic tape recorders and transmitters. Diagnostic and status telemetry signals are provided to the spacecraft telemetry subsystem. A power regulator and dc-to-dc converter in the multiplexer remove transients on the spacecraft bus, provide dc isolation from the bus, and generate several supply voltages required by the multiplexer.

2.2.1.1 Commutation

Figure 2-32 shows the input portion of the multiplexer which organizes the incoming video into a single pulse stream with amplitudes corresponding to the channel video levels at the instant of sampling. These pulses can then be sent directly to the analog-to-digital (A/D) section for binary encoding or directed through a nonlinear amplifier for signal compression. The basic output bit rate of the multiplexer is approximately 15 Mbps, and each digital word is 6 bits in length, so that the word rate is 2.5 MHz. There are 25 words between successive samples of each sensor signal, resulting in a sample rate of approximately 100,000 samples per second for each sensor signal.

To provide accurate A/D conversion of the signals, track and hold circuits are used to provide a fixed analog voltage to the 6 bit A/D converter while a conversion is being performed. While the output of one track and hold is being held for conversion, the second track and hold is tracking the signal which is to be converted during the succeeding word time. These relative operations are shown in Figure 2-33.

2.2.1.2 Digitization

The A/D converter shown in Figure 2-34 is used to perform one 6 bit conversion in two steps - 3 bits at a time each word period. The 3-bits-at-a-time converter permits two word times for settling of the integrated circuit elements. This was done to reduce sample to sample cross talk.

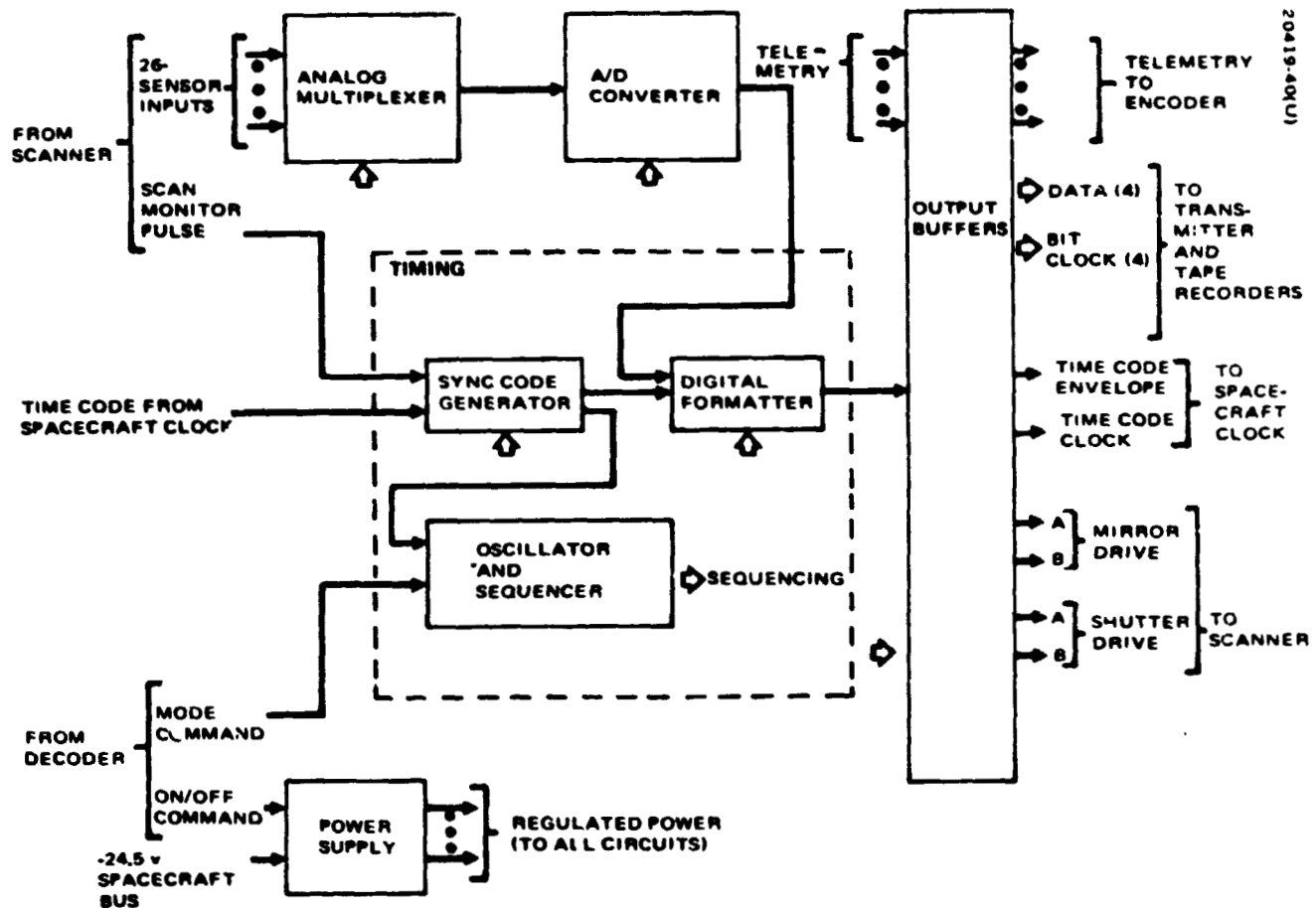


Figure 2-30. Multiplexer Functional Block Diagram

20419-41(U)

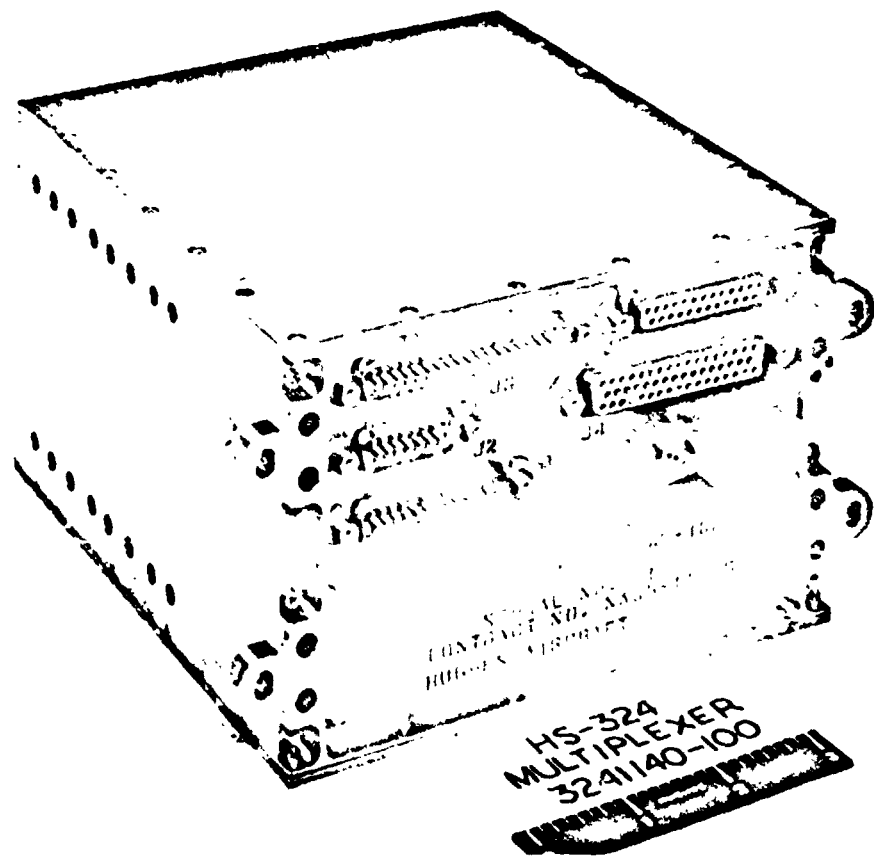


Figure 2-31. Multiplexer Configuration
(Photo 72-11680)

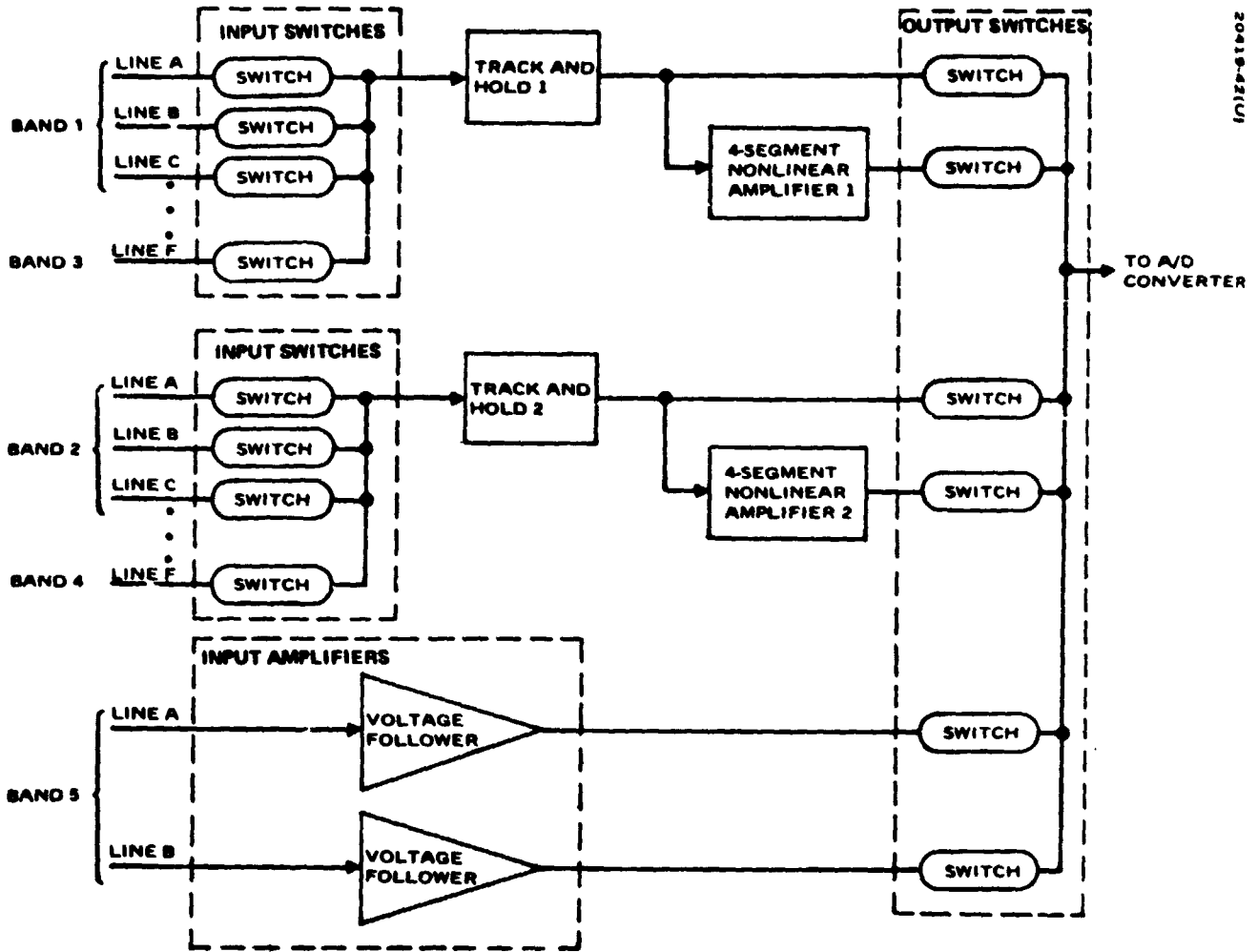


Figure 2-32. Analog Multiplexer Block Diagram

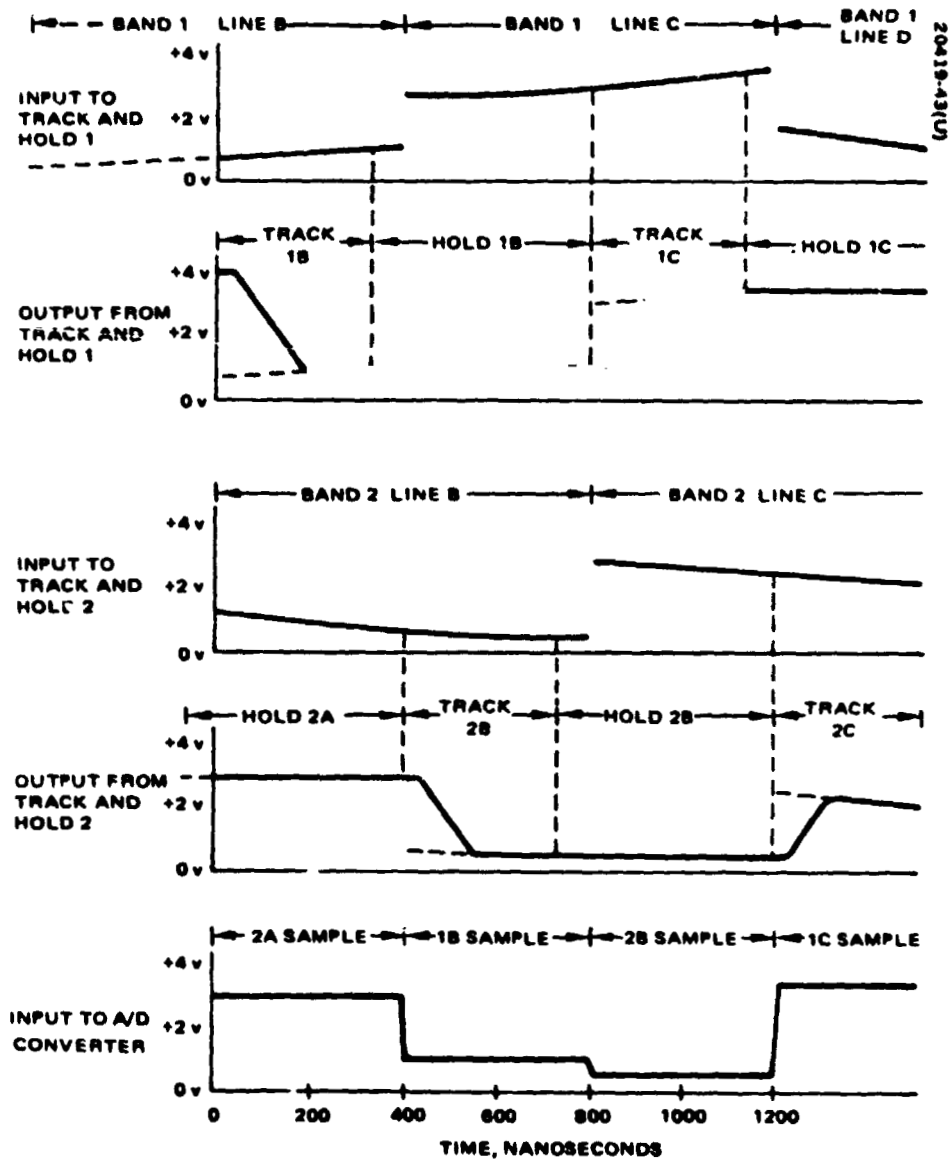
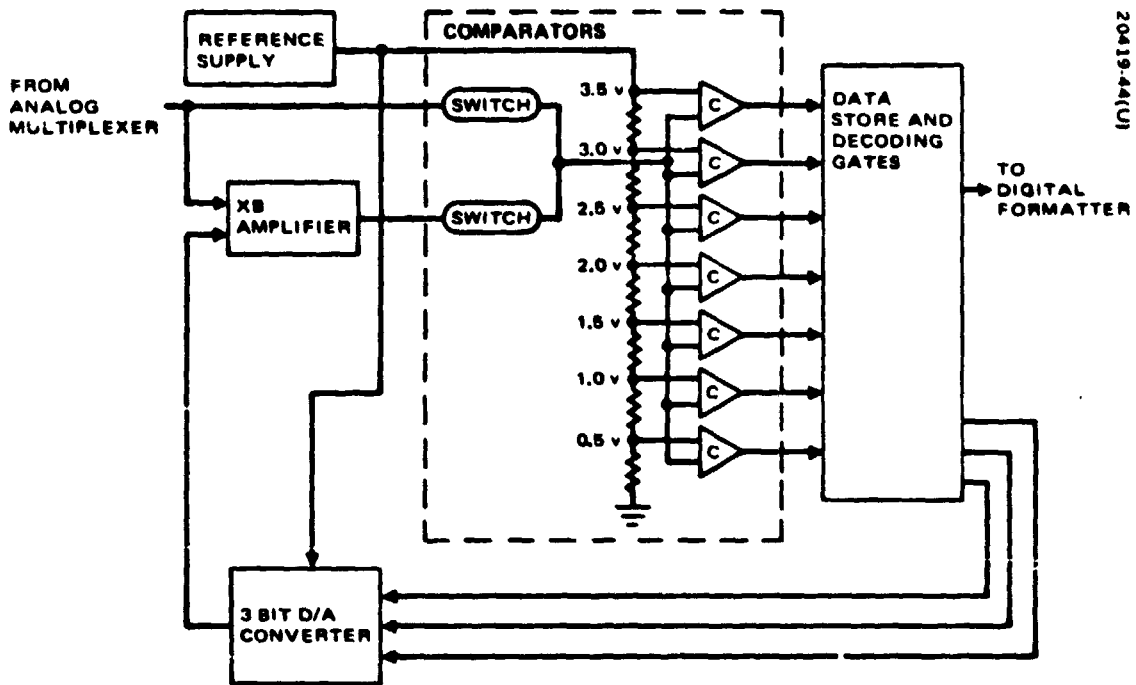
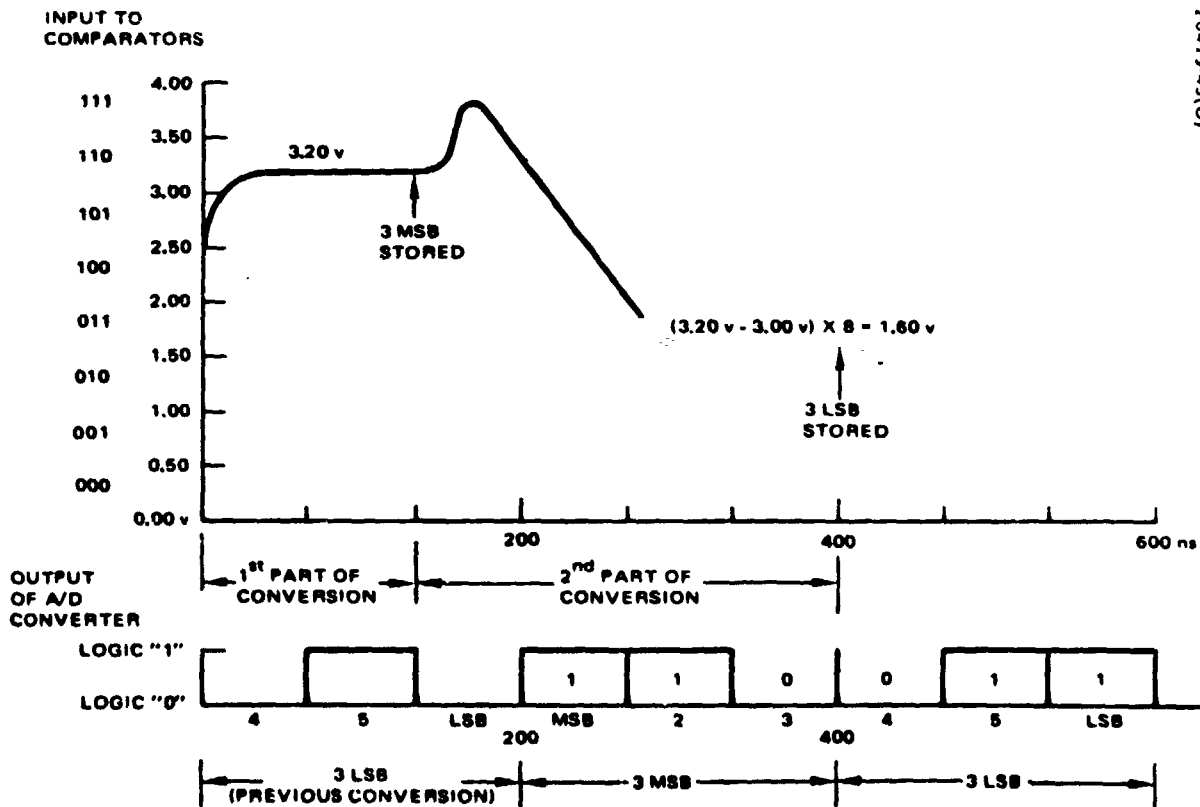


Figure 2-33. Analog Multiplexer Timing



20419-44(U)

Figure 2-34. Analog-to-Digital Converter Block Diagram



20419-45(U)

Figure 2-35. Analog-to-Digital Conversion Cycle

Each 6 bit conversion is done in two parts, shown on a time scale in Figure 2-35. The first 3 bits or 3 most significant bits (MSB) are determined during the first part of the conversion. The 3 MSB are used to provide a bias level to the X8 amplifier. The output of this amplifier is then used in the second part of the conversion to determine the 3 least significant bits (LSB). The 6 bit word is gated sequentially out of the A/D converter, most significant bit first. Each A/D conversion is performed with an accuracy of ± 30 mv, ± 0.5 LSB.

2.2.1.3 Format

The multiplexer major frame format is shown in Figure 1-8. A major frame consists of one complete scan/retrace cycle of the scan mirror, which is driven by the multiplexer at its frequency of 13.62 Hz.

The start of the major frame is defined by transmission of a repeated 6 bit preamble pattern (000111...) and is initiated in the multiplexer. Approximately 11.5 ms after the start of the major frame, the start-of-line scan monitor pulse (SMF-1) will be received from the scanner. At the next word time, the preamble pattern ceases and the start-of-line scan monitor code, SMC (111000), is transmitted. Immediately following this code, the 6 bit minor frame sync code (MFSC) is transmitted, signaling the first minor frame of data transmission of the line scan. A 48 bit time code received from the spacecraft clock is inserted into the data bit stream. Each bit of the time code is transmitted as a 6 bit pattern so that the code occupies 48 words of data. Following the time code, normal transmission of sensor data is begun, and the MFSC and its complement are inserted into the data bit stream in their proper sequence within the minor frame.

Sensor data is pre-empted at the next word time immediately following receipt of either the end-of-line scan monitor pulse (SMP-3) or midscan monitor pulse (SMP-2), (if enabled by ground command). A code is then transmitted depicting SMP-2 or SMP-3, which consists of black level data for exactly four rows (100 words), and thereafter by white level data for exactly four rows, after which normal transmission of sensor is resumed. The sensor data transmitted after occurrence of SMP-3 will be samples of the internal calibration wedge signal during alternate retraces interleaved with black level data when no calibration signal is present. Data transmission is terminated and a new preamble is initiated 73.42 ms after the previous preamble pattern.

2.2.1.4 Sensor Data Coding

In the multiplexer digitized data stream, bits 3 and 4 of each 6 bit digital word are complemented before transmission. This is to ensure a minimum average transition density in the event that either all black or all white scenes are encountered. The inversion of the two middle bits is provided for in the internal storage and decoding logic of the A/D converter. Since the 6 bit patterns for preamble, start-of-scan line monitor pulse code, and MFSC and its complement contain data transitions, the two middle bits of these patterns are not inverted.

2. 2. 1. 5 Data Signal Compression

The outputs of the 24 sensors are to be quantized into 64 levels prior to conversion into binary pulse code modulation. These 64 quantum levels are evenly spaced across the entire 4 volt signal range. For sensors 1 through 18 (comprising bands 1, 2, and 3), however, this linear quantization scheme is not optimum, because the noise in the signal diminishes as the square root of the signal. For example, a 4 volt signal contains twice as much rms noise as a 1 volt signal. For this reason, shaping the signal according to a square root law will equalize the noise throughout the range of the signal. After this process, a linear quantization will match the quantization errors precisely to the signal noise.

The compression amplifier consists of four linear segments which approximate the square root response curve.

2. 2. 2 Analog Multiplexer (MX05, MX06)

The analog multiplexer input switches selectively connect 24 separate signal sources to a pair of sample and hold amplifiers. The timing for the switching is developed by MX22, the timing section of the multiplexer. The sample and hold amplifiers operate in an alternate cycle and the resultant "held" voltages are alternately selected as the input reference for the A/D converter.

Figure 2-36, the multiplexer block diagram, shows the arrangement of MX05 and MX06 within the multiplexer. The input switches are closed for 12 clock periods, and the selected input signal is sampled during the 7th through the 11th clock period. The sample switch is opened at the end of the 11th clock period, which is approximately 66 ns, before the input to the channel is opened.

An abbreviated timing diagram of an alternate cycle of the upper and lower channel is shown in Figure 2-37.

2. 2. 3 Reference Supply (MX13)

The reference supply provides a constant voltage to the comparators and the 3 bit D/A converter.

The accurate reference is obtained by using a zener diode driven by a constant current source. The stable zener voltage is applied to an operational amplifier with precise gain adjustment to give the required low impedance precision output.

2. 2. 4 Comparators (MX14)

The comparators compare the analog signal, either MX12TO1 or MX17, against seven reference levels from 0.0 to +3.5 volts in 0.5 volt steps. If the analog signal exceeds the reference voltage of a specific comparator, that comparator's output will be a TTL logic "1"; if it is less than the reference voltage, the output will be a "0".

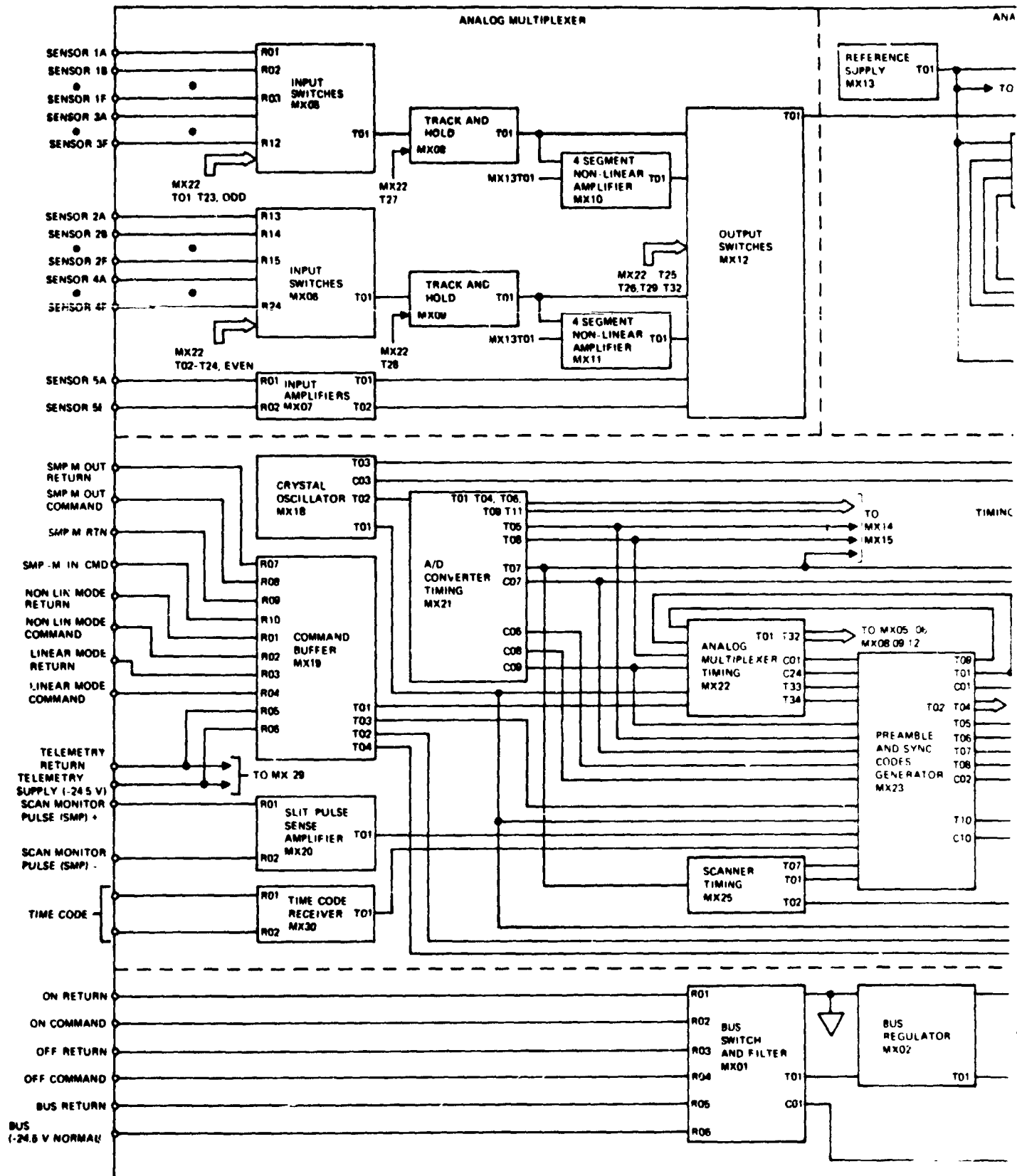
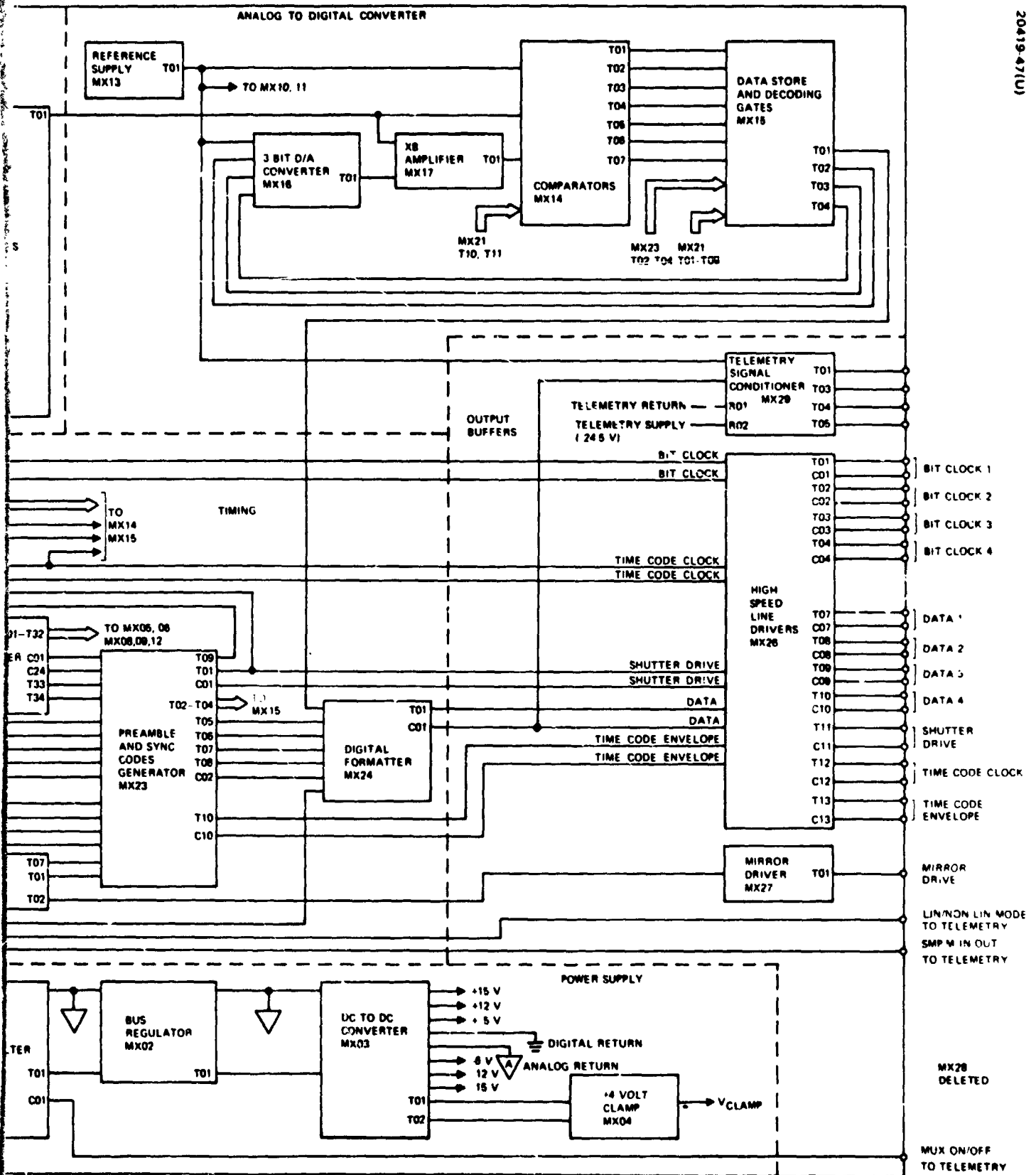


Figure 2-36. MSS Multiplexer Block Diagram

20419-47(U)



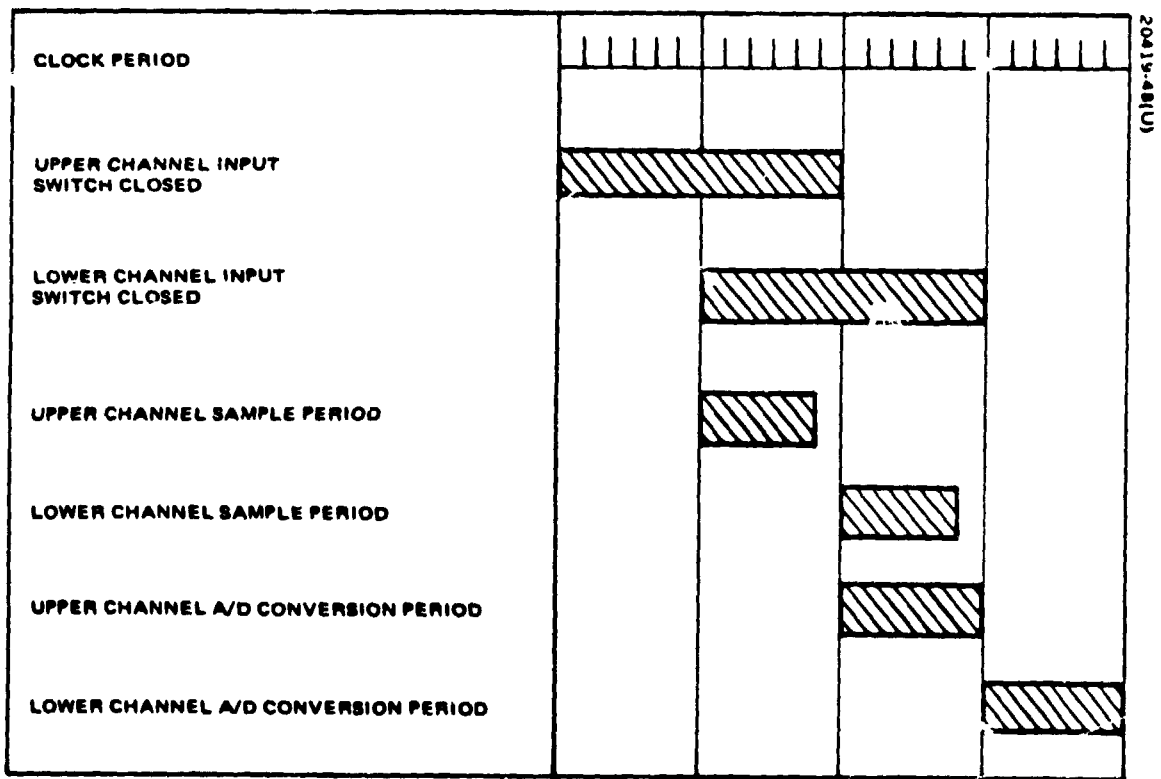


Figure 2-37. Abbreviated Timing Diagram

2.5 Data Store and Decoding Gates (MS15)

The data store and decoding gates perform the following logic functions in the D/A converter:

- 1) Stores the comparators unary code outputs for subsequent readout
- 2) Decodes the stores information into true binary
- 3) Outputs the 6 bits of each conversion (with bits 3 and 4 complemented) at separate gates, which are scanned serially by timing signals MX21T04 - T09
- 4) Outputs the 3 MSB of each conversion to the 3 bit D/A converter.

Inputs MX²³T03 and MX23T04 are timing signals which set and reset, respectively, the storage flip-flops for the purpose of inserting several lines of zero scale (black) followed by full scale (white) data each time the end-of-scan slit pulse occurs.

2.2.6 D/A Converter (MX16)

The 3 bit D/A converter provides a bias current to the X8 amplifier. The current has eight discrete levels, from 0.0 to 3.5 ma, in steps of 0.5 ma each.

The current is achieved by means of a precision reference supply which is switched to binary weighted resistors through saturated transistor switches operating in the inverted mode for low V_{EC} (sat).

2.2.7 Preamble and Sync Codes Generator (MX23)

The preamble and sync codes generator provides various digital codes which enable the ground equipment to synchronize with each mirror scan and each minor frame of data transmission and inserts into the data bit stream a time code received from the spacecraft clock.

2.2.8 Scanner Timing (MX25)

The scanner timing generates mirror drive and shutter drive signals for the scanner for synchronization with the multiplexer. It also provides the signals required by the multiplexer to detect start-of-scan and end-of-scan pulses which are received from the scanner.

2.2.9 High Speed Line Drivers (MX26)

Each line driver converts a pair of complementary transistor-transistor logic signals into a pair of complementary current source outputs for noise immune transmission via a twisted, shielded pair.

2. 2. 10 Time Code Receiver (MX30)

The time code receiver detects the differential voltage created by complementary current inputs and produces a transistor-transistor logic compatible output.

3. CALIBRATION PROCESSING THEORY

3.1 PURPOSE OF CALIBRATION SYSTEM

The purpose of the MSS system is to accurately produce images of the earth from a low altitude satellite. The energy received from the earth's surface, both reflected and emitted, is sensed and digitized by the system. The digitized data are transmitted to the ground where they are recorded for later processing. The recorded data are either analyzed directly by a computer or transferred first to a photographic transparency. For meaningful analysis of the digital information, the correct relationship between each digital word and the input scene radiance must be known. Likewise, for proper analysis of photographic transparencies, the density of the film must have a known relationship to the scene energy levels. The density of film is related to its transmission, which is the ratio of the transmitted light energy to the incident light energy, by the formula, $Density = \log (1/transmission)$.

The earth scenes are identified from the digital data or transparency by the relative amount of energy received by the system in four spectral bands. The reflectivity of the earth scene, which varies as a function of wavelength, establishes the energy distribution received by the system. The sun's rays are scattered from the earth's surface and the system senses the energy directed toward it. In the case of agricultural observables from orbit, each commodity has a different energy distribution across the four spectral bands, which is called its signature. Consequently, knowledge of the relationships between digital word and film density to scene radiance in all spectral bands is of paramount importance to the successful operation of the MSS system.

The MSS system functions as a transducer that transforms the energy received in each spectral band to a density on a photographic transparency as shown in Figure 3-1. Since there are 24 independent channels in the system, the transfer function illustrated in this figure must be determined for each channel. This is necessary in order to produce high quality pictures of the earth scenes, because the six channels involved in making a band picture must be well matched in the densities which they create in order to produce a stripe-free picture. Also, for signature analysis, the transfer function from the scanner input to the multiplexer output must be known accurately. For these reasons, a calibration system is required in the MSS system. Furthermore, since the scanner is the element sensitive to change,

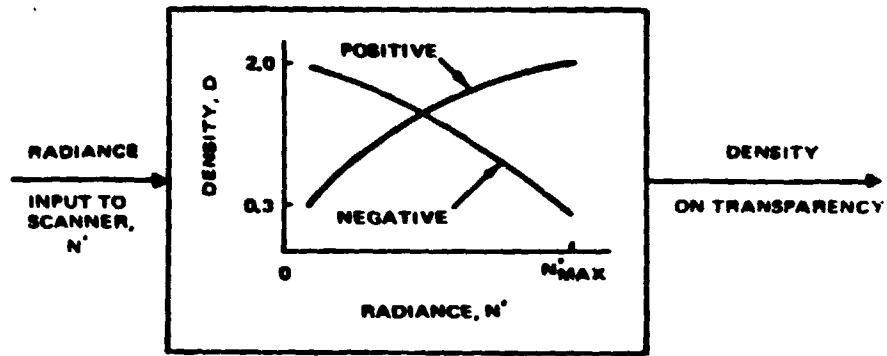


Figure 3-1. MSS System as Transducer

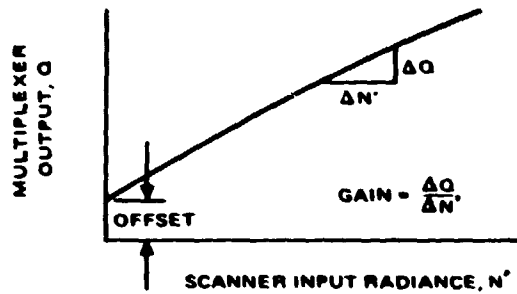


Figure 3-2. Definition of Gain and Offset

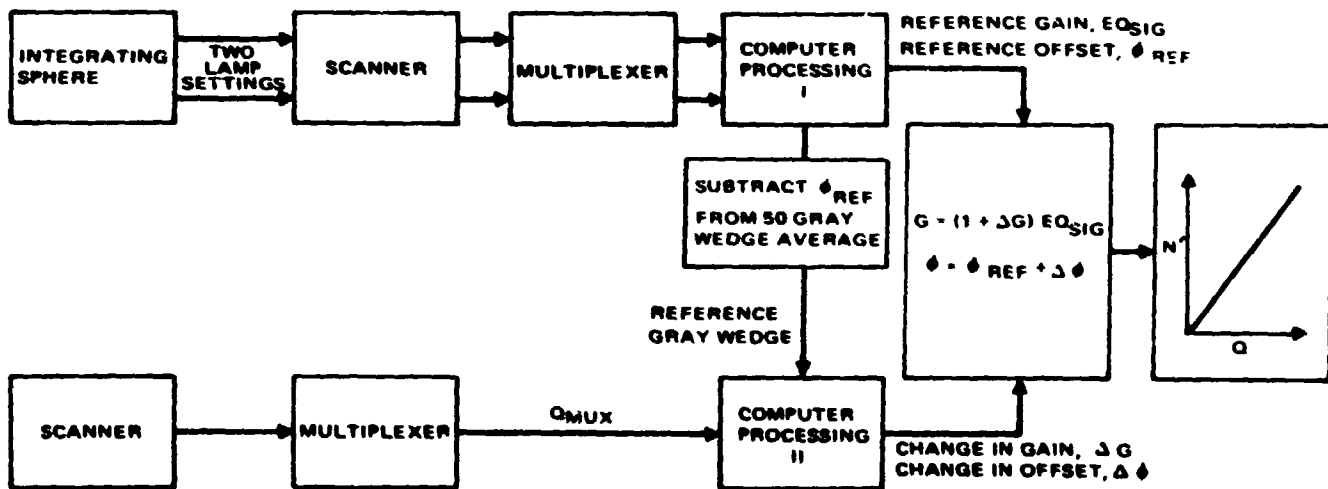


Figure 3-3. Channel Gain and Offset Processing

the calibration system is incorporated in it. The calibration system may be viewed as a device that keeps surveillance on each of the scanner channels and reports periodically on their status so that knowledge of their transfer functions can be current.

3.2 PROCESSING REQUIREMENTS

To produce a perfect picture of the scene imaged by the scanner, the transfer function (i. e., the channel gain and dc offset) of each of the six channels in a band must be known exactly. This is necessary so that the correct film density can be assigned to the digital words generated by the multiplexer. If this condition is met, the individual lines in the picture at almost all density levels will not be discernible. However, if the gains and offsets are in error in one or more channels, the individual adjacent lines which should have nearly the same scene information will have different average levels of density in each line and, consequently, will be displayed as stripes in the picture. The calibration system is also used in signature analysis to maintain accurate relative response between the four bands.

Over a wide range of shades of gray, the eye responds to ratios, instead of absolute levels. The eye can detect a sharp-edged junction between two fields that differ by little more than 2 percent in level. As a result, the calibration system processing techniques have been designed to compute the gains of all channels in a band to within an uncertainty of 2 percent peak to peak. Furthermore, based on visual impressions of a test transparency, it has been determined that an acceptable offset spread in a band for stripe-free pictures is 30 mv. This maximum uncertainty in the knowledge of the channel offsets has also been accounted for in the processing techniques.

3.3 CALIBRATION SYSTEM PROCESSING IN GENERAL

The purpose of the calibration system is to determine the gain and offset of each channel in a band within the accuracy requirements stated above. The gain and offset are defined in Figure 3-2. This is done by processing the gray wedge in conjunction with the sun calibration pulse. The sun pulse is used to modify the gain and offset computed from the gray wedge. The processing of the gray wedge will be considered first.

Since the calibration gray wedge is different for each scanner channel, each gray wedge is processed individually. Figure 3-3 shows the steps used to obtain the gain and offset for a single channel. The first step in the procedure is to establish the initial (reference) gain and offset of the scanner/multiplexer subsystem. This is necessary because the calibration gray wedge can only provide information to compute the change in gain and offset from a previously recorded reference gray wedge. The integrating sphere, which is a radiance standard provided by GSFC for MSS calibration tests, is all that

is needed to obtain the reference calibration data. Two different radiance outputs are used to establish the initial offset. One of these two settings, or an average of several settings, is used to establish the gain. A reference gray wedge is computed during this calibration period by averaging 50 gray wedges. All these procedures cannot be performed simultaneously but for short periods the scanner is assumed to be stable so that the data are assumed to be taken under the same conditions. All subsequent gray wedges are compared to the reference gray wedge and the change in offset and gain is determined. The gain as shown in Figure 3-2 for the scanner/multiplexer is decomposed as follows:

$$G = (1 + \Delta G) EQ_{sig} \quad (1)$$

For the reference gain calibration, $\Delta G = 0$, and therefore, $G = EQ_{sig}$. The parameter EQ_{sig} has been referred to as the signal equalization factor, but it is actually the reference gain. The gain was divided in this manner for the convenience it provides in tracking gain changes. The reference gain, or EQ_{sig} , is computed from the following relationship:

$$EQ_{sig} = \frac{(Q_{MUX} + 0.5) - \theta_{ref}}{N'} \quad (2)$$

All parameters in this equation are known as follows:

- N' = calibrated radiance of integrating sphere
- Q_{MUX} = multiplexer quantum level output for N' input to scanner
- θ_{ref} = computed subsystem offset

The 0.5 factor added to Q_{MUX} in Equation 2 is needed because the multiplexer is nominally biased negatively by 0.5 quantum levels. This can be seen, for example, by noting that the decision between quantum level 0 and quantum level 1 is nominally made at a level of 62.5 mv. All voltages between 0 and 62.5 mv are converted to digital word 0 and all voltages between 62.5 and 125 mv are converted to digital word 1. Assuming all inputs to the multiplexer are equally likely, the average input that will be converted to digital word 0 is 31.25 mv. This 31.25 mv average input corresponds to 0.5 quantum levels. Therefore, for inputs to the multiplexer between 0 and 62.5 mv, the multiplexer outputs digital word 0, but the average input is 0.5 quantum levels higher. This occurs at all decision points and, consequently, a 0.5 quantum level bias needs to be added to the multiplexer output.

The details for computing all the gains, offsets and gray wedges are given below. The processes assume the shape of the new calibration gray wedge results solely from a change in the gain and offset of the

subsystem and not to any change in the calibration device (NDF, lamp, and relay optics). Any change in the calibration system is assumed to be correctable with the sun calibration pulse.

3.4 PROCESSING TECHNIQUES

As was shown in Figure 3-3, two sets of data must be known to compute the subsystem gain and offset; the reference data and the changes from the reference data. Details of these processes are explained below.

The integrating sphere and a computer are the only pieces of equipment needed to obtain the reference data. The reference offset, θ_{ref} , is computed from two different nonsaturating radiance outputs from the integrating sphere. Scanning the integrating sphere aperture creates a video waveform approximating the one shown in Figure 3-4. In this figure, the outputs for both radiance levels are superimposed. Either the leading edge or trailing edge of the two waveforms is used to determine the offset. From the figure, it can be seen that the offset is the point where the extrapolations of both edges of the waveforms intersect. Mathematically, this may be described in the following way. If the system output is modeled as

$$Q(i) = \theta_{ref} + f(i) \quad (3)$$

where

$Q(i)$ = the multiplexer output for word i

θ_{ref} = the unknown subsystem offset

$f(i)$ = an unknown function equal to the output for zero θ_{ref}

And if the basic illumination level of the image is changed without changing its spatial distribution,

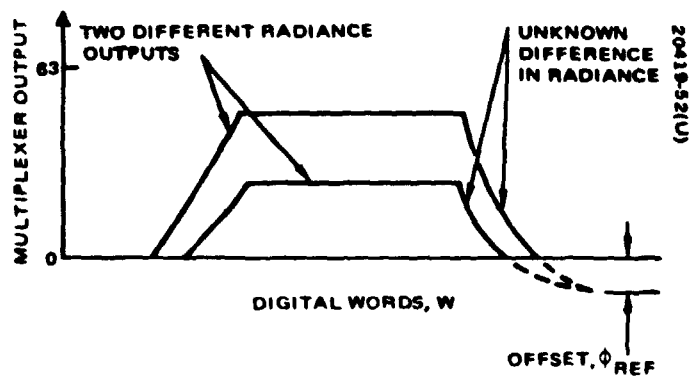
$$Q'(i) = \theta_{ref} + Rf(i) \quad (4)$$

where

R = the ratio of the new illumination level to the original level.

Then, if $Q(i)$ and $Q'(i)$ are known for a number of different word counts, using the same i or word count for both outputs, the offset can be solved by substituting Equation 3 into Equation 4 to obtain

$$Q'(i) = \theta_{ref}(1-R) + RQ(i) \quad (5)$$



NOTE: POSITIONING OF SPHERE TO ALLOW IMAGE TO GO FROM FULL RADIANCE TO ZERO SCALE PRIOR TO END OF SCAN, ENHANCES ACCURACY OF OFFSET DETERMINATION.

Figure 3-4. Integrating Sphere Outputs for Reference Offset Computation

This equation has the form

$$Q'(i) = A + RQ(i) \quad (6)$$

and the constants A and R are determined by a least squares fit on a plot of Q(i) versus Q'(i), with R being the slope and A the intercept. The system offset, θ_{ref} , is then estimated as

$$\theta_{ref} = A/(1-R) \quad (7)$$

This technique is used because the individual offsets of the scanner and multiplexer which are calibrated in unit tests do not add linearly when connected together. Furthermore, negative offsets are not observable at the output of the multiplexer, since all voltage levels below zero are quantized to level zero by the multiplexer.

The reference gain, or EQ_{sig} , is simply computed from the knowledge of the input radiance which at the plateau of the image is an accurately known function of the integrating sphere lamps, the output multiplexer quantum level, and the offset of the subsystem. The relationship between these parameters was given by Equation 2.

The reference calibration wedge is an average of 50 individual gray wedges. Figure 3-5 illustrates how this average is obtained. Each individual calibration wedge is detected and its leading edge is assigned a zero reference for the gray wedge word count. The reason for this is that the time interval from the line start pulse to the gray wedge may change slightly from one scan to the next scan on which a gray wedge appears because of scan mirror and shutter wheel irregularities. The detection procedure is shown in Figure 3-6. A total of 30 words in a row at quantum level 32 or greater is needed to assure the detection of a gray wedge after word 4100 from the line start pulse is received. The first word received in the string of 30 is then assigned gray wedge word 0.

After the detection of the gray wedge, a table is generated that gives the gray wedge word assignments for all 64 quantum levels. This table is generated by counting the number of words from zero which are equal to or exceed each quantum level. Figure 3-7 illustrates this technique for a single gray wedge at quantum level 32. The word count is picked up at word 300 and continues without interruption to word 305. However, the next two digital words received are below quantum level 32 and therefore are not counted. The next digital word is again above quantum level 32 and so the word count is incremented by one to 306. From here, all digital words received are below quantum level 32 and are not counted. The final result is that word count 306 is assigned to quantum level 32. This process is completed for all 64 quantum levels of the gray wedge.

The multiplexer 0.5 quantum level bias is eliminated when using this technique as illustrated in Figure 3-8. For the unquantized gray wedge output, equivalent quantum level 32 would be assigned to word count W_1 , and equivalent quantum level 31 to word count W_2 . With the quantized gray wedge output, the result will be the same using the 64 gray level computation technique. Consider, for example, quantum level 31 in Figure 3-8. All digital words greater than or equal to digital word 31 are counted, so that the count would reach word count W_1 before the first digital word of quantum level 31 is received. However, the counting would continue from W_1 to W_2 , because over this range all the digital words are at quantum level 31 and must be counted according to the algorithm. Therefore, quantum level 31 would be assigned word count W_2 as before, and consequently, a 0.5 quantum level bias does not have to be added to the multiplexer output.

The procedure to determine the 64 level gray wedge is completed 50 times and the 50 word counts corresponding to each quantum level are arithmetically averaged. The resultant average is called the 64 level gray wedge. This table of word count versus quantum level for all 64 levels is the basic reference gray wedge for that particular channel. Reference data for all other gray wedge computations for the channel are derived from this table. For instance, after this table of word count versus quantum level for all 64 levels is generated, eight preassigned word counts are selected and their respective quantum levels chosen. This process requires an interpolation between quantum levels, because the 64 level gray wedge program determined the word count corresponding to each quantum level, while this procedure calls for the quantum level corresponding to preassigned word counts. The eight preassigned word counts are selected to reduce the degree of error in the computation of the gain and offset from a single word count with a practical number of samples (less than 64). These eight word counts differ from band to band and from low to high gain. The location of the words affects the estimation error. The result of this process is called the reference 8 level gray wedge.

With the techniques for computing the reference parameters established, the processing of the subsequent gray wedges and the computation of the change in gain and offset will now be discussed. Figure 3-9 illustrates this procedure. The reference gray wedge is obtained in the linear mode; thus, a conversion to linear is required if the scanner is operating in the compression mode. The compression curve is obtained by comparing the linear gray wedge output to the compression gray wedge output of the scanner at approximately the same time by commanding on the two modes sequentially. The 64 level gray wedge program which produces a 50 gray wedge average is used to process each gray wedge as shown in Figure 3-10. The two gray wedges are compared on a word count basis. The compression curve is determined by: 1) selecting a quantum level output in compression mode, 2) finding the word count associated with this quantum level on the compression gray wedge, and 3) finding the quantum level output on the linear gray wedge associated with this same word count. The last step requires interpolation on the linear gray wedge to locate the correct quantum level.

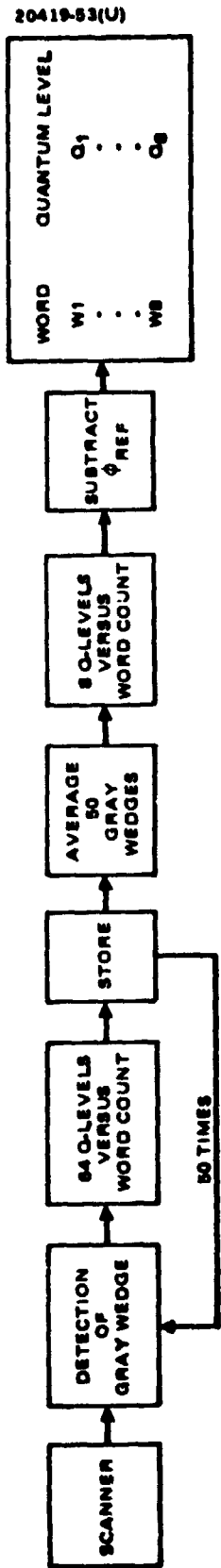


Figure 3-5. Computation of Reference Wedge

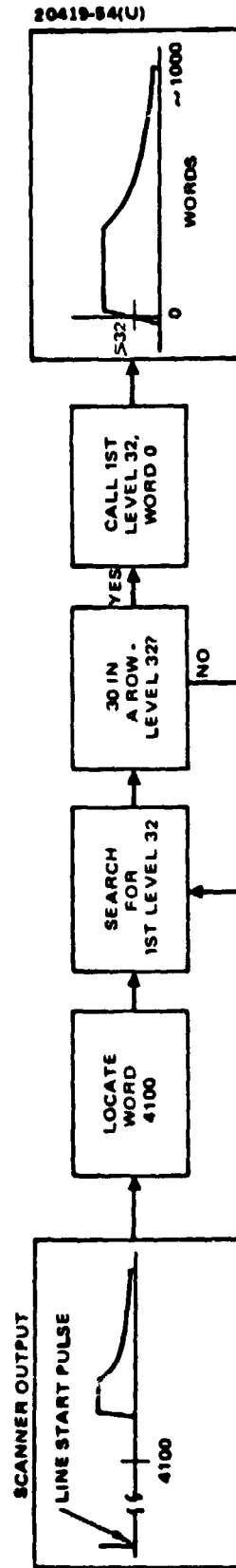
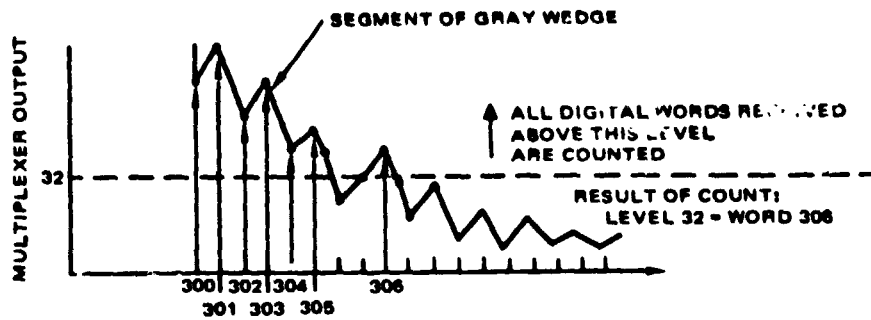
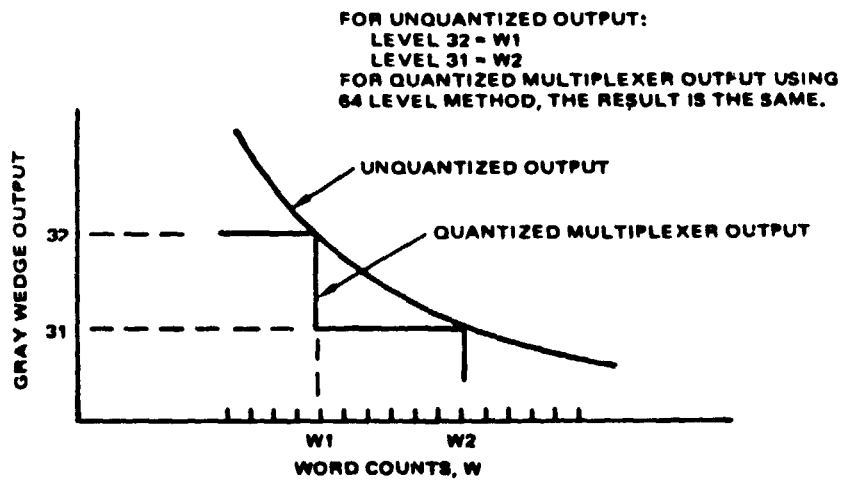


Figure 3-6. Detection of Gray Wedge



20419-55(U)

Figure 3-7. Sixty-Four Level Gray Wedge Computation Procedure for Level 32



20419-56(U)

Figure 3-8. No Multiplexer 0.5 Quantum Level Bias in 64 Gray Wedge Computation

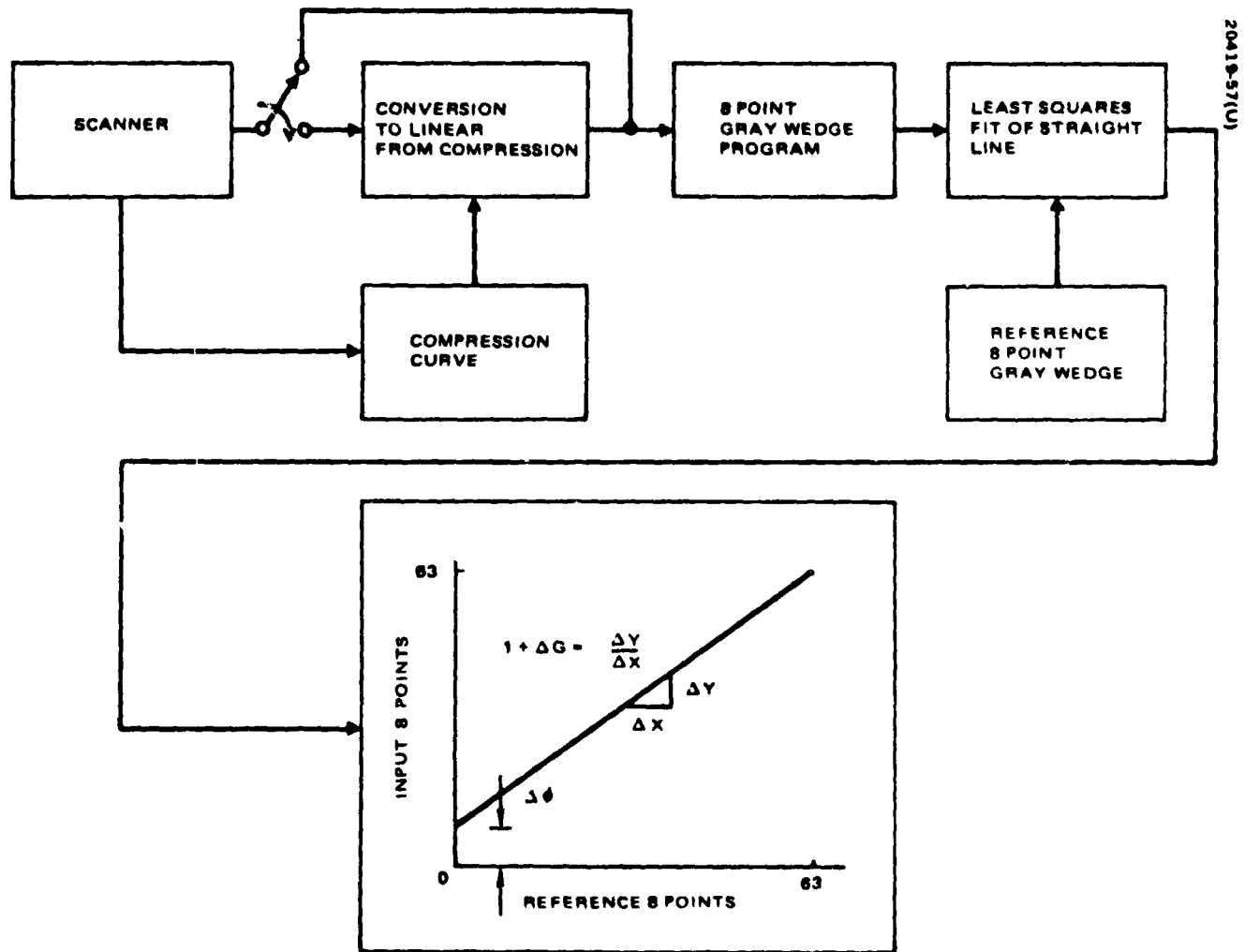


Figure 3-9. Computation of Changes in Gain and Offset for Subsequent Wedge Outputs

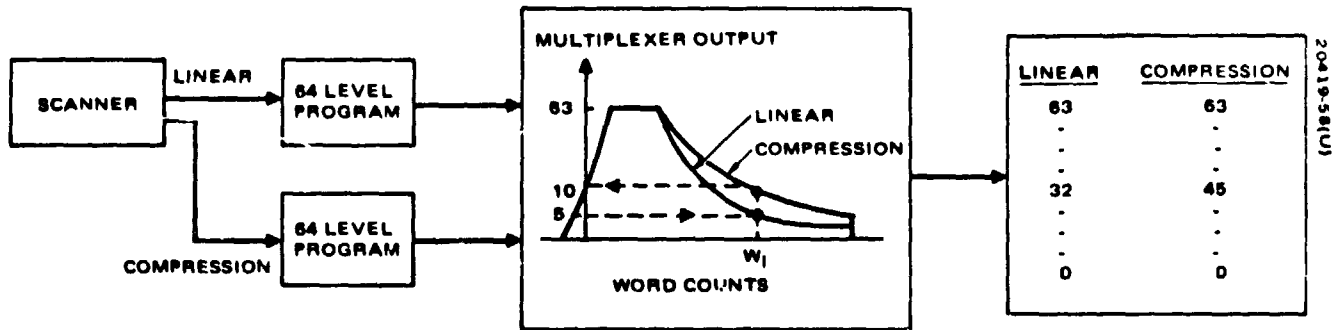


Figure 3-10. Calculation of Multiplexer Compression Curve

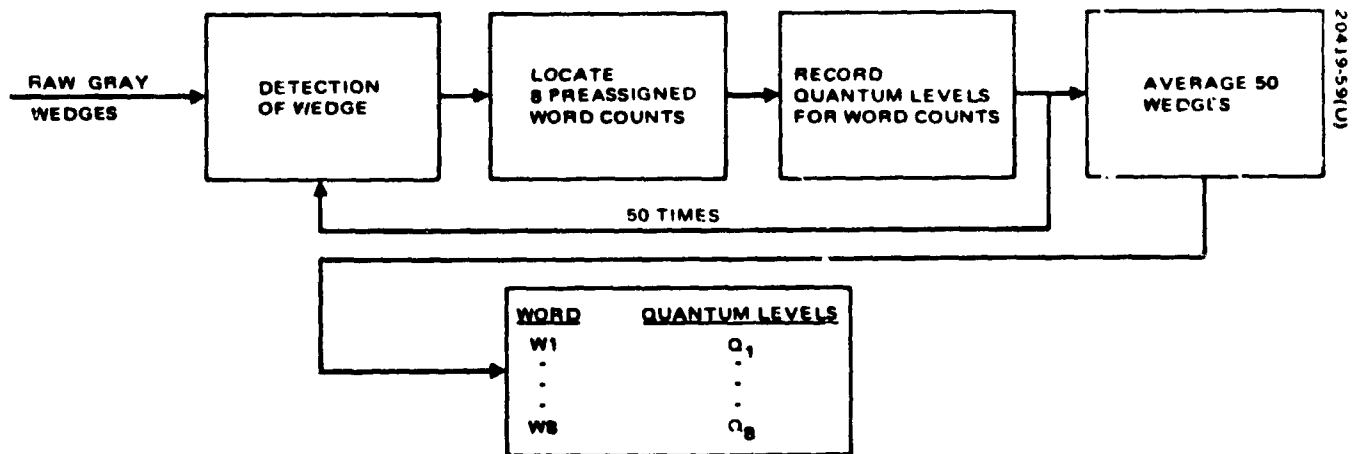


Figure 3-11. Eight Level Gray Wedge Calculation

Repeating this procedure for all 64 linear quantum levels gives a table of linear quantum level versus compression quantum level, which is the input-output characteristic of the compression amplifier.

After the completion of the compression to linear quantum level conversion, if required, the gray wedge is processed by an 8 level gray wedge program which is different from the one used at the output of the 64 level gray wedge program used for the reference data in that the 8 levels are compiled directly. The operator of this program is given in Figure 3-11. The detection of the wedge follows the same algorithm discussed in the 64 level gray wedge program. In this program, a search is made for eight preassigned word counts and their associated quantum level outputs in each of 50 wedges. The 50 quantum levels are averaged arithmetically at each word count and the resultant table is the new 8 level gray wedge.

The change in gain and offset is determined solely from the 8 level reference gray wedge and the subsequently computed 8 level gray wedge. For each of the 8 word counts there is a quantum level for the reference wedge and a quantum level for the new wedge. All eight sets of quantum levels are plotted and a least squares best fit straight line is placed through them. The slope of the straight line gives one plus the change in gain (i. e., ratio of measured gain to reference gain), and the intercept on the input axis is the change in offset. Figure 3-9 illustrates this calculation.

3.5 INGREDIENTS NEEDED FOR LOOKUP TABLE COMPUTATION

The ultimate objective is the correct assignment of film density to the input radiance to the scanner. The linkup between the computed gain and offset of the scanner/multiplexer subsystem and the film density is performed in the digital processor by a lookup table. Figure 3-12 illustrates this process. The relationship between input radiance is determined from

$$N' = \frac{(Q_{MUX} + 0.5) - (\theta_{ref} + \Delta\theta)}{(1 + \Delta G) EQ_{sig}} \quad (8)$$

which has all known parameters in it. The compression amplifier polynomial is used to make the correct conversion for the computer mode. The procedure for obtaining the compression curve data was discussed earlier. Calibration of the digital processor and photorecorder acting together gives a table of input quantum level versus output film density to which a polynomial is fit for computational convenience. The GPE calibration includes the crater lamp, film, and developer characteristics. The inputs required to develop the lookup table are shown in Figure 3-13. Gamma, and maximum and minimum film density are inputs selected as desired by the user of the pictures. Now, all the ingredients are available to assign each 6 bit multiplexer output to an appropriate 8 bit GPE digital word.

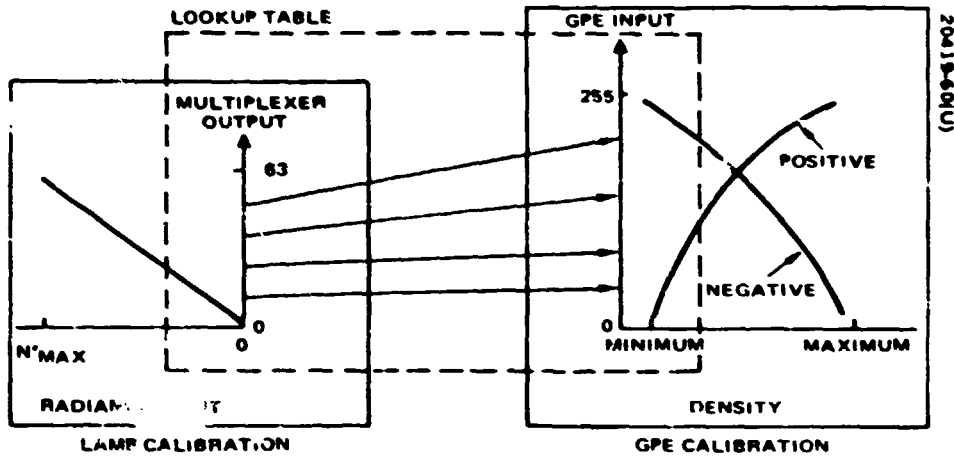


Figure 3-i2 Lookup Table is Linkup Between Radiance Input and Density

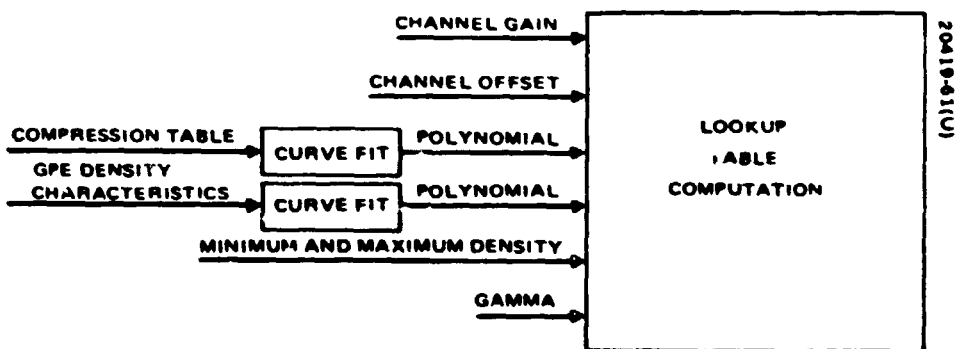


Figure 3-13. Ingredients for Lookup Table

3.6 GENERATION OF LOOKUP TABLE

The 6 to 8 bit lookup table permits any one of 256 possible film densities to be assigned to a particular multiplexer quantum level output for each channel. An 8 bit GPE digital word was selected primarily because the GPE density versus input voltage level (or input digital word) curve is nonlinear with a slope at its center approximately equal to two. Therefore, to have a density resolution at the center equivalent to that on the edges of the curve, more possible density values had to be made available over the full input voltage range. The problem is to select the appropriate density given the channel gain and offset and the multiplexer output level. In this last step of the calibration process, the important consideration is the avoidance of striping in the pictures.

Within the band, all channels do not saturate at the same maximum light level. Therefore, to avoid striping in bright scene areas, all channels in a band must be limited to the lowest radiance that will saturate any sensor. This point can be explained by Figure 3-14. In this figure, it is assumed that each channel has zero offset and that the gains of each channel decreases in numerical order. To simplify the discussion, consider only channels 1 and 2. At N'_{max} , channel 1 has an output of 63 and channel 2 an output less than 63, say 60. Therefore, channel 2 is not saturated and is capable of responding linearly to a higher radiance. However, channel 1 is saturated, and any increase in radiance will not increase the channel 1 output above quantum level 63. If a density, say D_1 , is assigned to N'_{max} , channel 1 must continue to be assigned density D_1 as the radiance is increased above N'_{max} , because it continues to report quantum level 63 for the radiance it receives. However, channel 2 will report linearly from quantum levels 60 through 63 as the radiance is increased. If different densities are assigned to quantum levels 60 through 63, the net result will be striping as illustrated in Figure 3-15. That is, channel 1 will maintain a constant density as the radiance is increased, and channel 2 will change progressively until it reaches saturation and remains at a constant density.

This effect does represent a loss in signal space and an increase in quantization noise for channels 2 through 6. To illustrate this increase in quantization noise, consider channel 6 in Figure 3-15. For this channel, the full range of input radiance from 0 to N'_{max} is quantized into only 40 parts, instead of 64. This means that channel 6 has more quantization noise than channels 1 through 5, which are divided up into more parts. However, to achieve stripe-free pictures, this loss is necessary. The loss does decrease as the gain and offset become more balanced among the channels, which emphasizes the need for good adjustment of the scanner channels.

This effect also takes place in a similar way on the lower portion of the channel response curves as shown in Figure 3-16. Because of offset variations among channels, some channels may reach zero output at higher radiance inputs than other channels. For exactly the same reason as explained above for the upper portion, this causes striping in the pictures.

REPRODUCIBILITY OF THE ORIGINAL PAGE IS POOR.

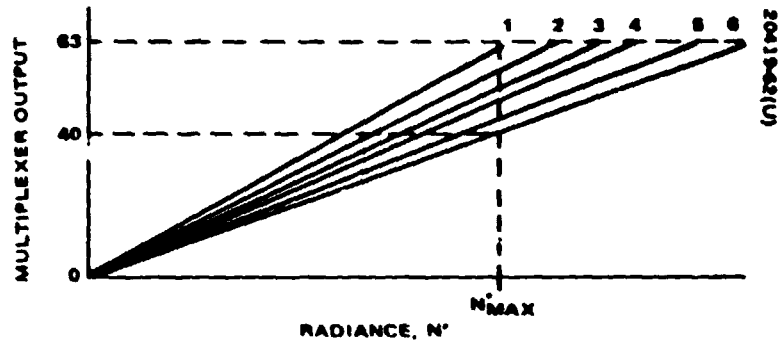


Figure 3-14. Channel Responses Using Gain and Offset Data

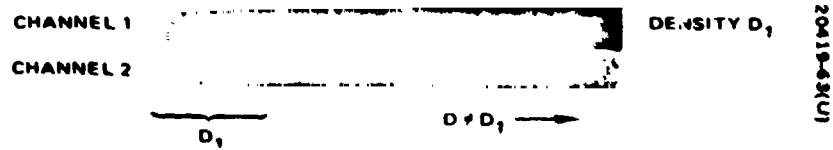


Figure 3-15. Striping Effect

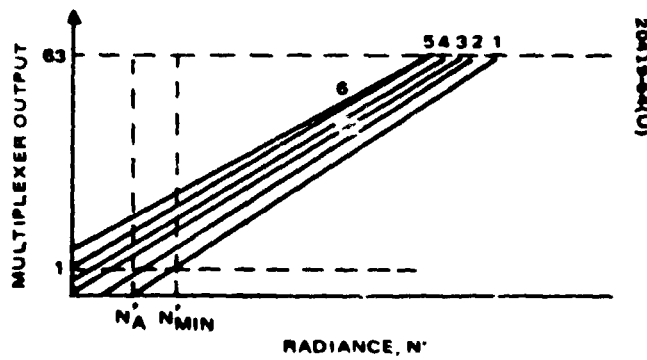


Figure 3-16. Offset as Limitation on Signal Space for Stripe-free Pictures

At N_A' , channel 1 reaches zero quantum level output, and any further decrease of radiance input would only continue a zero output response from the channel. Channel 2, for example, can still respond linearly to radiances below N_A' , but if new density assignments were made to these radiance levels, striping would occur. Present practice is to limit all sensors at low light levels to the light level corresponding to quantum level 1 for the sensor with the greatest negative offset. The limit at quantum level 1 rather than zero is necessary because of constraints on the density limits available. It is generally difficult to obtain densities outside the range of 0.3 to 2.0.

Therefore, limits have now been set on the range of input radiances in a band which can be transferred into the desired limits, D_{min} and D_{max} . The composite effect is shown in Figure 3-17. The selection of the densities to go with the quantum levels in each channel depends on whether a positive or negative is desired. If a positive is desired, the N'_{max} is set equal to D_{min} , and if a negative is wanted, N'_{max} is assigned to D_{max} . The density will then vary as a function of radiance as follows:

$$D = D_{min} - (\text{Gamma}) \log \left(\frac{N'}{N'_{max}} \right) \quad (9)$$

for a positive where gamma is positive, and as

$$D = D_{max} - (\text{Gamma}) \log \left(\frac{N'}{N'_{max}} \right) \quad (10)$$

for a negative where gamma is negative. The proper selection of gamma allows the full desired density range to be assigned to the full radiance range from N'_{max} to N'_{min} . Constraining gamma to a fixed value will limit the density range or the radiance range. This is illustrated in Figure 3-17 for a positive. For gamma too large, only the radiance range between N'_2 and N'_{max} will be converted into the desired density range. For gamma too small, the full radiance range from N'_{max} to N'_{min} will be converted into the density range from D_{min} to something less than D_{max} .

With the selection of gamma, D_{max} and D_{min} to obtain the desired transparency, all information needed to generate the lookup table is now ready. Figure 3-18 shows how one single multiplexer quantum level is converted to the correct GPE 8 bit word. The multiplexer output is converted first to linear mode, using the compression amplifier calibration curve, if the system is in the compression mode. Then, the correct radiance input corresponding to the multiplexer output is established from the computed gain and offset of the channel. From here, the density to be assigned to the input radiance is determined from either Equation 9 or 10, depending on whether a negative or positive is desired. In this transfer function, the user

may select the gamma and maximum and minimum density desired on the film. The density is finally used to obtain the GPE 8 bit word by utilizing the calibration characteristics of the GPE equipment. This process is completed for all 64 multiplexer quantum levels. The computer program which performs these operations punches a paper tape to be used in the GPE digital processor to perform the actual 6 to 8 bit conversion.

3.7 SUN CALIBRATION PULSE

The sun pulse is used to modify the gain and offset data obtained from the lamp calibration system. In the lookup table computation, the only parameters that change are the gain and offset. The total technique just discussed above remains the same. Techniques for processing the sun pulse have not yet been developed. Preliminary analysis of this problem indicates that the gain information provided by the sun pulse is probably the most significant contribution and the easiest of the two to compute. The offset information provided by the sun pulse is seemingly hard to determine and of less significance. In addition, smoothing of the sun pulse may be necessary to remove effects of tiny optical imperfections which cause intensity variations as the small beam of acceptance sunlight scans the optics. Also, it has been found that a failure to receive the sun pulse during the mission does not preclude the possibility of computing the correct gain. A flat scene, averaged over many scan lines, can be used to determine gain information.

3.8 LIMITATIONS

The primary limitations are in the capability of the film to produce a wide range of densities and in the reduction in signal space needed to produce stripe-free pictures. The film is limited in minimum density by "base fog" and in maximum density by the crater lamp. The reduction in signal space was fully discussed earlier.

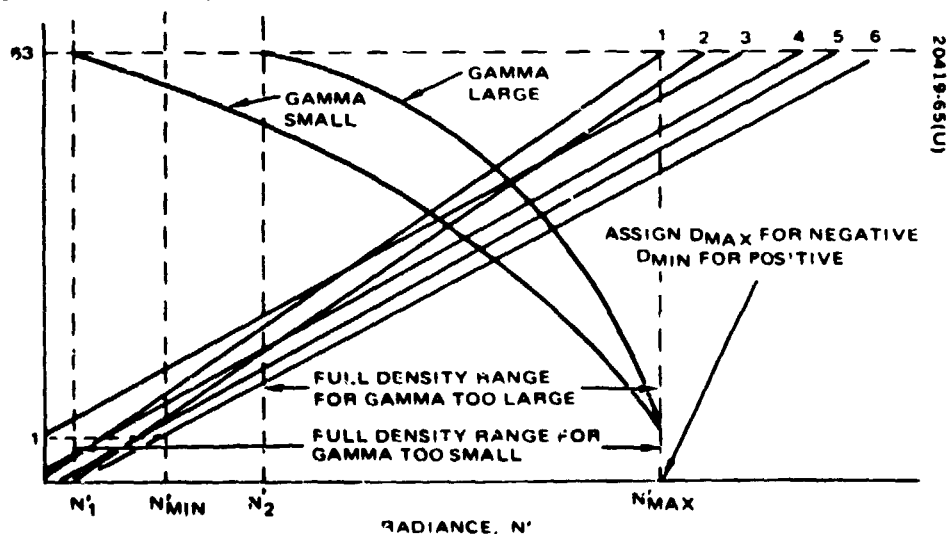


Figure 3-17. Composite Effect

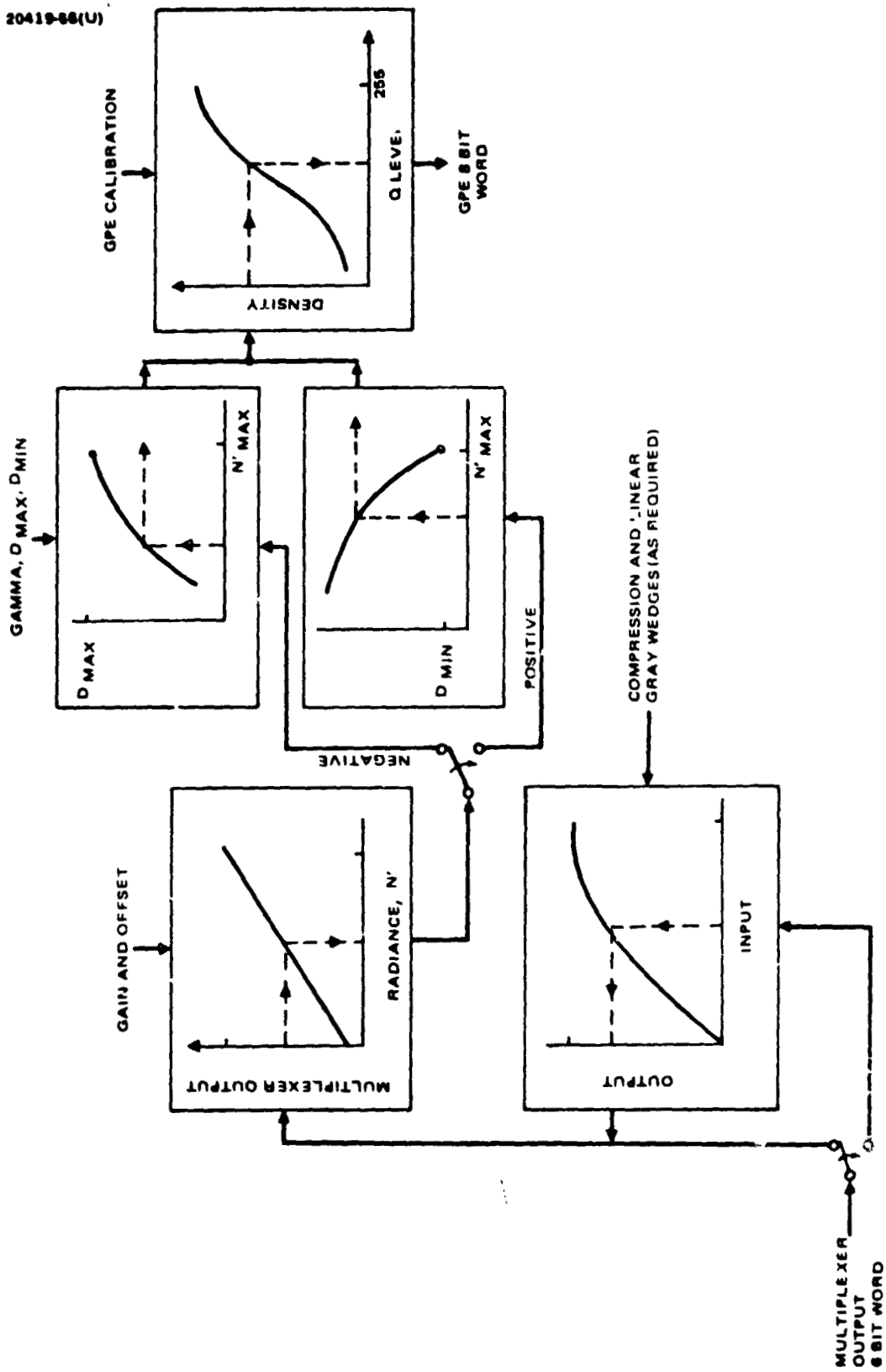


Figure 3-18. Procedure for Generating Lookup Table for One Channel at One Multiplexer Output Level

4. CALIBRATION DATA

4.1 SCANNER SPECTRAL RESPONSE

The relative spectral response of each channel for the prototype (S/N 001) and backup (S/N 002) scanners are given in Figure 4-1 and 4-2, respectively. These figures are plots of the normalized voltage output of each scanner channel versus a constant radiance input at different wavelengths. The measurements were made with a monochromator. These data are the spectral responses of the complete scanner, which is the composite effect of the spectral responses of the scan mirror, primary and secondary telescope mirrors, fiber optics, optical filters, and detectors.

4.2 RADIOMETRIC RESPONSE

4.2.1 Subsystem Response Versus Radiance

The GSFC integrating sphere was used as a light source to establish absolute gain/sensitivity for the scanner. This sphere had been previously calibrated with a primary standard at GSFC and supplied to Hughes Aircraft Company for calibration purposes. The data generated in this calibration has been presented in the Acceptance Test Report (HS324-5196). This section summarizes the data.

Table 4-1 is a listing of the radiance required for each channel to produce full scale signals (4.0 volts) at the output of the multiplexer. The scanner mode for this test was linear/low gain. It is discussed in more detail in Appendix H of the reference report.

Additional important data derived from the integrating sphere test is presented in Table 4-2. This data is a listing of nominal (or reference) gain and offset for each channel of the scanner. The scanner mode for this testing was also linear/low gain. This is discussed in subsection 2.7.2 and Appendix J of the reference report.

4.2.2 Integrating Sphere Radiance Versus Wavelength

As mentioned in the previous section, the integrating sphere was calibrated at GSFC using a primary source. A summary of this calibration data is shown in Table 4-3.

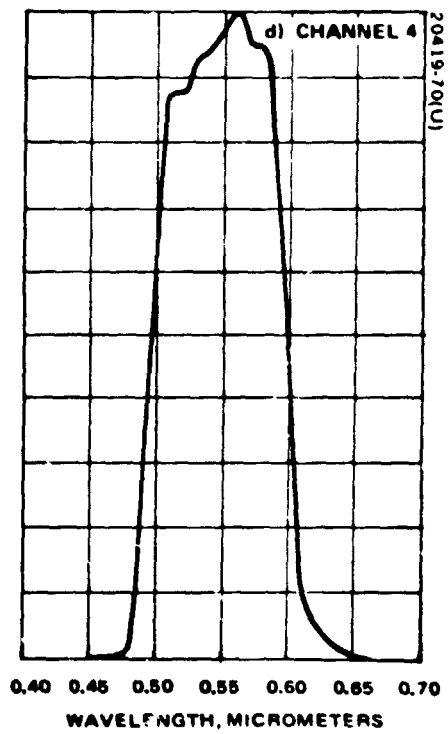
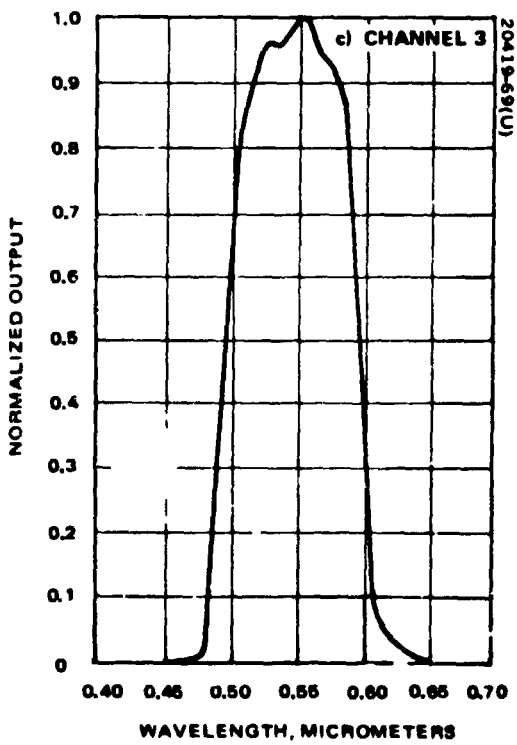
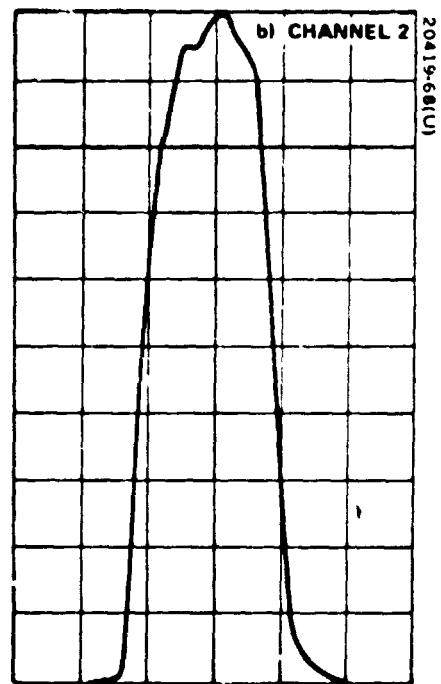
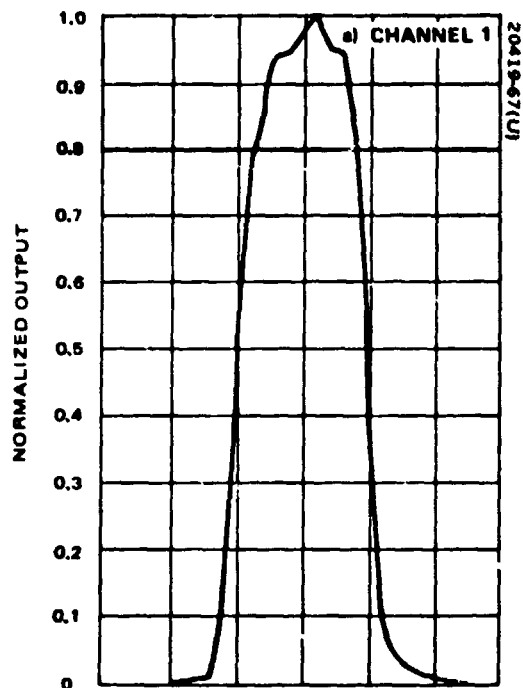


Figure 4-1. Prototype (S/N 001) Relative Spectral Response

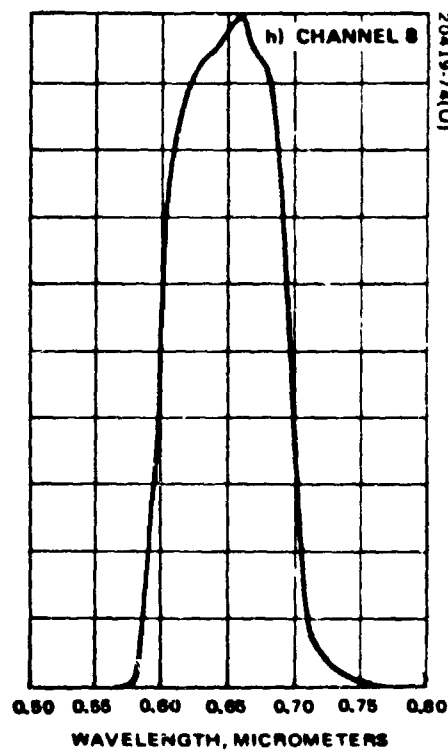
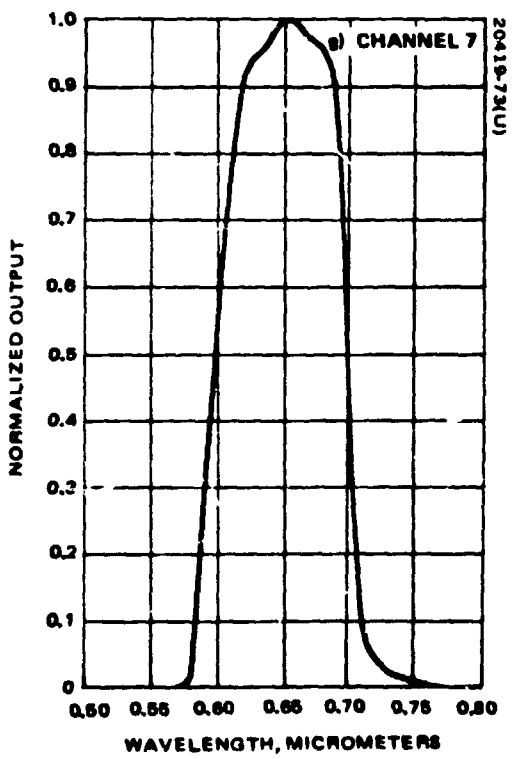
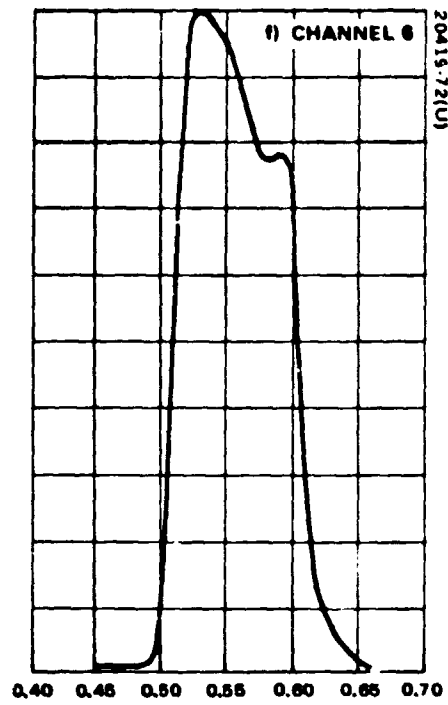
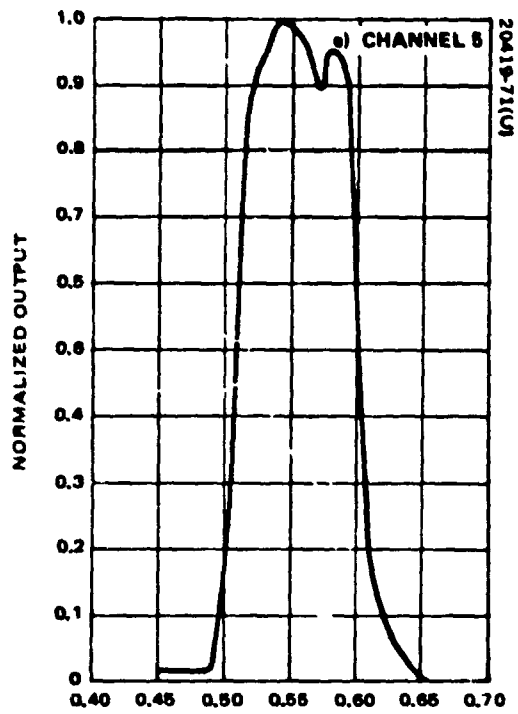


Figure 4-1 (continued). Prototype (S/N 001) Relative Spectral Response

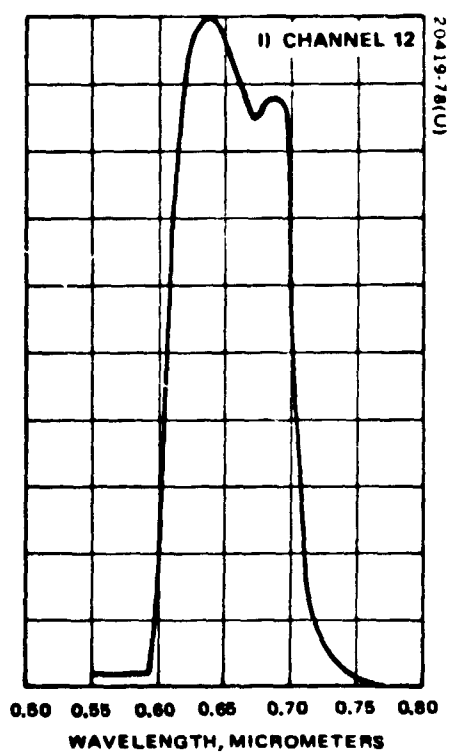
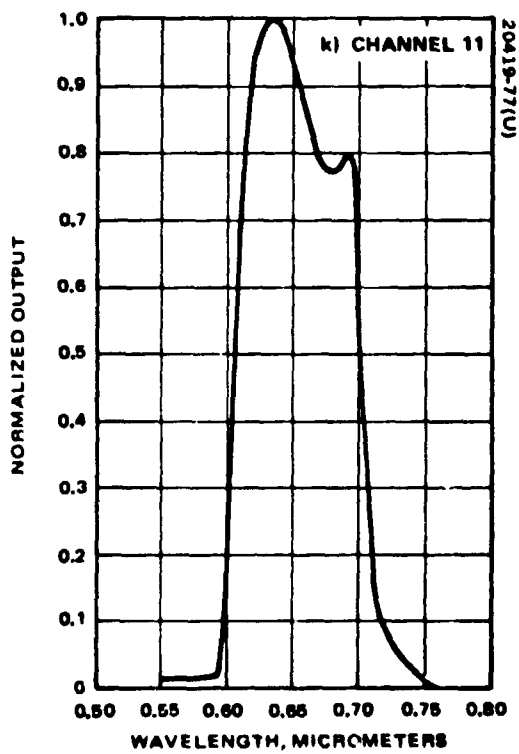
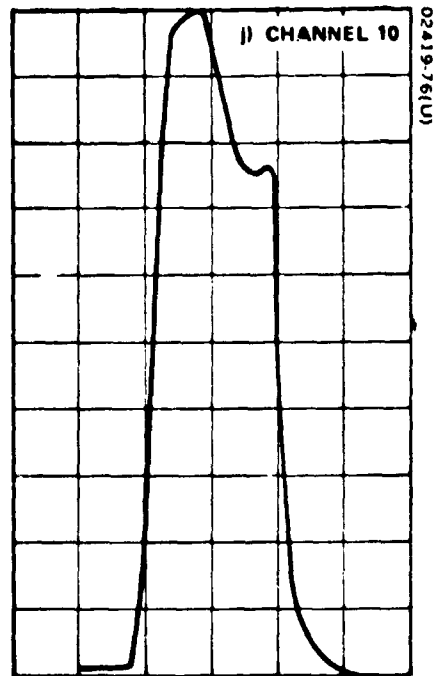
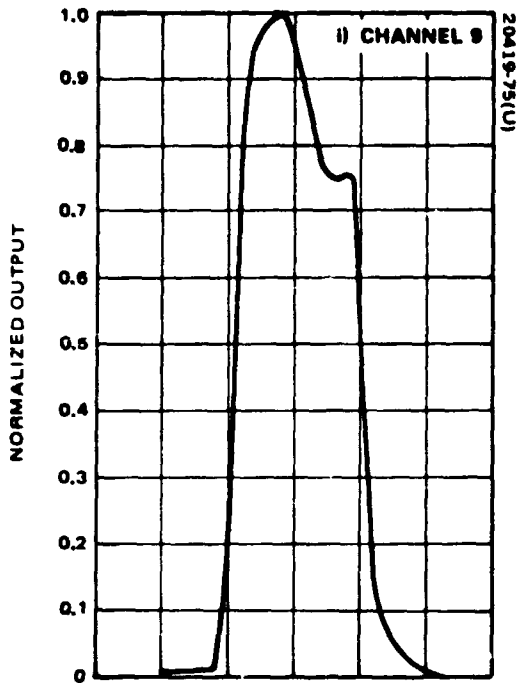


Figure 4-1 (continued). Prototype (S/N 001) Relative Spectral Response

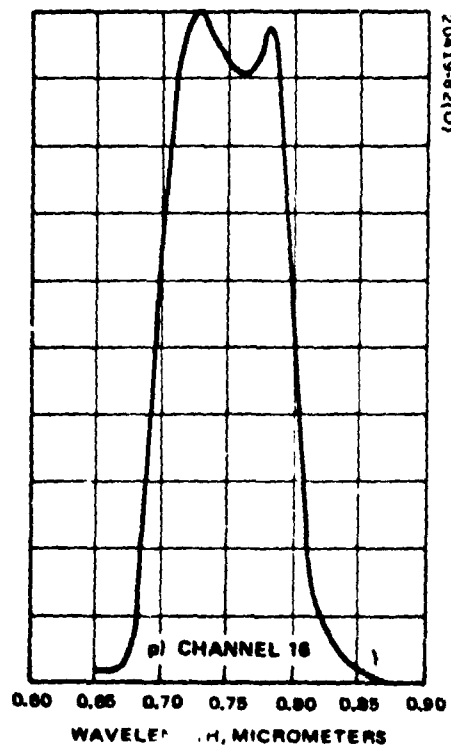
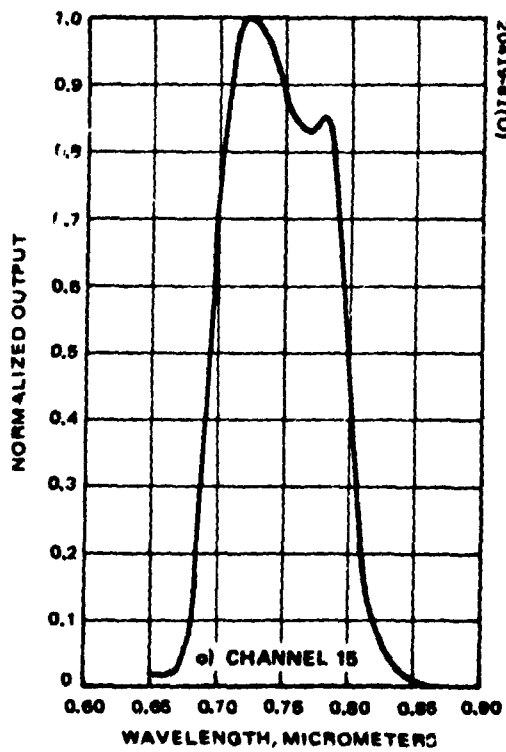
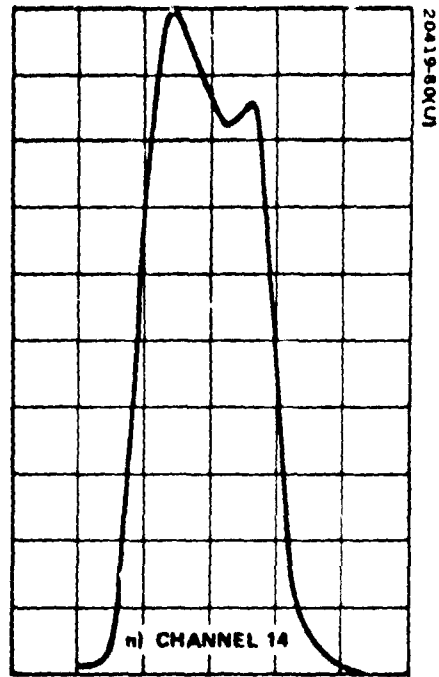
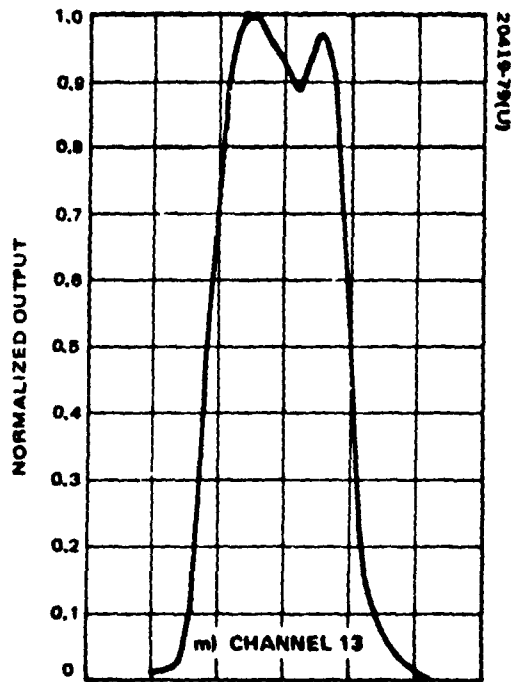


Figure 4-1 (continued). Prototype (S/N 001) Relative Spectral Response

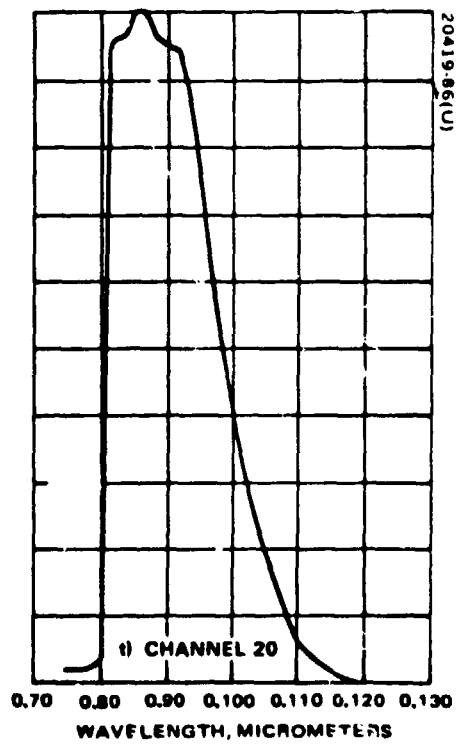
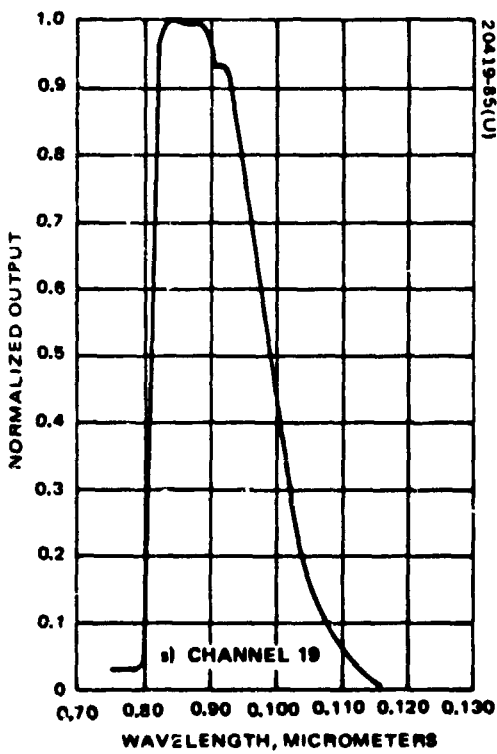
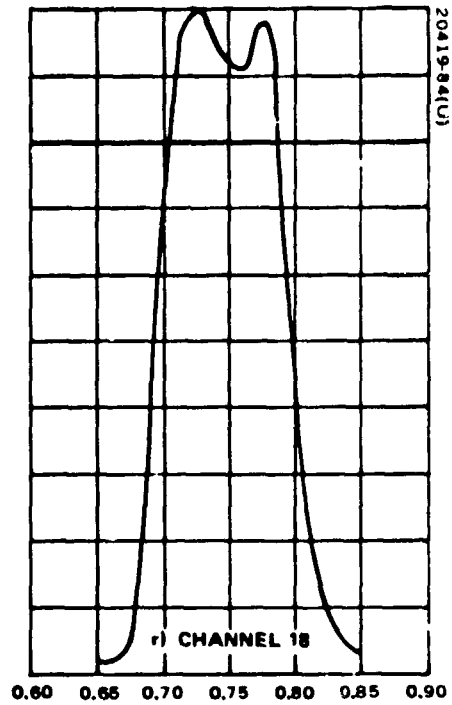
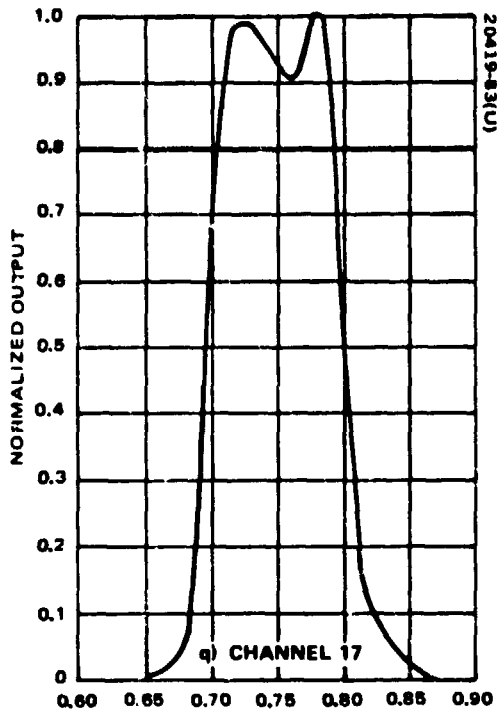


Figure 4-1 (continued). Prototype (S/N 001) Relative Spectral Response

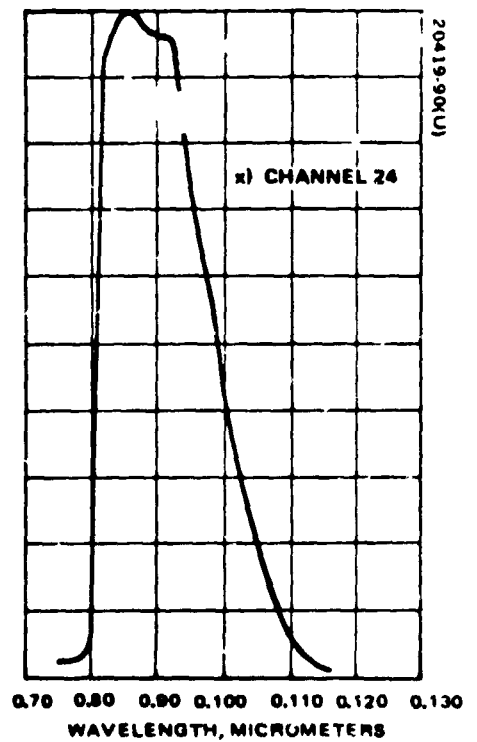
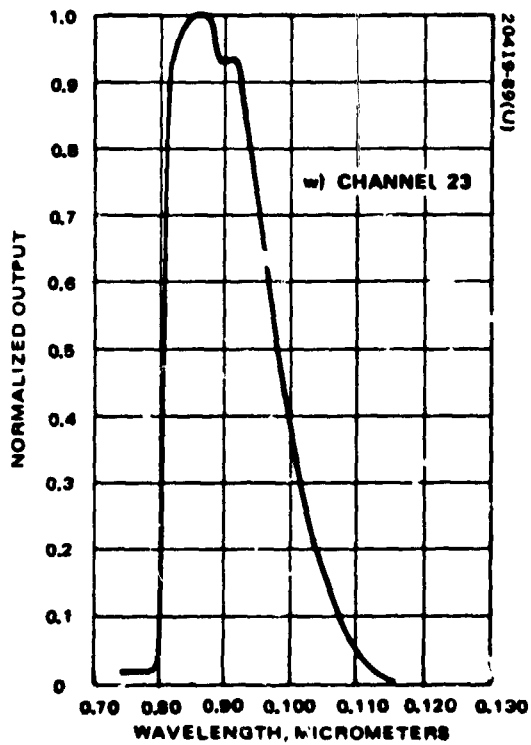
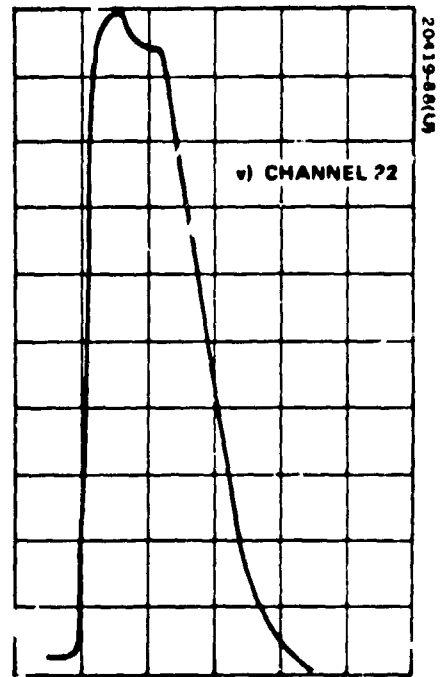
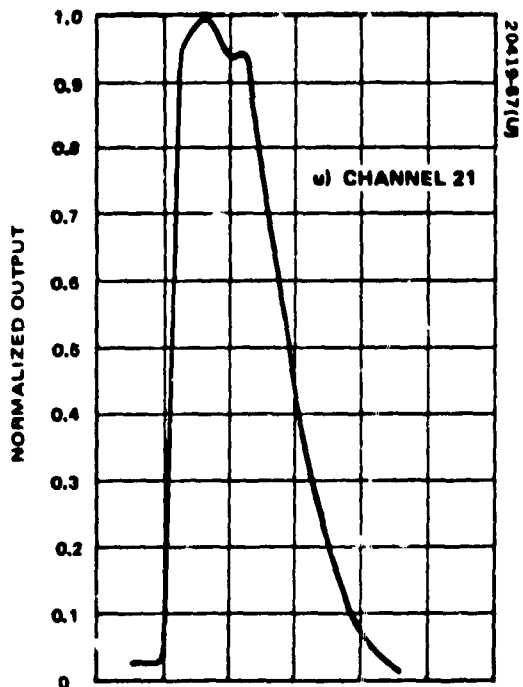


Figure 4-1 (continued). Prototype (S/N 001) Relative Spectral Response

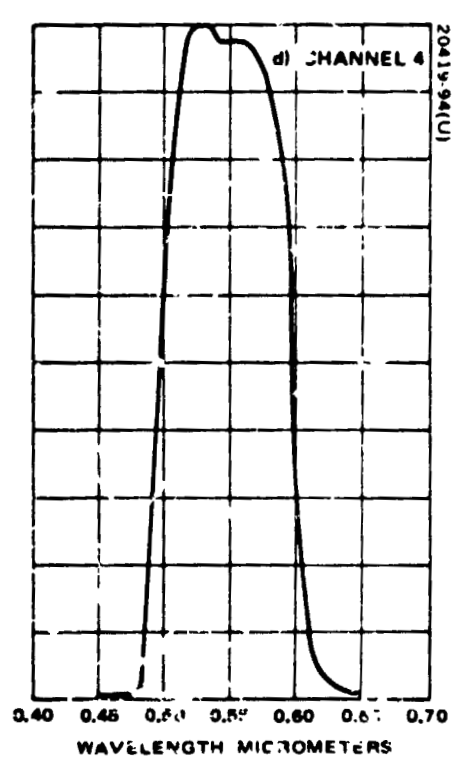
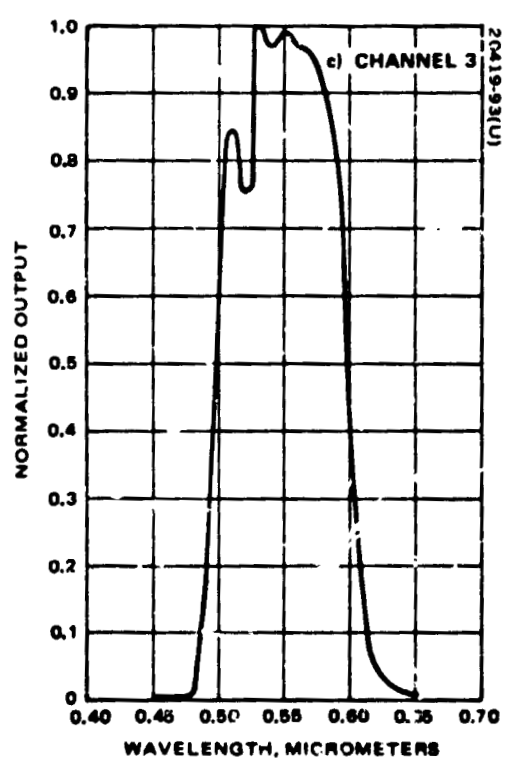
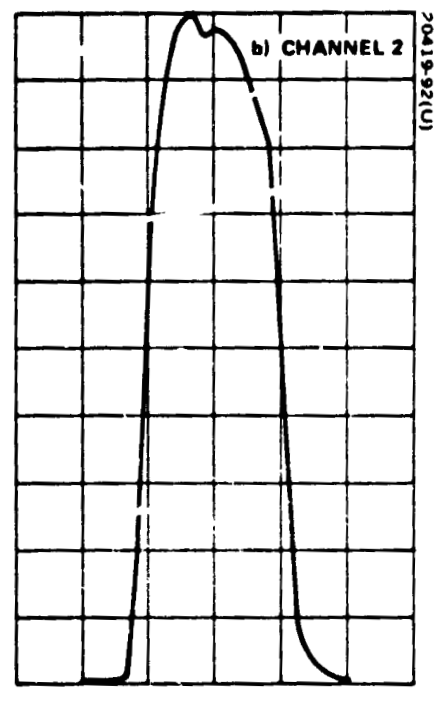
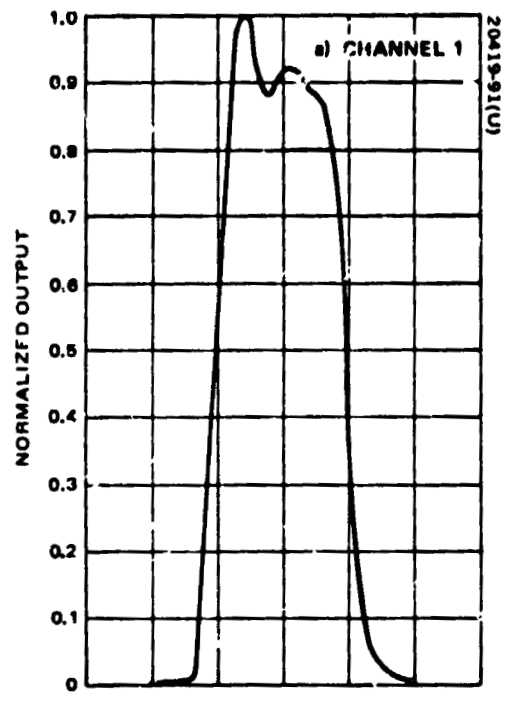


Figure 4.2. Backup (S/N 002) Relative Spectral Res. onse

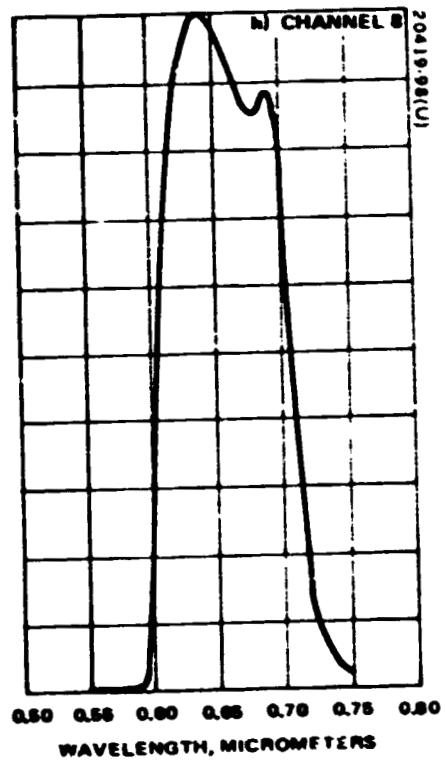
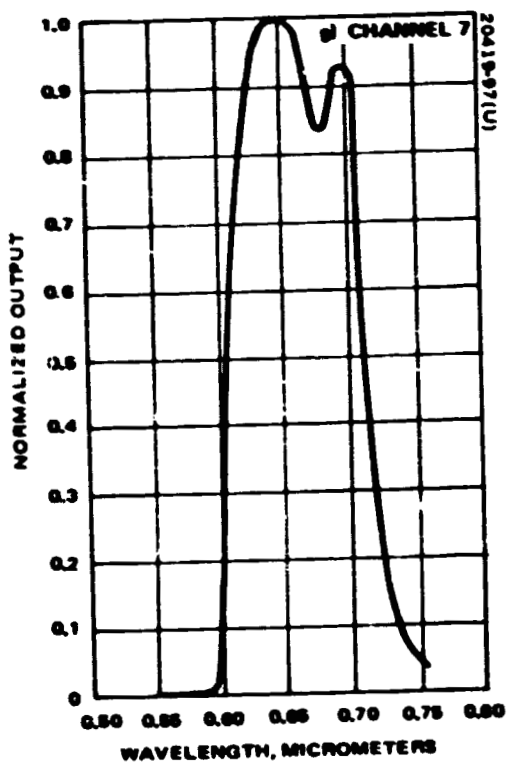
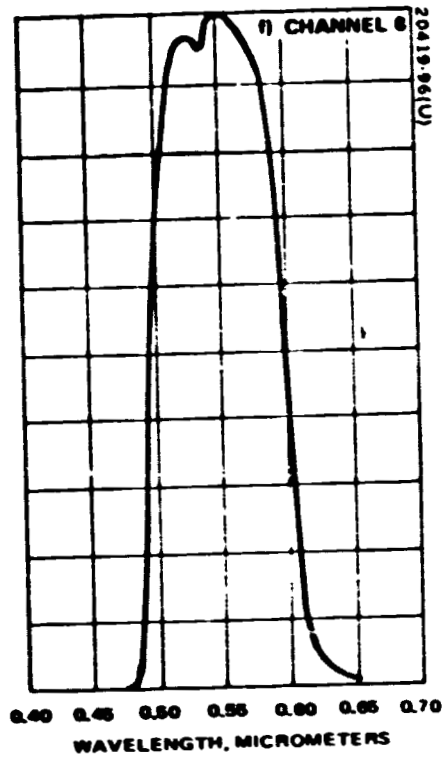
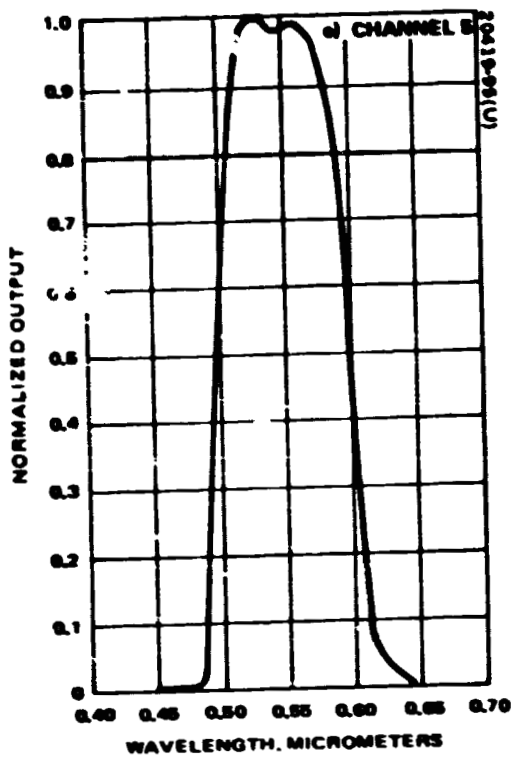


Figure 4-2 (continued). Backup (S/N 002) Relative Spectral Response

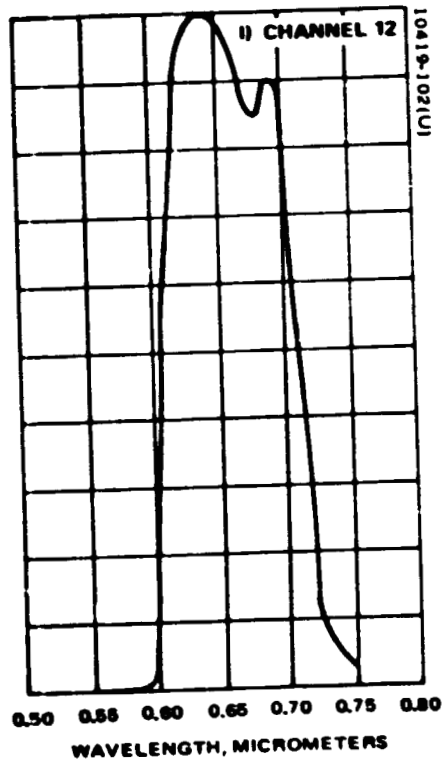
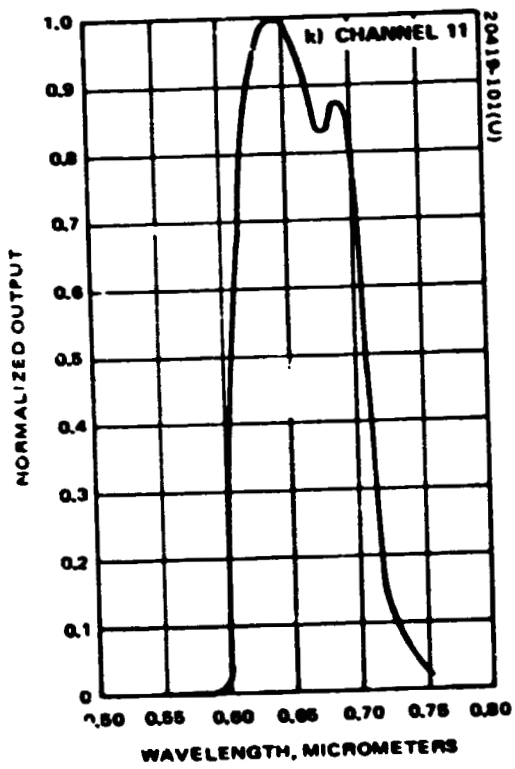
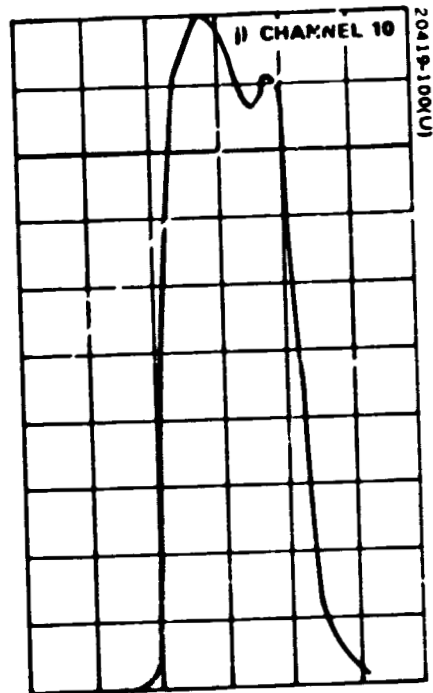
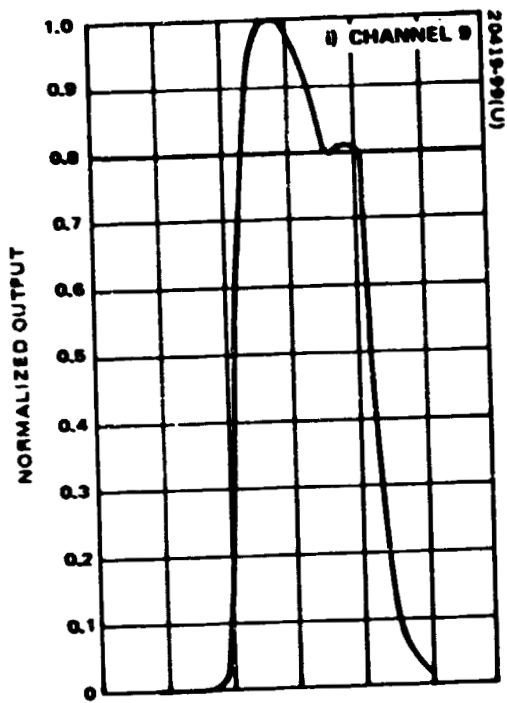


Figure 4-2 (continued). Backup (S/N 002) Relative Spectral Response

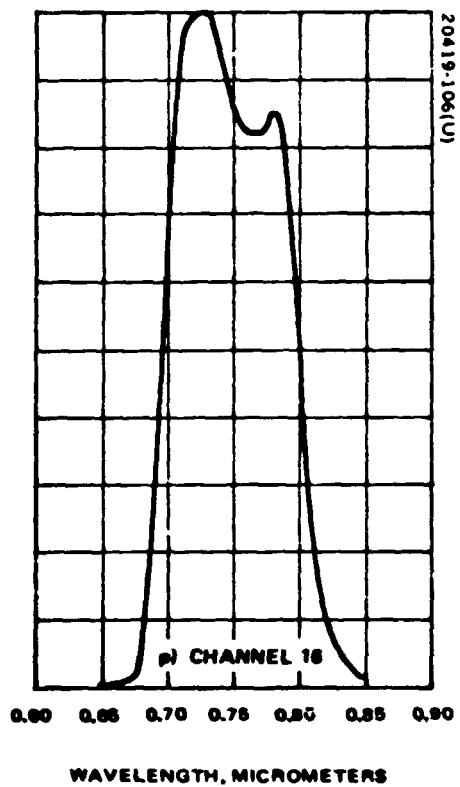
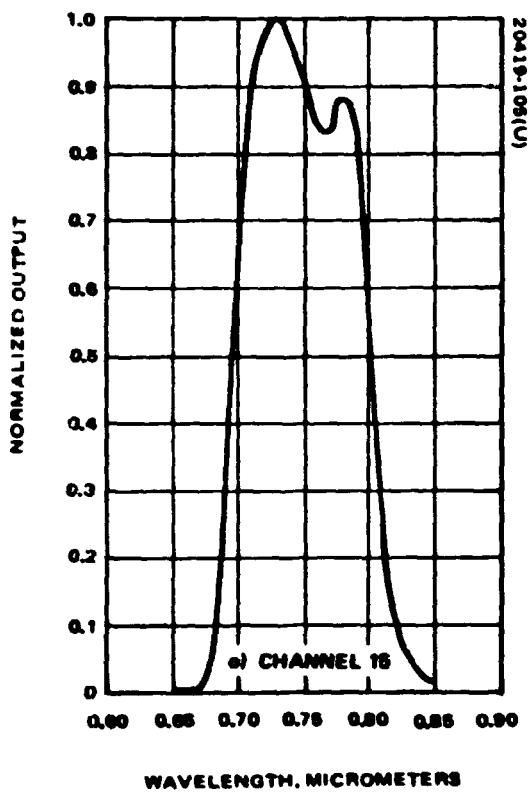
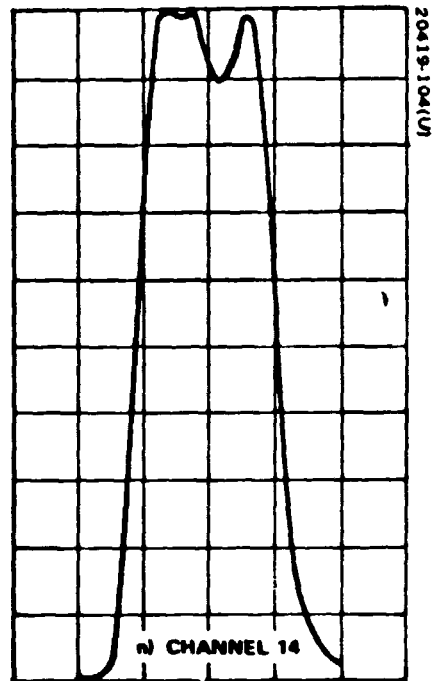
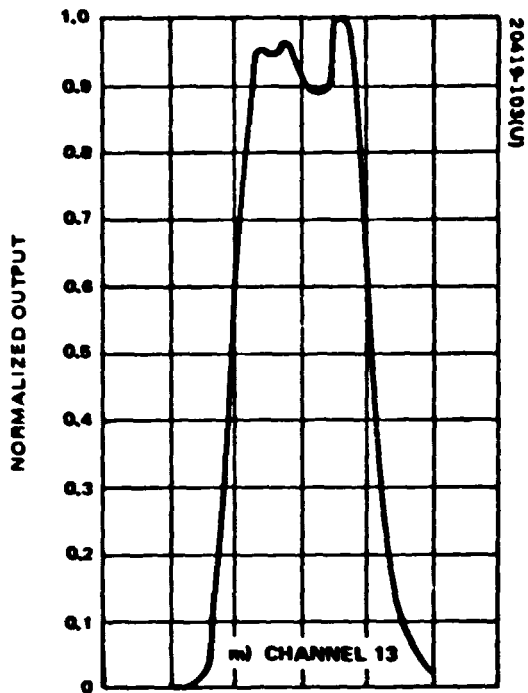


Figure 4-2 (continued). Backup (S/N 002) Relative Spectral Response

REPRODUCIBILITY OF THE ORIGINAL PAGE IS POOR.

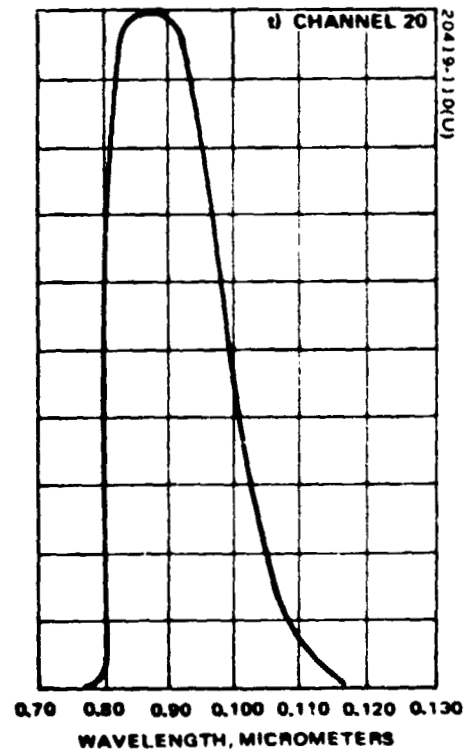
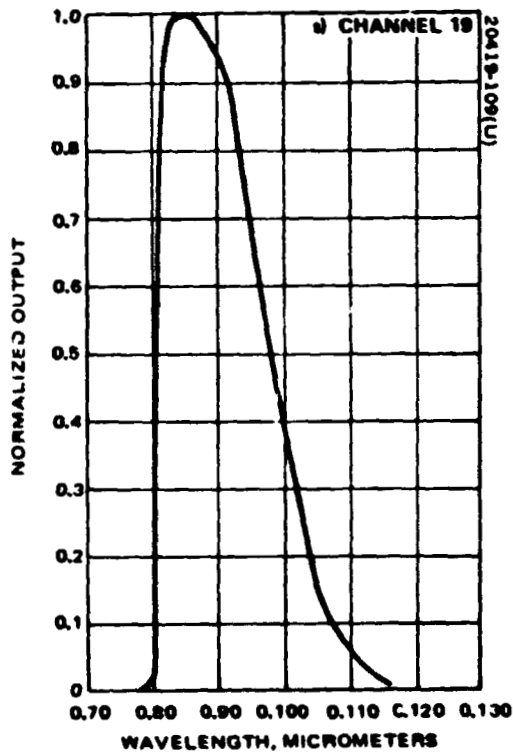
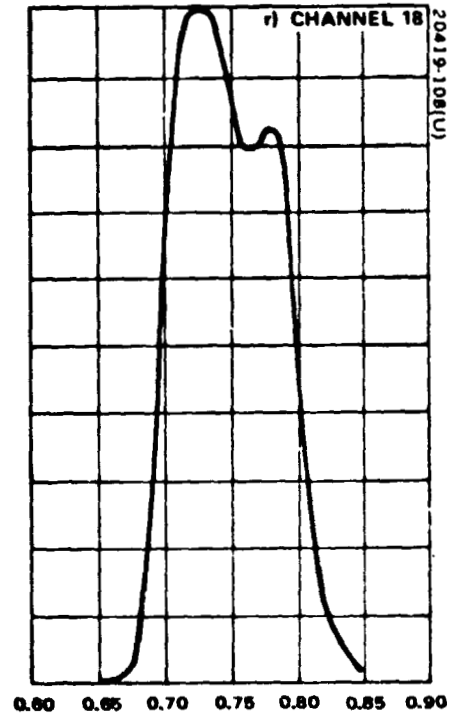
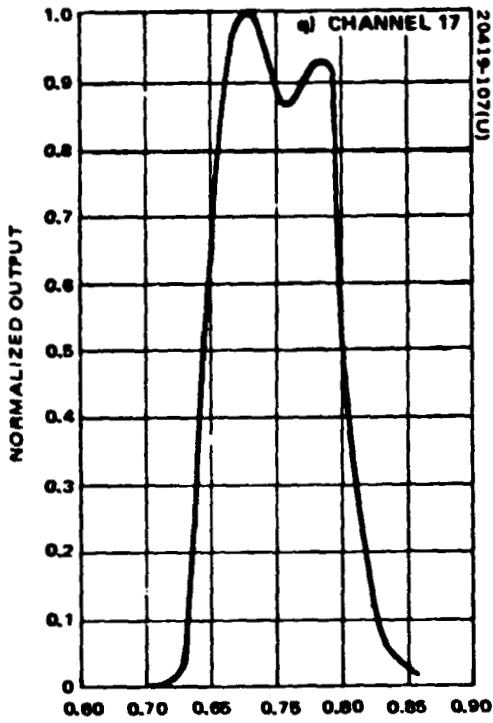


Figure 4-2 (continued). Backup (S/N 002) Relative Spectral Response

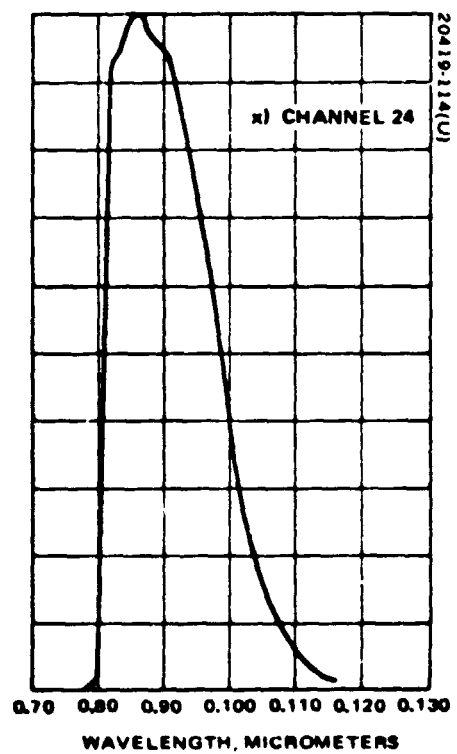
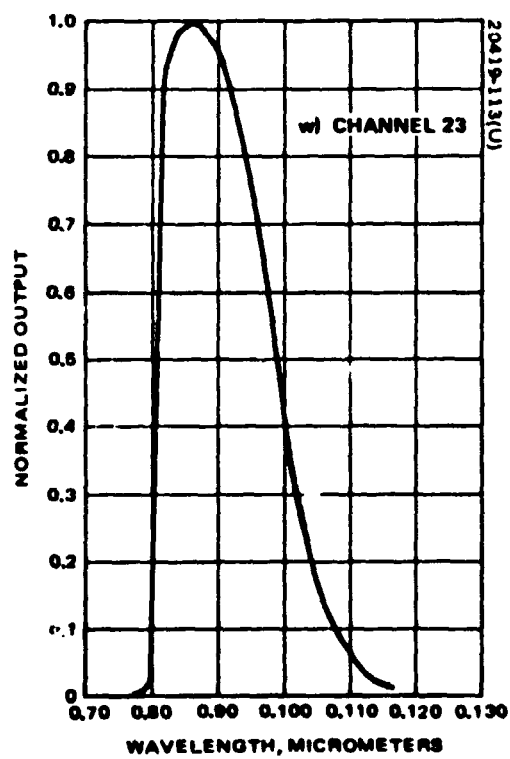
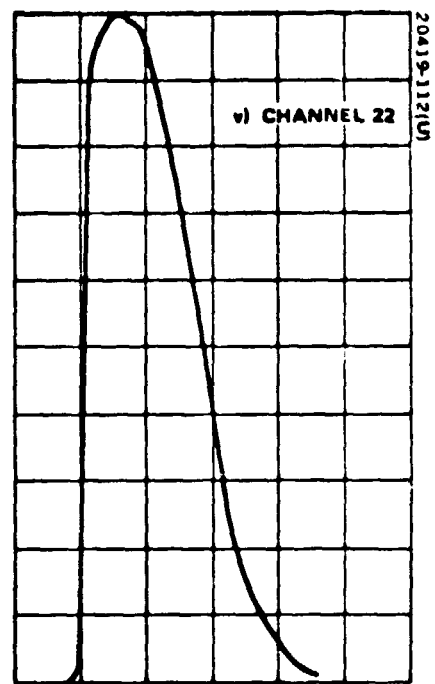
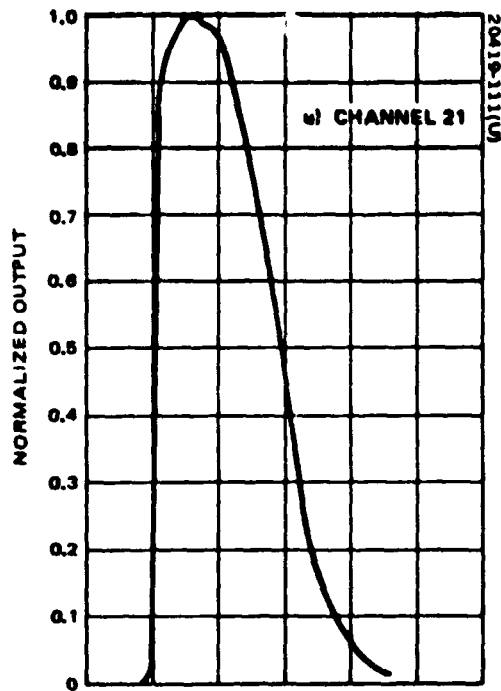


Figure 4-2 (continued). Backup (S/N 002) Relative Spectral Response

TABLE 4-1. RADIANCE NECESSARY TO PRODUCE FULL SCALE AT THE MULTIPLEXER OUTPUT
(mw/cm² · ster)

Channel	Band			
	1	2	3	4
A	2.45	1.86	1.84	4.81
B	2.43	1.95	1.68	4.80
C	2.34	1.94	1.73	4.76
D	2.33	1.87	1.80	4.74
E	2.39	1.92	1.74	4.70
F	2.35	1.96	1.78	4.70

4.2.3 Gain Factors - High Gain to Low Gain

The gain factors for the prototype and backup scanners is presented in Table 4-4. The data for the prototype is based on four orbits, while backup is based on two orbits.

4.3 REGISTRATION AND IFOV

The registration accuracy between bands is a function of the multiplexer sampling sequence, the scan profile, and the fiber matrix pattern. The instantaneous field of view (IFOV) of each channel is obtained from the telescope focal length and the dimensions of the optical fiber terminations in the fiber matrix. Calibration data for all these parameters for both the prototype and backup subsystems are presented in this section.

4.3.1 Multiplexer Sampling Sequence

The multiplexer sampling sequence is defined in Figure 3 of the Design Requirements Specification for MSS Spacecraft Equipment for ERTS, DR31324-001. The sequence is part of the design of the flight subsystem and not calibration data, but its existence and location is stated for the convenience of those calculating registration accuracy.

4.3.2 Scan Profile

The scan profile for the prototype and backup scan mechanisms is given in Figure 4-3. The figure is a plot of the difference between the displacement function and a truly linear displacement function which passes through the two end points of the curve. This figure was obtained by fitting

TABLE 4-2. SYSTEM NOMINAL GAIN AND OFFSET FROM
PRETHERMAL-VACUUM TESTING

Channel	Gain*	Offset**
1	25.4256	0.4280
2	25.0441	0.7415
3	25.8145	0.1360
4	26.2599	0.5285
5	24.2256	0.8345
6	24.8795	0.7265
7	34.4582	0.0605
8	30.8778	0.5155
9	32.4830	0.1050
10	32.8372	0.3605
11	33.0025	0.4345
12	30.5510	0.5830
13	37.6270	0.2365
14	36.2802	0.2515
15	38.6872	0.3040
16	34.7568	0.7470
17	37.3887	0.7755
18	36.5568	0.4790
19	13.9490	0.5055
20	13.8835	0.3020
21	13.8380	0.9910
22	13.7275	0.4275
23	14.1585	1.0745
24	14.1595	0.6890

*Quantum/mw cm⁻² ster⁻¹
**Quantum level

TABLE 4-3. INTEGRATING SPHERE CALIBRATION - NOVEMBER 1971
RADIANCE (mw/cm² ster) IN EACH OF FOUR BANDS

Band	Number of Lamps				
	12	4	3	2	1
1	20.951	7.058	5.194	3.507	1.686
2	37.350	12.553	9.218	6.278	3.059
3	51.232		12.726	8.484	4.242
4	178.667			29.676	14.847

TABLE 4-4. RATIO OF HIGH/LOW GAIN ($G_{H/L}$)

Channel	Prototype (S/N 001)		Delta	Backup (S/N 002)	
	Range*			Range**	
1	3.06 - 3.47		0.41	3.17 - 3.24	
2	3.03 - 3.09		0.06	2.87 - 3.11	
3	3.06 - 3.10		0.04	3.12 - 3.59	
4	3.009 - 3.05		0.04	3.14 - 3.71	
5	2.99 - 3.02		0.03	3.15 - 3.23	
6	2.67 - 3.09		0.42	3.16 - 3.33	
7	2.81 - 2.94		0.13	3.08 - 3.14	
8	2.91 - 2.95		0.04	2.49 - 31.2	
9	2.89 - 2.94		0.05	3.15 - 3.29	
10	2.90 - 2.94		0.04	3.14 - 3.42	
11	2.88 - 2.96		0.08	3.16 - 3.38	
12	2.92 - 2.98		0.06	3.009 - 3.47	

* Based on data from four orbits (1, 3, 5, 7)

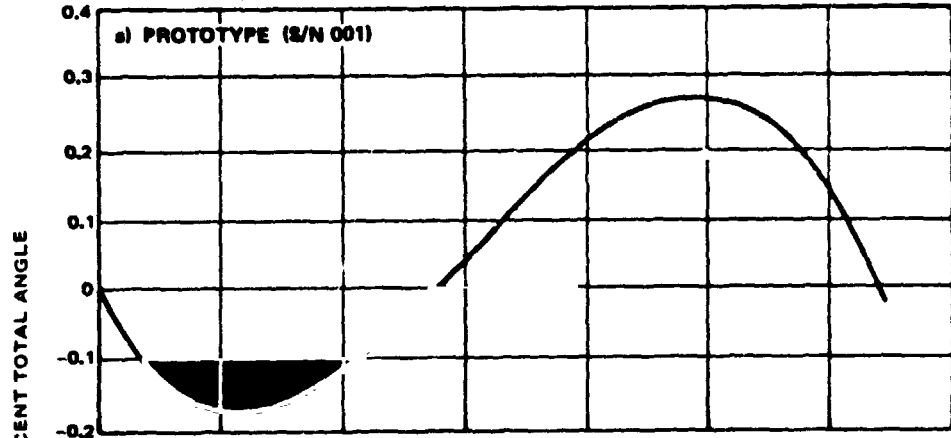
** Based on data from two orbits (102, 203)

$$\text{ERROR} = \left\{ \frac{[A \sin(\omega t + B) + C] - (\theta_s/t_s)}{\theta_s} \right\} 100$$

WHERE A = 0.384045 rad
 B = -0.261320 rad
 C = 0.096806 rad
 W = 16.8248 rad/sec = RADIANT NATURAL FREQUENCY
 θ_s = 0.201498 rad = TOTAL SCAN ANGLE
 t_s = 0.032130 sec = TOTAL SCAN PERIOD

20419-115(U)

THE TIME FROM LINE START TO MIDSCAN WAS 0.016036 sec



$$\text{ERROR} = \left\{ \frac{[A \sin(\omega t + B) + C] - (\theta_s/t_s)}{\theta_s} \right\} 100$$

WHERE A = 0.309540 rad
 B = -0.267250 rad
 C = 0.097588 rad
 W = 17.0903 rad/sec = RADIANT NATURAL FREQUENCY
 θ_s = 0.201586 rad = TOTAL SCAN ANGLE
 t_s = 0.032330 sec = TOTAL SCAN PERIOD

20419-116(U)

THE TIME FROM LINE START TO MIDSCAN WAS 0.016146 sec

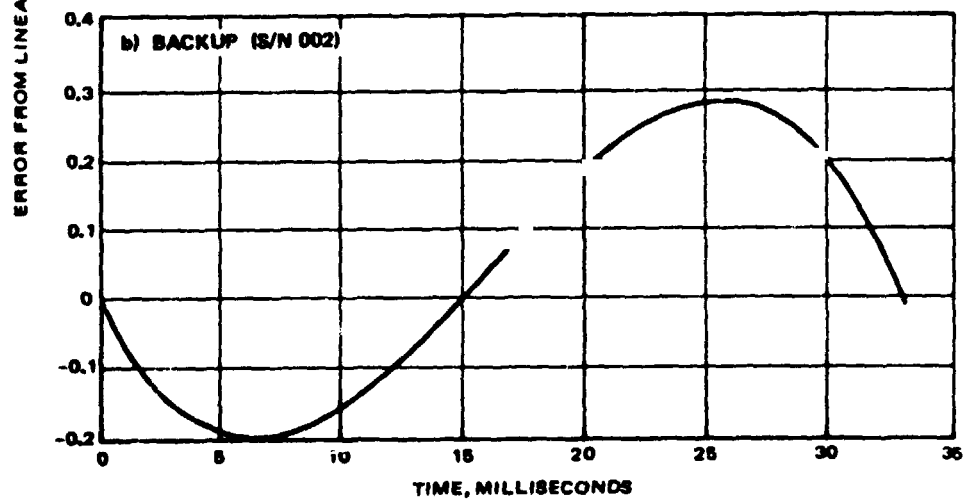


Figure 4-3. Scan Profile

a sinusoidal function to measurements of the time interval from the line start pulse to the midscan pulse, the line start to line end scan period, the scan angle given in 4.5.3, and the natural frequency given in 4.5.1. The analytical expressions are given in the figure.

4.3.3 Fiber Matrix Pattern

A polaroid picture and a drawing of the matrix array with dimensions for the prototype and backup fiber matrices are given in Figure 4-4. The dimensions on the drawing are actual measurements which were made from the polaroid pictures. The dimensions missing from the drawing can be obtained by scaling the new distances from the given dimensions.

4.3.4 Telescope Focal Length

The telescope focal length for the prototype is 32.32 inches and, for the backup, it is 32.4 inches.

4.4 MULTIPLEXER CALIBRATION

4.4.1 A/D Conversion Accuracy

A table for each scanner channel of the input voltage level corresponding to the threshold between adjacent quantum level outputs is given in HS324-5210. The data is given in both the compression and linear modes and at different temperature levels. The threshold (or decision) level between adjacent quantum level outputs is not a discrete voltage level, but occupies a small band of voltages. Maximum and minimum values for these bands are given in the tables.

4.4.2 Compression Amplifier Characteristics

The input/output characteristics of the compression amplifier can be obtained directly from the A/D conversion accuracy data described above. All the data in compression mode gives the relationship between input voltage level and output quantum level. The output quantum level can be transferred to output voltage by using the conversion from voltage level to quantum level presented in the linear mode data.

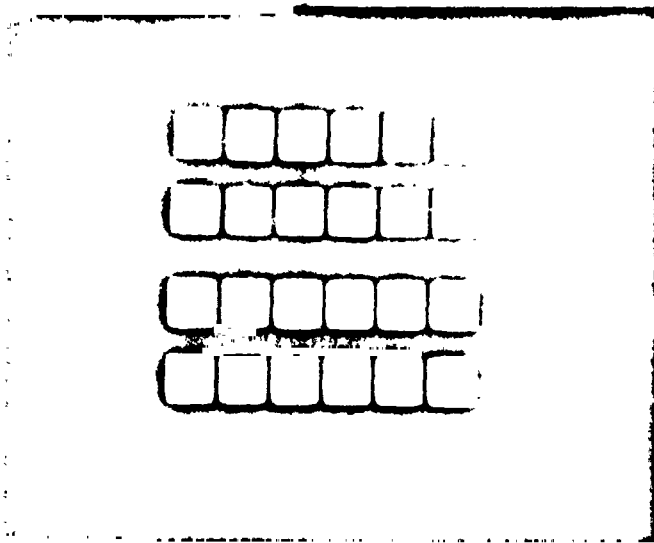
4.4.3 Sampling Frequency

The nominal sampling frequency is 100.4175 kilosamples/second.

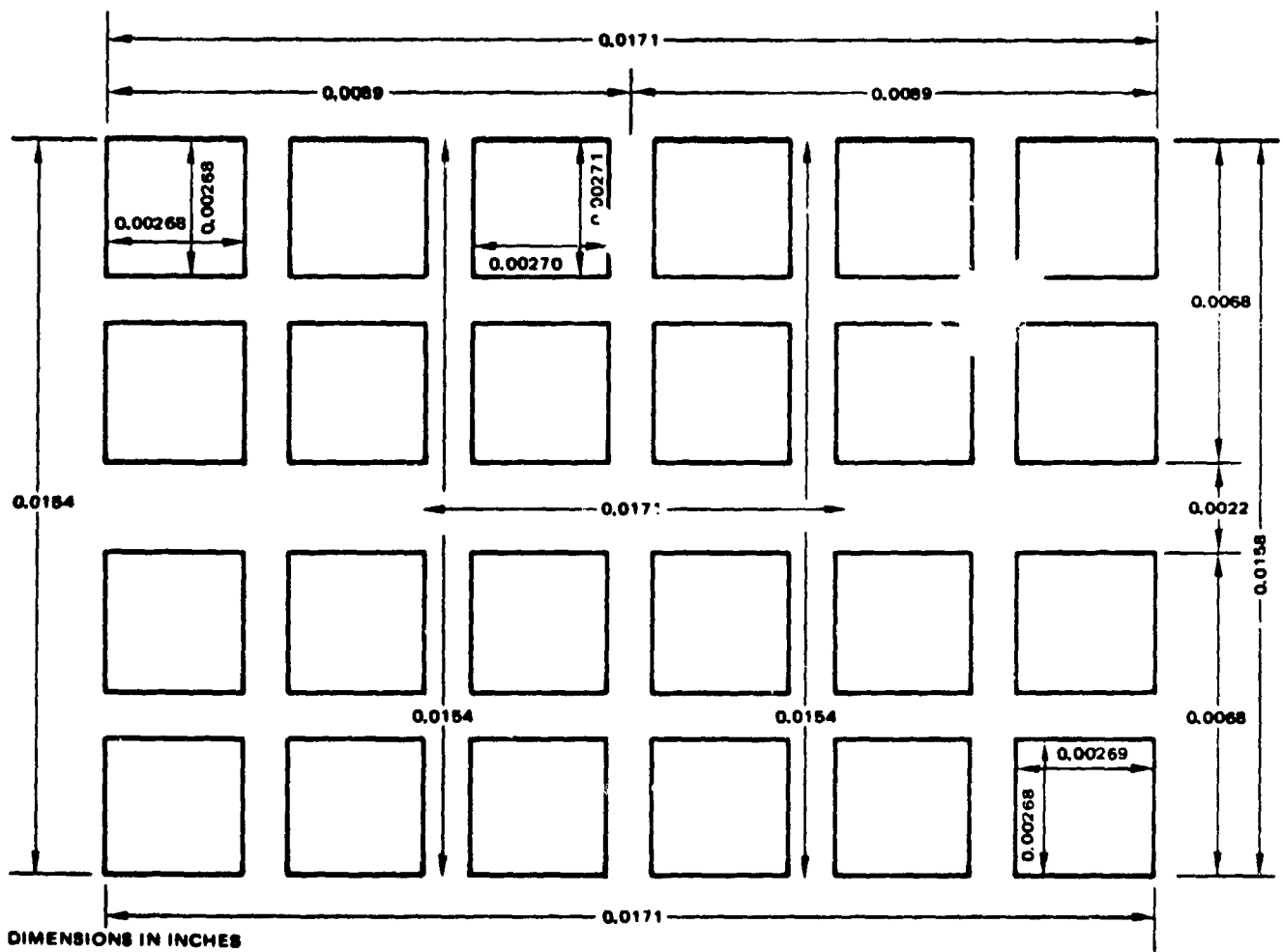
4.5 SCAN CHARACTERISTICS

The characteristics which describe the scan are the natural frequency of the scan mechanism, the time interval between the line start and line finish pulses (i. e., linear portion of scan mechanism scan profile), the scan angle, and the scan profile. Measurements of these parameters are given in this section, except for the scan profile which was presented in section 4.3.

2049-1181(1)



S/N 3



b) Backup Scanner

Figure 4-4 (continued). Fiber Matrix Pattern

4.5.1 Natural Frequency

The natural frequency of the prototype and backup scan mechanisms is 2.63 and 2.72 Hz, respectively. These frequencies are accurate to 5 percent.

4.5.2 Active Linear Period

The time interval between line start and line finish pulses for both the prototype and backup units is given in Table 4-5. These measurements were made during the thermal vacuum test cycle in system test.

4.5.3 Scan Angle

The scan angles for the prototype and backup subsystem are 11°32'43" and 11°31'0", respectively.

4.6 SUN CALIBRATION SYSTEM

The sun calibration system consists of a four-faceted mirror and an entrance aperture for each mirror facet. The characteristics of this system are presented in this section.

TABLE 4-5. ACTIVE LINEAR PERIOD DURING THERMAL VACUUM TESTS FOR PROTOTYPE AND BACKUP SUBSYSTEMS

Test	Prototype	Backup
0	32.1	*
5	*	32.4
10	32.1	32.3
15	32.1	*
20	32.0	32.3
25	32.0	*
30	32.0	32.3
35	*	32.2
40	31.9	*
*Data not taken		

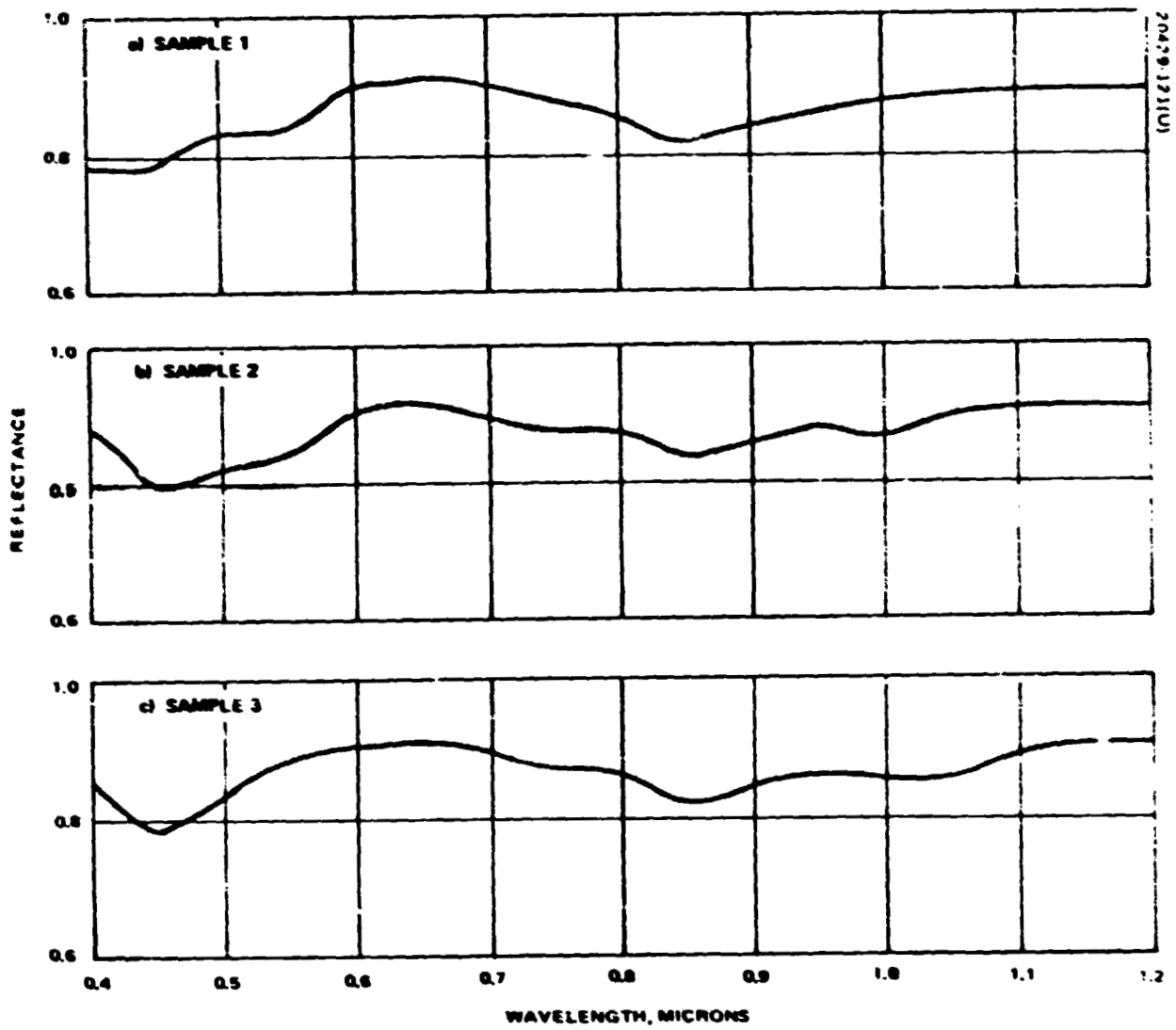


Figure 4-5. Prototype Sun Calibrate Witness Mirror

4.6.1 Aperture Dimensions

The prototype and backup sun calibrate apertures are all within the limits of 0.0196 to 0.020 inch. This variation produces a maximum spread in sun signal of ± 2 percent.

4.6.2 Mirror Reflectance

The spectral response of the reflectance of three witness mirror samples for the prototype four-faceted mirror is presented in Figure 4-5. The backup reflectance data is approximately the same. Averaging the three curves over the four bands gives the reflectance data shown in Table 4-6.

4.6.3 Mirror Alignment

The measured elevation and azimuth angles for the prototype and backup sun calibrate mirrors are presented in Table 4-7. The angles are defined in Figure 4-6. The nominal value stated in the table for reference information has a specified tolerance of ± 0.5 degree. The measurement accuracy is less than 5 minutes.

4.7 INTERNAL CALIBRATION SYSTEM

The internal calibration system uses redundant tungsten lamps and a neutral density filter (NDF). These elements are considered here.

4.7.1 Spectral Distribution of Tungsten Lamps

The spectral distribution of the tungsten lamps used in the prototype and backup systems were not measured. However, a typical spectrum for the type of tungsten lamp with filters used in these units is presented in Figure 4-7 for reference.

TABLE 4-6. REFLECTANCE FOR EACH BAND FROM WITNESS MIRROR SAMPLES FOR PROTOTYPE SCANNER

Band	Reflectance
1	0.85
2	0.90
3	0.88
4	0.86

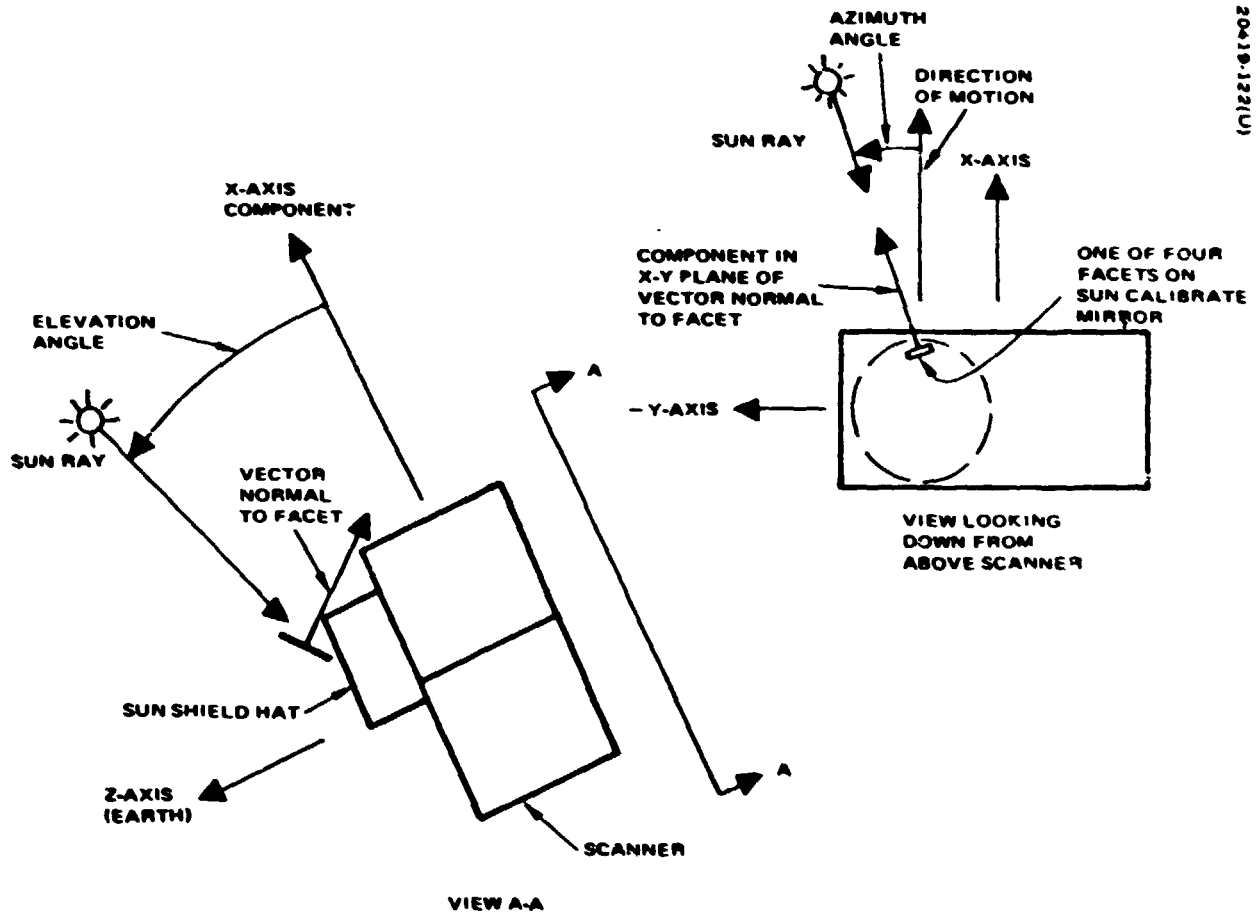


Figure 4-6. Sun Calibrate Mirror Angles

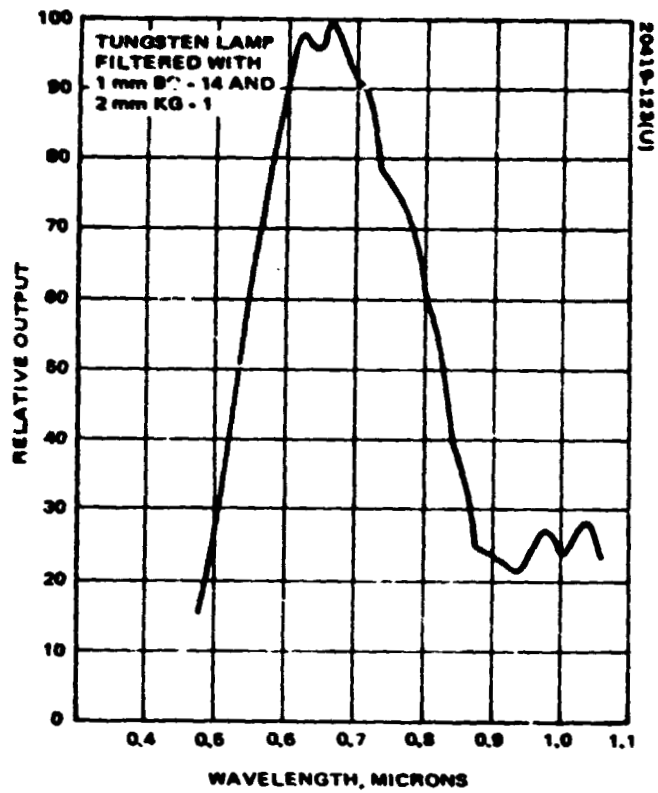


Figure 4-7. Relative Spectral Distribution of Calibration Lamps

TABLE 4-7. SUN CALIBRATE MIRROR ALIGNMENT ANGLES FOR PROTOTYPE AND BACKUP UNITS

Facet No.	Azimuth			Elevation		
	Nominal	Prototype	Backup	Nominal	Prototype	Backup
1	26°	25°59.35'	25°51.80'	19°	19°3.75'	19°3.70'
2	32°	31°57.00'	31°49.30'	19°	19°3.75'	19°3.70'
3	38°	37°51.50'	37°48.70'	19°	19°3.75'	19°3.70'
4	44°	43°51.50'	43°50.20'	19°	19°3.75'	19°3.70'

4.7.2 Neutral Density Filter

The density versus shutter wheel angle characteristics of the NDF at three different wavelengths are given in Figures 4-8 and 4-9 for the prototype and backup units, respectively. The wavelengths used for the measurements are 0.533, 0.8 and 1.0 micron.

4.8 TELEMETRY CALIBRATION

All the telemetry calibration data for the prototype flight subsystem is contained in the Flight Equipment, Operation and Maintenance Manual, Volume 1. The backup telemetry calibration data is essentially the same, so that the prototype data can be used for backup with negligible error.

4.9 SPECIAL ENGINEERING MODEL SUN CALIBRATE MEASUREMENTS

The response of the sun calibration function of the MSS Engineering Model was measured against the sun in a series of tests performed at the Jet Propulsion Laboratory Table Mountain Facility.

The solar spectral irradiance through the atmosphere was measured at the same time by GSFC personnel with equipment which had been used in a program of airborne solar measurements * Further information on the instruments can be found in the referenced article. The particular instruments, and the experimenters who operated them at Table Mountain, were the following:

- 1) Perkin-Elmer monochromator, M. P. Thekaekara, A. Winker.
- 2) Ångström pyrheliometer 7635, C. H. Duncan.

* Thekaekara, Kruger and Duncan, Appl. Opt. 8, 1713 (1969).

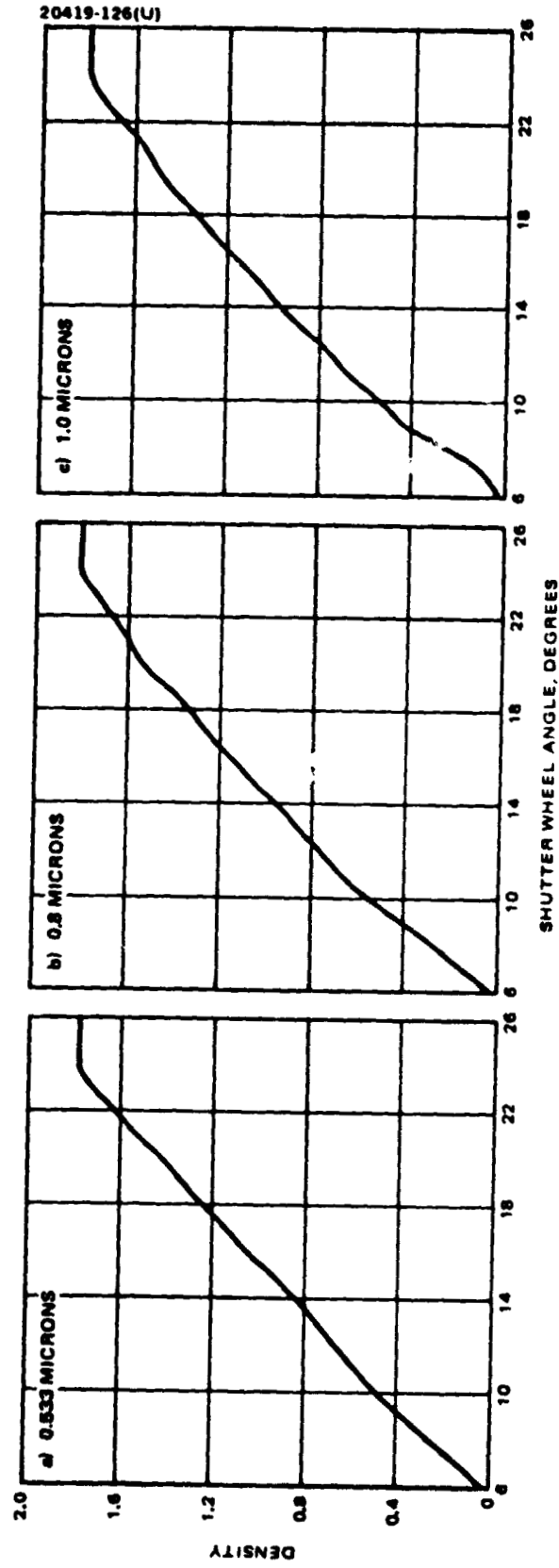


Figure 4-8. Neutral Density Filter For Prototype

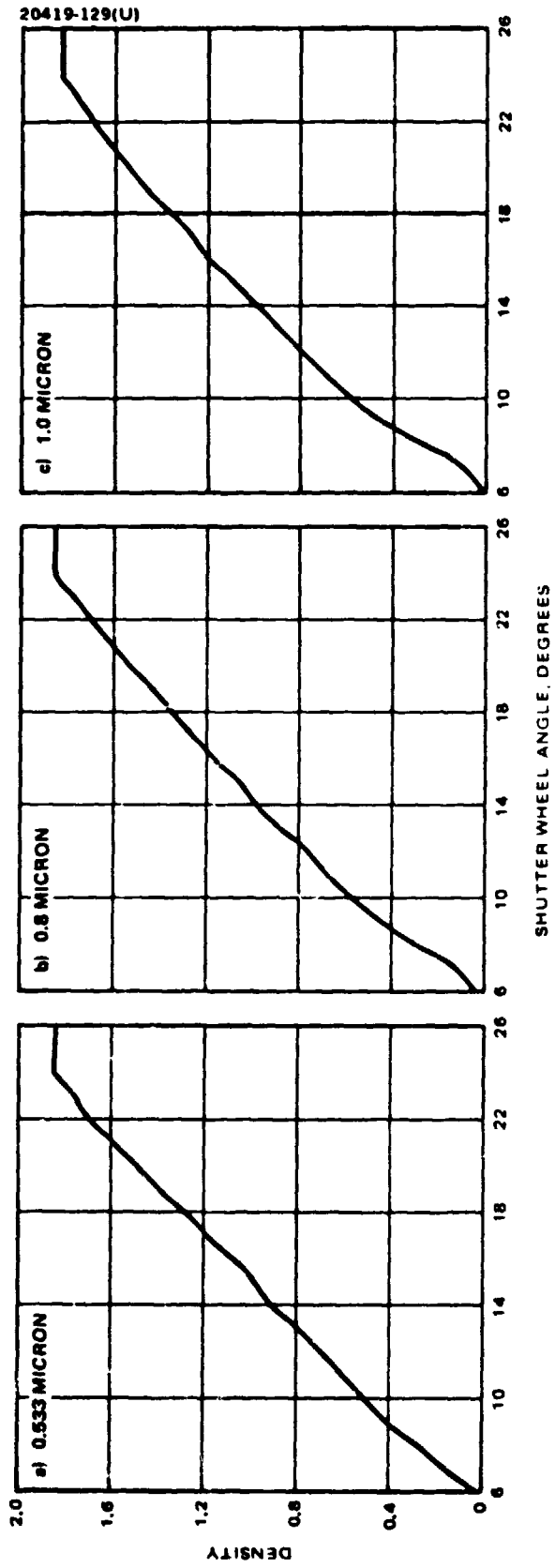


Figure 4-9. Neutral Density Filter For Flight A

3) Leiss monochromator, S. Parke.

The data was reduced by the experimenters and has been furnished for use in scanner data reduction.

The scanner output voltage is the integral over wavelength of the product of various scanner constants, the normalized spectral response, the solar spectral irradiance at the scanner, and other solar characteristics. If the ratio of voltage under the atmosphere to voltage outside the atmosphere is formed, for the scanner field of view centered on the solar disk, all factors cancel out except those which are wavelength dependent, leaving the form:

$$\frac{V}{V_o} = \frac{\int R(\lambda) H(\lambda) d\lambda}{\int R(\lambda) H_o(\lambda) d\lambda} \quad (1)$$

where

V = voltage under the atmosphere

R(λ) = the normalized spectral response of the scanner

H(λ) = solar spectral irradiance under the atmosphere

Subscript o indicates outside the atmosphere.

A typical R(λ) was selected for each band and the indicated integrations performed using H(λ) values supplied by Dr. Thekaekara. The resulting ratios appear in Table 4-8.

From Table 4-8 a set of atmospheric extinction coefficients was generated satisfying the equation

$$V/V_o = e^{-K \sec Z} \quad (2)$$

where

K = extinction coefficient

Z = sun zenith angle

The values of K are tabulated, including averages for each band, in Table 4-9.

Equation 2 was used to translate all voltage measurements outside the atmosphere.

TABLE 4-8. ATMOSPHERIC TRANSMISSION

MSS Band	Sec Z		
	1.4	1.5	1.6
1	0.817	0.804	0.793
2	0.881	0.873	0.866
3	0.923	0.919	0.912
4	0.905	0.899	0.893

TABLE 4-9. EXTINCTION COEFFICIENT

MSS Band	Sec Z			
	1.4	1.5	1.6	Average
1	0.1493	0.1448	0.1443	0.1461
2	0.0911	0.0908	0.0906	0.0908
3	0.0562	0.0568	0.0578	0.0569
4	0.0706	0.0708	0.0708	0.0707

The measurements made may be summarized as follows:

- 1) Test conditions:
 - a) Scanner on the special mounting described above
 - b) The main aperture was covered, giving no signal
 - c) Scan mirror operating
 - d) Rotating shutter operating
 - e) Low gain
- 2) Test procedure:
 - a) Select a representative channel for each band
 - b) Photograph output from the calibration wedges

- c) Measure sun output on the channels for each of the four sun calibrate channels
- d) Repeat (c), and photograph the sun pulse in each case
- e) On one facet, measure sun output for all channels
- f) Measure the sun apertures

Several repetitions of (c) above were made at different times. The values of output voltage obtained were translated outside the atmosphere as described above and all runs averaged. These were then corrected for the aperture size, to the nominal aperture used in the prototype and backup scanners, and then corrected to nominal gain (4.0 volts for the specification maximum scene), using the last available gain measurement (5/71). The results of this process are shown in Table 4-10. The facet numbering starts with the one nearest the X axis. The "calculated fraction" column of this table results from correcting values previously calculated* to the prototype - backup aperture sizes. The agreement between the corrected measured values and the calculated values is remarkable, considering that the measurements were made only to the nearest 5 percent.

The measurements of (e) in the above procedure were performed twice, and the results used as an indication of gain relative to nominal shown in Table 4-11. From this table, the assumed relative gain of channel 1A may be high, since the other channels are all high compared to the previously measured gain. This comment would also apply to channel 2A.

TABLE 4-10. PREDICTED SOLAR RESPONSE OF MSS SCANNERS FROM ENGINEERING MODEL TESTS AND FROM CALCULATIONS

Spectral Band	Corrected Exoatmospheric Voltage					Fraction of Full Scale	Calculated Fraction
	Facet 1	Facet 2	Facet 3	Facet 4	Average		
1	2.83	2.71	2.74	2.80	2.77	0.69	0.68
2	2.77	2.68	2.69	2.75	2.72	0.68	0.72
3	2.48	2.38	2.40	2.50	2.44	0.61	0.64
4	1.76	1.71	1.79	1.73	1.75	0.44	0.46

* J. Lansing, "Sun Calibration Signals," SBRC Memo HS324-1967A, dated 22 December 1971.

TABLE 4-11. ALL-CHANNEL MEASUREMENTS

Band	Channel	Corrected Voltage Exoatmosphere			Relative Gain*	Relative Gain as Measured in April 1971
		1st Run	2rd Run	Average		
1	A	2.82	2.60	2.71	0.99	0.99
	B	2.93	2.60	2.76	1.01	0.98
	C	2.93	2.72	2.82	1.03	0.97
	D	3.27	3.07	3.17	1.16	1.03
	E	3.50	3.19	3.35	1.23	0.98
	F	2.93	2.72	2.82	1.03	0.99
2	A	2.61	2.52	2.56	0.96	0.96
	B	3.02	2.74	2.88	1.08	0.98
	C	2.71	2.57	2.64	0.99	0.95
	D	2.81	2.63	2.72	1.04	0.97
	E	3.02	2.74	2.88	1.08	0.99
	F	3.44	3.18	3.31	1.24	1.02
3	A	2.28	2.30	2.29	0.96	0.96
	B	2.48	2.41	2.44	1.02	0.97
	C	2.08	2.09	2.08	0.87	0.95
	D	2.38	2.35	2.36	0.99	0.98
	E	2.28	2.20	2.24	0.94	0.99
	F	2.58	2.41	2.49	1.04	0.96
4	A	1.82	1.92	1.87	1.03	--
	B	1.62	1.81	1.71	0.95	--
	C	1.92	2.13	2.02	1.12	1.20
	D	2.32	2.34	2.33	1.29	1.27
	E	1.92	1.92	1.92	1.06	1.06
	F	Noisy	Noisy	Noisy	Noisy	Noisy

*The boxed value is assumed and the other values in the band are relative to it.

The photographs of step 4 of the procedure are shown in Figure 4-10. The general shape and width of the pulses are as expected. The departures from smooth shape, aside from the electronic noise, which is particularly obvious in band 4, appear to be caused by dirt and defects in the optics. The points in the optics traversed by the rays producing the different pictures of Figure 4-10 are not necessarily the same. For different facets the points are necessarily different.

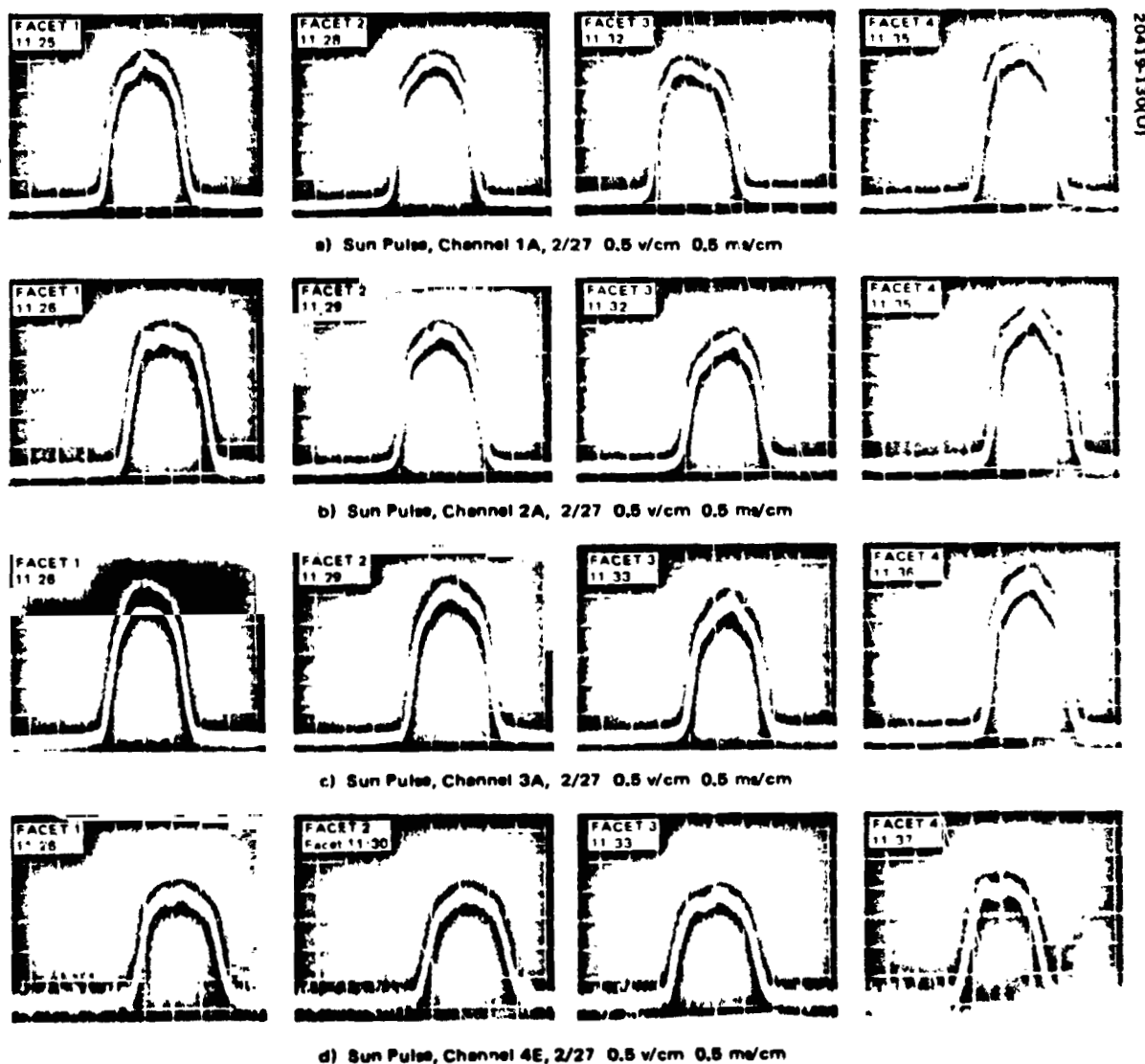


Figure 4-10. Sun Pulse Photographs. Scale 0.5 volts and 0.5 ms Per Major Reticule Divisions.

REPRODUCIBILITY OF THE ORIGINAL PAGE IS POOR.

In Figure 4-11 the scanner pointing was changed slightly between the two pictures so that the sun pulse was shifted, while the dip in the sun pulse remained at the same point, as indicated by the time relationship to the end-of-scan pulse, also on the photographs.

Figure 4-12 shows an area of the scan selected for obvious defects, by moving the scanner pointing about while observing the oscilloscope. Later the scanner was studied visually and an abraded area was apparent on the primary mirror at the location this sun ray would reflect from.

The Engineering Model optics were noticeably dirty, and less of the variations observed in these pictures would be expected in the flight (S/N 001, 002) units.

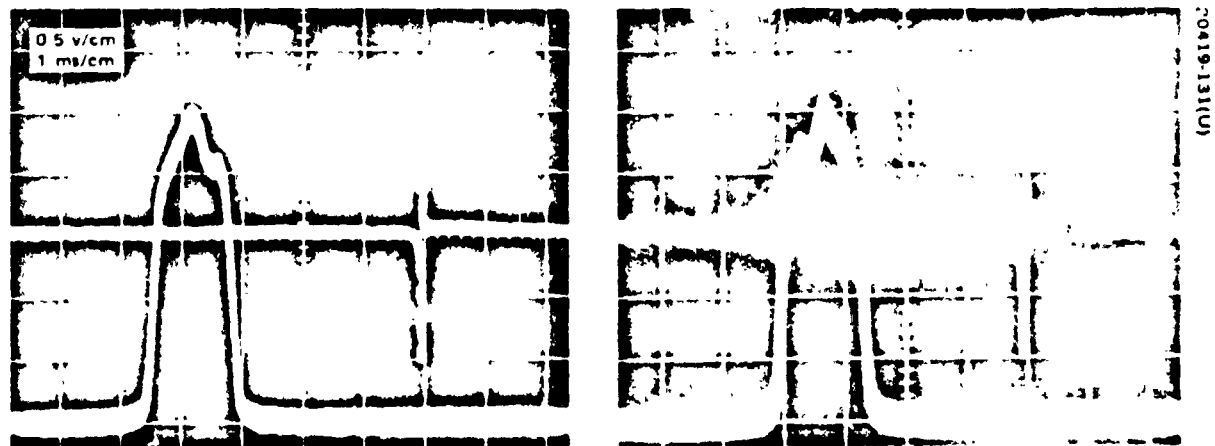


Figure 4-11. Sun Pulses Showing Stationary Defect and End of Scan

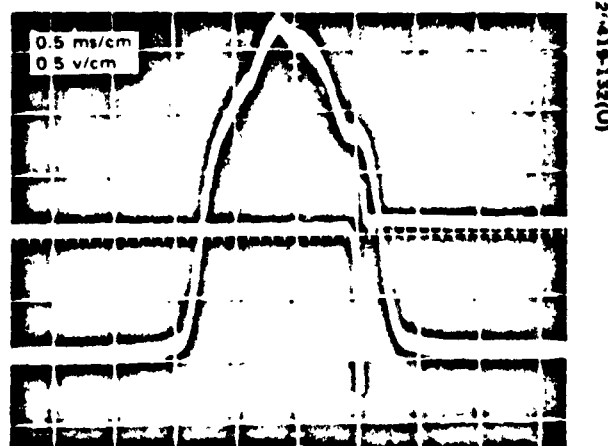


Figure 4-12. Example of Defects End of Scan Pulse Shown

5. PERFORMANCE EVALUATION

A comprehensive evaluation of the MSS subsystem performance has been accomplished during the environmental qualification and acceptance testing of two MSS subsystems; i. e. , the prototype subsystem (S/N 001) and the backup subsystem (S/N 002). The results of these tests are summarized in this section. More complete details may be found in the Environmental Qualification Test Report (HS324-4859) and the Environmental Acceptance Test Report (HS324-5196).

5.1 PROTOTYPE SUBSYSTEM (S/N 001) TEST PROGRAM SUMMARY

The environmental qualification test program was initiated with a low-level sinusoidal vibration test of the scanner to determine structural resonances and provide some confidence prior to qualification level vibration. This test was followed by establishment of a pre-environmental performance baseline in the long form performance test (LFPT). This was followed by environmental exposure (EMI, vibration, and thermal vacuum) and was concluded with a final performance baseline LFPT prior to delivery to the spacecraft.

The performance during the subsystem environmental qualification testing was verified by extensive measurements of all significant performance parameters at regular intervals throughout the test program. Measurements were made before and after every environmental exposure and during those exposures where in-orbit operation is required (i. e. , EMI and thermal vacuum).

Some anomalies were uncovered during vibration and thermal-vacuum exposures which required rework and retest. Performance measurements made at the completion of the rework and retest indicated that the revised configuration suffered no detectable degradation or significant performance anomalies either before and after or during environmental exposure. The subsystem exhibited no performance anomalies during subsequent spacecraft environmental testing, which included acceptance vibration, EMI interference tests, and two thermal-vacuum exposures. Performance measurements made at the conclusion of spacecraft testing prior to shipment to WTR verified that performance was essentially unchanged from the time of completion of subsystem environmental testing.

Two significant deviations to the planned subsystem environmental test sequence were required because of performance anomalies. The planned three axis qualification vibration test was interrupted after the Z and Y-axis and before the X-axis vibrations because of the failure of a relay in the scanner. The relay was replaced and the scanner successfully completed the X-axis vibration. An exhaustive review of the failed relay revealed no component or system design deficiencies; however, a redundant relay was subsequently designed and assembled into the system to provide additional reliability.

The second major deviation to the planned test program was the division of the thermal-vacuum test into two exposures because of three major problems; i. e. , improper scan monitor performance, a PMT failure in channel 13, and marginal signal-to-noise performance. The scan monitor anomaly was the result of initial optical-mechanical misalignments caused by improper mechanical interface between the sun shield and the scanner structure. This initial misalignment caused a mechanical distortion which was aggravated by thermal gradients at the cold temperature extremes in thermal-vacuum. The mechanical interface was redesigned to provide a more precise mechanical interface fit; performance during a special thermal cycle test and during the second thermal-vacuum exposure verified that the scan monitor met all operational requirements.

The PMT failure (a cracked glass envelope) was attributed to mechanical stresses caused by thermal expansion action of the conetic shield, epoxy coating, and glass envelope. The crack occurred because of an envelope scratch incurred in the manufacturing process which, on this particular assembly, was serious enough to result in a failure. A comprehensive review of the manufacturing processes and thermal cycling data on all other PMT assemblies indicated a low probability of occurrence of similar failures in remaining PMT assemblies. Channel 13 PMT was replaced and performance was verified during the second thermal-vacuum exposure.

The signal-to-noise anomaly was caused by 100 kHz noise interference in the video outputs which were generated in the inverter of the scanner power supply. Isolation of this noise from the video was achieved by reducing the inverter switching current transient (by adding an inductor current limiter) and isolating the high voltage power supply from the inverter (by adding an isolation transformer). Signal-to-noise performance verification was accomplished by measurements in all channels at many different light levels in all modes of operation during the second thermal-vacuum exposure and in the post thermal-vacuum LFPT.

During the second thermal-vacuum exposure, intermittent arcing observed in the video output at channel 9 resulted in the replacement of the PMT after thermal-vacuum. This failure was due to a break in the high voltage lead to the PMT, which pressed the shield sufficiently close to the center conductor to cause intermittent arcing. The break apparently occurred sometime during the assembly of the scanner; an examination of all other PMT assemblies at the time of replacement verified that similar problems

were not present. Performance verification under thermal-vacuum conditions was accomplished subsequently during two exposures at the spacecraft level.

5.2 PROTOTYPE SUBSYSTEM (S/N 001) PERFORMANCE RESULTS

Performance evaluation during the environmental test program was accomplished through an extensive series of repetitive performance measurement before, during, and after each environmental exposure. This provided a continuous assessment of performance and resulted in a massive quantity of measurement data under all types of conditions. The historical performance during significant events in the test sequence is contained in the Qualification Test Report; however, Table 5-1 compiled from the final LFPT prior to spacecraft delivery, represents performance which can be expected in orbit under operational condition.

5.3 BACKUP SUBSYSTEM (S/N 002) TEST PROGRAM SUMMARY

Subsystem S/N 002 environmental acceptance test program was initiated with the LFPT which established the pre-environmental performance baseline. This was followed by environmental exposure (vibration, thermal-vacuum, and EMI) and was concluded with the final performance baseline LFPT prior to delivery. The MSS subsystem was then delivered to GSFC for special magnetic radiation and moment tests and finally delivered to the spacecraft contractor's facility.

As in the test program for S/N 001, the performance of S/N 002 was verified by extensive measurements of all significant system parameters at regular intervals throughout the environmental test program. Measurements were made before and after every environmental exposure and during those exposures where in-orbit operation is required: i. e., thermal-vacuum and EMI. These measurements indicate that the subsystem suffered no detectable degradation or significant anomalies either before and after or during environmental exposure.

One significant deviation from the planned environmental test sequence was required. The planned thermal-vacuum exposure was divided into two separate exposures because of an optical/mechanical misalignment in the scan monitor subsystem which resulted in a performance anomaly when the system was exposed to cold temperature extremes (only in redundancy configuration B). The subsystem was removed from the environment and alignment was improved to provide more margin at nominal temperatures. The MSS subsystem was then reexposed to the thermal-vacuum environment and satisfactorily met all scan monitor and other performance requirements. A minor anomaly in the scan monitor was noted at the cold temperature extremes; however, it was not considered significant because it would not influence mission performance; furthermore, adequate margins were demonstrated at operational temperature extremes.

TABLE 5-1. CHARACTERISTIC PERFORMANCE SUMMARY MSS SUBSYSTEM S/N 001

Characteristic	Requirement	Performance
Scan repeatability, microradian	24 maximum	4
Cross-axis variation, microradian	33 maximum	3
Modulation transfer function (MTF)	0.35 minimum	0.42
Internal calibration system performance (corrected signal stability)		
Absolute stability, percent (over an orbit)	±2 maximum	Data unavailable
Channel-to-channel, percent (picture striping)	±1 maximum	2.4*
Band-to-band, percent (relative radiometric accuracy)	±1.5 maximum	3.6**
Signal-to-noise (S/N)		
Band 1 (at 2.48 mw/cm ² ster.)	71 minimum	112.9
Band 2 (at 2.00 mw/cm ² ster.)	57 minimum	86.2
Band 3 (at 1.76 mw/cm ² ster.)	38 minimum	72.1
Band 4 (at 4.60 mw/cm ² ster.)	77 minimum	122.6
GPE picture quality (at simulated orbital conditions)		
Interference:		
Wood grain: barely visible, acceptable		
Microphonics: barely visible, acceptable		
Video correction: complete compensation for gain variations		

*GE Launch Readiness Review, May, 1972, pp 6-9.

**GE Public Information Release, ERTS 214, March 15, 1972.

An additional adjustment, (i. e., the internal calibration signal level) was made to the subsystem configuration near the beginning of the environmental testing. After a series of tests, it was concluded that a more optimum tradeoff of dynamic range in this signal could be achieved between the low and high gain modes. This adjustment was not the result of any degradation or environmental exposure and may possibly have been acceptable without readjustment. However, to ensure greater margin under all expected environmental extremes (temperature, vacuum, etc.), the adjustment was made to provide an increased dynamic range in the high gain mode. The performance at the adjusted level was verified during both thermal-vacuum exposures. The adjustment required a change to the value of one resistor.

5.4 BACKUP SUBSYSTEM (S/N 002) PERFORMANCE RESULTS

Based on the measurements made during the acceptance test program, Table 5-2 has been compiled to illustrate the characteristic performance of MSS subsystem S/N 002. Performance measurements were made under a wide variety of conditions (temperature, pressure, electromagnetic radiation, etc.); Table 5-2 is a composite summary which is illustrative of the performance which can be expected in orbit.

5.5 TYPICAL S/N AND MTF PERFORMANCE

The S/N performance indicated in Tables 5-1 and 5-2 is a summary of measurements made on all 24 channels. Typical measured signal, noise, and S/N values for each of the 24 channels under all modes of operation for subsystem S/N 001 and 002 are included in Tables 5-3 and 5-4, respectively. The measurements have been made from the subsystem response to specific radiance inputs available from the test collimator.

The collimator calibration was changed between measurements made on S/N 001 and S/N 002, making the radiance inputs slightly different. Although a precise quantitative comparison is not directly possible, the radiance differences are so small that a direct comparison can be made for all practical purposes.

Similarly, the MTF performance illustrated in Tables 5-1 and 5-2 is a summary of measurements made on all 24 channels. Typical measured values of MTF for both subsystems S/N 001 and 002 are included in Tables 5-5 and 5-6, respectively. The measurements were compiled from test data using different computational algorithms, and therefore are not directly comparable. However, quantitative estimates of differences between the two algorithms have been made by performing computations with the two algorithms on identical data (reference the acceptance test report HS324-5196 section). The results of this analysis indicate that the MTF estimates would differ by an average of 14 percent. Using this correction factor to scale down the S/N 001 measurement, the MTF performance of the two subsystems compare within an average of 1.3 to 4.7 percent.

TABLE 5-2. CHARACTERISTIC PERFORMANCE SUMMARY MSS SUBSYSTEM S/N 002

Characteristic	Requirement	Performance
Scan repeatability, microradian	24 maximum	8
Cross-axis variation, microradian	33 maximum	3
Modulation transfer function (MTF)	0.35 minimum	0.43
Internal calibration system performance (corrected signal stability)		
Absolute stability, percent (over an orbit)	±2 maximum	0.5
Channel-to-channel, percent (picture striping)	±1 maximum	1.9
Band-to-band, percent (relative radiometric accuracy)	±1.5 maximum	2.2
Signal-to-noise (S/N)		
Band 1 (at 2.48 mw/cm ² ster.)	71 minimum	129
Band 2 (at 2.00 mw/cm ² ster.)	57 minimum	98.5
Band 3 (at 1.76 mw/cm ² ster.)	38 minimum	75.7
Band 4 (at 4.60 mw/cm ² ster.)	77 minimum	129.8
GPE picture quality (at simulated orbital conditions)		
Interference:		
Wood grain: barely visible, acceptable		
Microphonics: barely visible, acceptable		
Video correction: complete compensation for gain variations		

TABLE 5-3. TYPICAL SIGNAL, NOISE, AND S/N MEASUREMENTS FOR SUBSYSTEM S/N 001

Mode	Channel	Radiance, mw/cm ² -ster.	Signal Level, Quantum Units	Noise Level, Quantum Units	Signal-to-Noise	Test Requirements
Linear/low 50 percent NDF	1	1.42	38.20	0.52	74.1	51.0 ↓
	2	1.48	37.44	0.48	78.2	
	3	1.44	38.14	0.53	71.4	
	4	1.47	36.92	0.52	71.0	
	5	1.49	35.07	0.48	72.4	
	6	1.50	41.23	0.55	75.6	
	7	1.72	53.99	0.69	78.1	52.9 ↓
	8	1.72	48.58	0.63	76.9	
	9	1.74	53.96	0.73	73.7	
	10	1.74	49.33	0.59	84.2	
	11	1.71	53.92	0.72	74.5	
	12	1.74	48.81	0.60	80.7	
	13	1.54	56.19	0.81	69.4	36.1 ↓
	14	1.57	55.43	0.81	68.3	
	15	1.57	53.63	0.79	67.5	
	16	1.52	52.32	0.75	69.6	
	17	1.54	55.87	0.82	68.0	
	18	1.52	52.96	0.92	57.4	
	19	4.08	53.19	0.51	103.9	68.5 ↓
	20	4.14	53.51	0.53	101.7	
	21	4.15	54.29	0.49	109.7	
	22	4.09	54.16	0.48	112.4	
	23	4.05	53.90	0.50	107.6	
	24	4.01	50.99	0.45	113.3	
Linear/high 10 percent NDF	1	0.28	23.04	0.68	34.1	25.8 ↓
	2	0.32	24.00	0.57	41.9	
	3	0.33	23.45	0.65	36.2	
	4	0.32	23.40	0.67	35.9	
	5	0.32	22.13	0.66	34.4	
	6	0.33	25.24	0.68	36.4	
	7	0.37	33.79	0.94	35.9	25.2 ↓
	8	0.37	29.93	0.90	33.1	
	9	0.36	33.10	0.91	34.0	
	10	0.35	31.75	0.80	40.0	
	11	0.36	32.39	1.01	32.0	
	12	0.36	30.89	0.87	35.4	
Compression/low 10 percent NDF	1	0.28	15.86	0.33	47.8	27.1 ↓
	2	0.32	15.86	0.36	44.6	
	3	0.33	16.13	0.46	39.9	
	4	0.32	15.42	0.44	35.2	
	5	0.32	15.27	0.44	34.5	
	6	0.33	16.97	0.45	33.1	
	7	0.37	21.53	0.47	45.8	29.9 ↓
	8	0.37	19.78	0.49	40.0	
	9	0.36	20.74	0.53	39.2	
	10	0.35	20.12	0.45	44.6	
	11	0.36	20.87	0.51	41.2	
	12	0.36	20.12	0.45	44.4	
	13	0.32	21.38	0.52	41.0	21.4 ↓
	14	0.32	21.14	0.52	40.5	
	15	0.33	20.89	0.53	38.2	
	16	0.31	19.95	0.51	39.0	
	17	0.31	20.81	0.56	37.2	
	18	0.31	20.19	0.62	32.6	
Compression/high 5 percent NDF	1	0.12	19.69	0.66	29.7	24.1 ↓
	2	0.16	21.70	0.54	39.8	
	3	0.15	20.75	0.62	33.5	
	4	0.15	21.01	0.63	33.5	
	5	0.16	20.99	0.59	35.7	
	6	0.16	21.66	0.67	32.2	
	7	0.18	27.92	0.74	37.3	25.1 ↓
	8	0.17	25.34	0.73	34.7	
	9	0.18	26.80	0.81	35.2	
	10	0.17	27.13	0.64	42.4	
	11	0.18	25.99	0.81	32.2	
	12	0.18	26.55	0.66	40.0	

TABLE 5-4. TYPICAL SIGNAL, NOISE AND S/N MEASUREMENTS FOR SUBSYSTEM S/N 002

Mode	Channel	Radiance, mw/cm ² -ster.	Measured Signal, Quantum	Measured Noise, Quantum	Signal-to-Noise Ratio	S/N Test Requirement
Linear/low 50 percent NDF	1	1.38 ↓	33.57	0.47	71.60	48.69 ↓
	2		34.76	0.45	76.55	
	3		35.84	0.44	80.80	
	4		37.18	0.45	81.91	
	5		33.83	0.45	74.89	
	6		34.49	0.46	76.69	
	7	1.63 ↓	54.65	0.62	88.88	50.88 ↓
	8		50.42	0.59	85.61	
	9		53.16	0.65	82.11	
	10		55.33	0.65	85.56	
	11		52.98	0.61	86.97	
	12		50.67	0.62	85.16	
	13	1.57 ↓	56.58	0.69	31.83	36.38 ↓
	14		56.48	0.92	61.35	
	15		61.13	0.83	73.47	
	16		54.73	0.86	63.86	
	17		57.85	0.77	75.21	
	18		57.35	0.82	70.91	
	19	4.29 ↓	56.18	0.45	124.59	71.54 ↓
	20		56.09	0.46	120.94	
	21		55.22	0.42	131.83	
	22		54.74	0.47	116.86	
	23		56.32	0.49	116.10	
	24		55.44	0.48	120.97	
Linear/high 10 percent NDF	1	0.29 ↓	21.18	0.63	33.94	24.05 ↓
	2		23.24	0.61	38.26	
	3		22.78	0.60	37.97	
	4		23.96	0.58	41.29	
	5		22.52	0.62	36.28	
	6		22.89	0.63	36.31	
	7	0.35 ↓	35.57	0.81	44.19	24.66 ↓
	8		32.58	0.83	39.09	
	9		34.17	0.87	39.31	
	10		35.43	0.83	42.15	
	11		32.33	0.86	37.79	
	12		31.50	0.83	38.19	
Compression/low 10 percent NDF	1	0.29 ↓	14.88	0.43	34.59	24.67 ↓
	2		15.85	0.39	40.31	
	3		15.37	0.45	34.37	
	4		16.31	0.44	37.13	
	5		15.87	0.40	39.39	
	6		15.44	0.48	32.39	
	7	0.35 ↓	21.44	0.48	44.49	29.07 ↓
	8		20.49	0.47	43.24	
	9		20.99	0.50	41.63	
	10		21.45	0.47	45.49	
	11		20.86	0.49	42.32	
	12		20.79	0.47	43.95	
	13	0.33 ↓	21.91	0.53	41.31	22.02 ↓
	14		21.69	0.62	34.83	
	15		23.48	0.57	40.93	
	16		21.64	0.62	35.11	
	17		22.19	0.56	39.44	
	18		21.94	0.57	38.63	
Compression/high 5 percent NDF	1	0.13 ↓	18.98	0.65	29.15	22.06 ↓
	2		21.71	0.55	39.18	
	3		20.57	0.57	36.16	
	4		21.75	0.55	34.24	
	5		21.43	0.56	38.18	
	6		21.58	0.57	37.63	
	7	0.17 ↓	29.18	0.68	42.92	24.54 ↓
	8		27.43	0.69	39.22	
	9		28.28	0.72	39.42	
	10		28.87	0.69	41.69	
	11		26.43	0.69	37.87	
	12		26.68	0.69	38.54	

TABLE 5-5. TYPICAL MTF MEASUREMENTS
FOR SUBSYSTEM S/N 001

<u>Channel</u>	<u>Measured MTF*</u>
1	0.378
2	0.401
3	0.406
4	0.420
5	0.420
6	0.458
Band 1 (average)	0.414
7	0.423
8	0.424
9	0.415
10	0.401
11	0.403
12	0.423
Band 2 (average)	0.415
13	0.394
14	0.382
15	0.406
16	0.412
17	0.395
18	0.427
Band 3 (average)	0.403
19	0.463
20	0.446
21	0.412
22	0.402
23	0.473
24	0.456
Band 4 (average)	0.442
All channels (average)	0.419

NOTE: MTF minimum test requirement = 0.35.

*Reduced by 14 percent to account for change in algorithm between S/N 001 and S/N 002 system tests.

TABLE 5-6. SUMMARY OF AVERAGE MTF FROM MEASUREMENTS OVER ACCEPTANCE TEMPERATURE RANGE FOR SUBSYSTEM S/N 002

<u>Channel</u>	<u>MTF Average</u>
1	0.45
2	0.43
3	0.415
4	0.405
5	0.415
6	0.425
Band 1	0.42
7	0.38
8	0.425
9	0.425
10	0.415
11	0.42
12	0.415
Band 2	0.41
13	0.395
14	0.415
15	0.395
16	0.425
17	0.42
18	0.445
Band 3	0.415
19	0.465
20	0.43
21	0.43
22	0.46
23	0.47
24	0.465
Band 4	0.45
All channels	0.43

NOTE: MTF minimum test requirement = 0.35.

APPLICABLE DOCUMENTS

1. Design Requirements Specification for Multispectral Scanner (MSS) Spacecraft Equipment for ERTS, DR 31324-001
2. Qualification Test Report MSS Prototype System, HS 324-4859
3. Acceptance Test Report MSS Backup System, HS 324-5196
4. Operation and Maintenance Manual, Volume I, MSS Flight Equipment, HS 324-4365
5. Operation and Maintenance Manual, Volume II, Receiving Site Equipment, HS 324-4367
6. Operation and Maintenance Manual, Volume III, Ground Processing Equipment, HS 324-4366
7. Operation and Maintenance Manual, Volume IV, Bench Test Equipment/Spacecraft Test Equipment, HS 324-4368